Optimal Planning of Distributed Generations in Distribution Network and Load Frequency Control of Microgrid using Meta-Heuristic Algorithms

Thesis
submitted in partial fulfilment of the requirements
for the award of the degree of

Doctor of Philosophy
in
Electrical Engineering

by

S. Kayalvizhi
(Roll No. 701340)

Supervisor

Dr. D.M. Vinod Kumar
Professor

Department of Electrical Engineering
National Institute of Technology Warangal
(An Institute of National Importance)
Warangal – 506 004, Telangana State,India
January – 2018

APPROVAL SHEET

This Thesis entitled "**Optimal Planning of Distributed Generations in Distribution Network and Load Frequency Control of Microgrid using Meta-Heuristic Algorithms**" by **S. Kayalvizhi** is approved for the degree of Doctor of Philosophy

Examiners

_____

_____

_____

Supervisor

Dr. D.M. Vinod Kumar
Professor
EED, NIT Warangal

Chairman

Dr. V.T. Somasekhar
Professor & Head,
EED, NIT Warangal

Date: _____

DEPARTMENT OF ELECTRICAL ENGINEERING
NATIONAL INSTITUTE OF TECHNOLOGY WARANGAL
WARANGAL – 506 004

DEPARTMENT OF ELECTRICAL ENGINEERING

NATIONAL INSTITUTE OF TECHNOLOGY WARANGAL

CERTIFICATE

This is to certify that the thesis entitled **"Optimal Planning of Distributed Generations in Distribution Network and Load Frequency Control of Microgrid using Meta-Heuristic Algorithms"**, which is being submitted by **Ms. S. Kayalvizhi** (Roll No. 701340), is a bonafide work submitted to National Institute of Technology Warangal in partial fulfilment of the requirements for the award of the degree of **Doctor of Philosophy** in Electrical Engineering. To the best of my knowledge, the work incorporated in this thesis has not been submitted elsewhere for the award of any degree.

Date:

Place: Warangal

Dr. D.M. VINOD KUMAR
(Thesis Supervisor)
Professor
Department of Electrical Engineering
National Institute of Technology Warangal
Warangal – 506 004

DECLARATION

This is to certify that the work presented in the thesis entitled "**Optimal Planning of Distributed Generations in Distribution Network and Load Frequency Control of Microgrid using Meta-heuristic Algorithms"** is a bonafide work done by me under the supervision of **Dr. D.M. Vinod Kumar,** Professor, Department of Electrical Engineering, National Institute of Technology Warangal, India and was not submitted elsewhere for the award of any degree.

I declare that this written submission represents my ideas in my own words and where others' ideas or words have been included, I have adequately cited and referenced the original sources. I also declare that I have adhered to all principles of academic honesty and integrity and have not misrepresented or fabricated or falsified any idea/data/fact/source in my submission. I understand that any violation of the above will be a cause for disciplinary action by the institute and can also evoke penal action from the sources which have not been properly cited or from whom proper permission has not been taken when needed.

Date: **S. Kayalvizhi**

Place: Warangal (Roll No: 701340)

ACKNOWLEDGEMENTS

I want to profusely thank my adviser **Dr. D.M. Vinod Kumar**, Professor, Department of Electrical Engineering, National Institute of Technology Warangal, for his valuable guidance, support and suggestions throughout my research period. It has indeed an honour to work under him. He has guided through my tough times both in my research and on the personal front. He taught me the success mantra of "patience" and "commitment" not only for academic research but for life in general. I thank him for being a wonderful supervisor.

I am very much thankful to, **Prof. V.T. Somasekhar** Head, Dept. of Electrical Engineering for his suggestions, comments and support. I would also like to express my sincere thanks to **Prof. N. Vishwanathan,** Former Head**,** Dept. of Electrical Engineering for his constant suggestions, support and encouragement.

I deem it my privilege to thank all my Doctoral Scrutiny Committee members, **Dr. S. Srinivasa Rao**, Associate Professor, Department of Electrical Engineering and **Dr. P. Suresh Babu,** Assistant professor, Department of Electrical Engineering and **Dr. G. Amba Prasada Rao**, Professor, Department of Mechanical Engineering for their constructive reviews, directions and the valuable comments provided by them at every juncture of my research. I would also like to thank **Dr. M. Raja Vishwanathan**, Assistant Professor, Department of Humanities and Social science for proofreading my thesis.

I would also appreciate the encouragement and support from the teaching, non-teaching members and fraternity of Department of Electrical Engineering of NIT Warangal. They have always been encouraging and supportive.

I wish to express my sincere thanks to **The Director**, NIT Warangal for his support and encouragement.

I take this opportunity to convey my special thanks to my batch mates K. Vijaya Babu and S. Venu, Department of Electrical Engineering, for their moral support which made me feel at home. I would also like to convey my gratitude to all my co- scholars in the department for their timely technical discussions, suggestions and support. The entire scholar group in the department has been a source of good friendship and support. I would

also like to thank my friends R. Hithavani, B. Mayuri and P. Dorca, Research Scholars, NIT Warangal for their love and care for me throughout my stay at NIT Warangal.

I am highly indebted to my friend T. Jayakumar, JTO, BSNL, Pondicherry and his family for being my well-wishers. I would like to thank my cousin B. Devanathan for shouldering some of my responsibilities at times and being a source of moral support. I also thank my friends V. Gunasri, A. Geetha and S. Santhoshraj for their support and advice in times of crisis.

I acknowledge my gratitude to all my teachers, colleagues and friends at various places for their advice, encouragements and prayers directly or indirectly which supported me and enabled the successful completion of my research.

I render my gratitude to all my family members for their never ending love and support, especially to my mother **Smt. S. Valarmathy** who has supported all my decisions in my education and life. Not only this research work but my entire education and life was made possible only because of my mom's sacrifice, prayers and support. She has been the real driver with her moral support and courage.

I feel abundantly blessed and thank God for everything that happened for me. I owe my deepest gratitude to the **"ALMIGHTY"** for the blessings showered on me during tough times in life and research.

S. Kayalvizhi

Ж

ABSTRACT

Continuous supply of electricity is the need of the hour in developing economies, more so in a rapidly industrializing country like India. The growing demand tends to change the conventional structure of power system to increase the flexibility of the existing system that generates power in bulk and deliver the power to the load centers through transmission network. To avoid transmission congestion and to assure continuous supply to scattered loads, Distributed Generations (DG) in small scale emerged as an alternative technology. Many of the DG technology sources include renewable energy sources such as wind power, photovoltaic cells, biogas, fuel cells, etc., in order to meet the environmental constraints. These DG technologies have been adopted to meet the future load with improved system efficiency, reliability, security and quality of service; they however have a critical impact on the system voltage, power quality, stability, fault level and protection coordination. In spite of promising improvement in reliable power supply with less green gas emission, the implementation of active distribution networks imposes a large number of technical and regulatory issues that need to be carefully evaluated. Hence, planning the DG plays a vital role in establishment of future smart grid.

It is essential to have suitable and efficient methods and models to plan an active distribution network operation, which involves many objectives and constraints. Conventional methods like analytical approaches and numeric methods have been adequately applied for DG planning in distribution network in various ways. But these methods sometimes arrive at local optimal solutions in spite of their computational burdens. They also lack handling multi-objective problem efficiently. Population based evolutionary algorithms have been found ideal in dealing with multi-objective DG planning. However, many such algorithms suffer from premature convergence due to limited exploration in the search space while a few algorithms have their own control parameters, which will influence the algorithm efficacy.

Thus, in this thesis, a parameter less novel multi-objective based Peer enhanced Teaching-learning based optimization (PeMOTLBO) algorithm is proposed and employed to find a set Pareto optimal solutions for planning DG in distribution system and fuzzy theory approach has been used to find the best compromising DG location and size. The

pareto front obtained by the proposed PeMOTLBO has been compared with basic Multi-Objective TLBO (MOTLBO) and Non-Dominated Sorting Genetic Algorithm –II (NSGA-II). The comparisons show the superiority of the proposed algorithm in terms of both better objectives and diversity among the solutions in the optimal fronts obtained. Two performance metrics have been evaluated to ascertain the two goals of the multi-objective optimization and the proposed technique exhibited better metric value compared to NSGA-II and MOTLBO.

It is well known that there are several DG technologies which are costlier and polluting, such as diesel and gas, as well as environment friendly technologies such as wind and solar. Planning the optimal operation of DGs to supply the load is the ultimate requirement of Active Distribution Network (ADN) operation. In view of this, a new hybrid Grid-based Harmony Search algorithm is proposed by incorporating the grid based strategy in the basic harmony search algorithm for multi-objective DERs planning model both in grid connected and autonomous microgrid operation with three conflicting objectives viz., i) Energy loss ii) voltage deviation and iii) cost of DG integration. A qualitative comparison is also made with two comparison metrics to ascertain the superiority of the proposed algorithm over robust NSGA-II and other form of multi-objective harmony search. A grid based multi-objective harmony search optimization is proposed to find the optimal mix of DG units for economic operation of grid connected distribution system and it has been extended to analyze autonomous operation of active distribution system in the presence of battery storage.

While planning the DGs and their economic feasibility for operation in microgrid, the main purpose of microgrid operation should not be ignored i.e. the active management of load that is directly linked with the approximately constant frequency of operation in the system. Thus, load frequency control of an isolated microgrid is also attempted in this thesis with two types of control techniques: first one with PI controller, whose gains are tuned with Levy-based spider monkey optimization algorithm. This method employs levy flights to explore the search space whereas spider monkey algorithm is utilized to intensify the search towards better optimal solution. And the second, a fuzzy adaptive Model Predictive Control (MPC), where the fuzzy controller is embedded into MPC algorithm for better adaptive performance of load frequency control in an isolated microgrid.

Contents

List of Figures

List of Tables

Abbreviations

ADN	Active Distribution Network
BFSA	Backward-Forward Sweep Algorithm
DG	Distributed Generation
DERs	Distributed Energy Resources
DEG	Diesel Engine Generator
COG	Centre Of Gravity
ESS	Energy Storage Systems
FA	Firefly Algorithm
FLC	Fuzzy Logic Controller
FAMPC	Fuzzy Adaptive Model Predictive Control
FC	Fuel Cell
GrMHS	Grid based Multi-objective Harmony Search
HSA	Harmony Search Algorithm
HMCR	Harmony Memory Consideration Rate
ITSE	Integral Time Squared Error
ISE	Integral Squared Error
LFC	Load Frequency Control
MPC	Model Predictive Control
NSGA-II	Non-Dominated Sorting Genetic Algorithm – II
ODGP	Optimal Distributed Generation Planning
PeMOTLBO	Peer-enhanced Multi-Objective Teaching Learning Based Optimisation
PAR	Pitch Adjusting Rate
PV	Photo Voltaic
PDF	Probability Density Function
PSO	Particle Swarm Optimisation
PI controller	Proportional Integral Controller
SMA	Spider Monkey Algorithm
TLBO	Teaching Learning Based Optimization

List of Symbols

a, b and c	Fuel cost coefficients
α, β	Parameters of the Beta distribution function
C_{gasoil}	Price of the gasoil
C_{ei}	The penalty for eth pollution source
CI_i	Investment cost coefficient
CAP_i	Capacity of installed units
D	Damping Coefficient
div	No. of divisions in the objective space
d_i	Minimum distance between objectives in the objective space
$\bar{d}$	Mean of d_i
$DLF_{i,t,h}$	Demand Level Factor for typical daily load at every bus in year t
E_{bat}	Energy Status of the battery
$f_w(v)$	Weibull distribution of wind velocity
$f_b(s)$	Beta distribution function of solar irradiance
FF	Fill factor
Δf	Frequency deviation
H	Inertia of rotating masses of the micro grid
I_c	Set coverage metric
I_{sc}	Short circuit current in A
I_{MPP}	Current at maximum power point in A
J	Cost function in MPC
K_v	Voltage temperature coefficient in V/°C
K_i	Current temperature coefficient in A/°C
k_{OMi}	M&O costs coefficient
K_{WT}	Annual M&O cost (per kW) for wind turbine

K_{PV}	Annual M&O cost (per kW) for solar cell
Kp	Proportional controller gain
K_i	Integral controller gain
ll_k	Lower limits of the grid in objective space
M	No. of objectives
μ_{ei}	The coefficients of eth pollution source
n	No. of buses in the system
N	Population size
N_{OT}	Nominal operating temperature of cell in ˚C
N_m	Number of PV modules
n_s	No. of PV cells
n_w	No. of wind turbine generator
η_{ch}	Charging efficiency of the battery
η_{disch}	Discharging efficiency of the battery
N_P	Prediction horizon
Nc	Control horizon
P_loss	The total real power loss in the system
P_{DG}	Real power of DG
P_{load}	Total load on the system
$P_{DG}^{\max}$	Maximum power of DG
$P_v\{G_w\}$	Probability of the wind speed in state w
$P_s\{G_y\}$	Probability of the solar irradiance in state y
P_w	Output power of the wind turbine during state w
P_s	Total solar power output
$P_m^{\min}, P_m^{\max}$	Minimum and maximum limits on m^{th} objective in population P
P_{Sy}	Output power of the PV module during state y
ΔP_L	Change in load power

ΔP_{s_inv}	Change in power outputs from inverter circuit of solar unit
ΔP_{s_filt}	Change in power outputs of filter circuit of solar unit
ΔP_{md}	Change in turbine mechanical power output from the diesel unit
ΔP_{gd}	Change in governor output of diesel unit
ΔP_{f_filt}	Change in power from filter circuit of fuel cell
ΔP_{f_inv}	Change in power from filter circuit of fuel cell
ΔP_{fc}	Change in power output from fuel cell
ΔP_{bat}	Change in the battery power
ΔP_{Cd}	Control inputs given to the diesel
ΔP_{Cf}	Control inputs given to the fuel cell
$\lvert Q \rvert$	No. of solutions in the pareto front
R	Frequency droop
r(k)	Reference input signal
R_w	Input tuning parameter in MPC
S_p	Space metric value
s	Solar irradiance in kW/m^2
$S^{D}_{i,base}$	Base load at each bus in the system
$S^{D}_{i,t,h}$	Demand level at each hour in the planning period
s_{ay}	Average solar irradiance of state y
s_{y1} s_{y2}	Solar irradiation limits in state y
T_F	Teaching –Learning factor
T_{Cy}	Cell temperature in ˚C during state y
T_A	Ambient temperature in ˚C
T_t	Turbine time constant
T_g	Governor time constant
T_{filt}	Time constant of filter circuit
T_{inv}	Time constant of inverter circuit
T_{fc}	Time constant of the fuel cell
T_b	Time constant of the battery

ul_k	Upper limits of the grid in objective space
ΔU	Control input vector
V_i	Voltage magnitude at bus i
$V_{i\min}, V_{i\max}$	Minimum and maximum limits on voltage at i^{th} bus
v_{aw}	Average wind speed
v_{ci} , v_{co}	Cut-in and cut-out wind speed
v_{w1} , v_{w2}	Wind speed limits at state w
V_{oc}	Open circuit voltage in V
V_{MPP}	Voltage at maximum power point in V
w_k	Width of hyper boxes in the objective space
Y	Output in the state space model of MPC

Chapter 1

Introduction

Chapter 1

1 Introduction

1.1 General Overview

The future electrical network is required to be flexible, accessible, reliable and cost-effective to become a smart grid, despite the changing regulatory and economic scenarios amidst the growing demand and its gap with the generation. The next generation electricity grid is expected to address major shortcomings of the existing grid. The required grid smartness is achieved by applying information technology, communication power electronics and digital technologies, tools and techniques to the existing grid to make it intelligent to tackle the future challenges [1] leading to smart grid operation. In short, Smart grid is defined as "Integrating advances in digital and information technology into the nation's electric delivery network for enhanced operational intelligence and connectivity" [2]. The keen interest on anticipated challenges in power grid proved that the roots of the power system issues might be found in the electrical distribution system, while the point of departure for grid overhaul is firmly placed at the bottom of the chain [3]. Thus, the initiatives taken to improve the smartness in the grid must start from the lower stream of the electrical grid i.e. distribution network. As one among the various future smart grid initiative worldwide, microgrid operation has emerged as one of the promising solutions to the active management of loads in distribution and remote networks [4] and it has claimed to be the building block of future smart grid.

There are several definitions for microgrid in many contexts [5], and these have evolved in various forms, such as Active Distribution Network (ADN), Cognitive Microgrid (CMG) and Virtual Power Plant (VPP) etc. The terms are interchangeably used in various research attempts in recent times. Candidates of microgrid operation are institute/campus, commercial/industrial facilities, remote "off grid" communities and military bases, data centers and municipalities etc. In this thesis, microgrid is conceived as an active distribution network and the medium voltage distribution networks are considered for the microgrid planning, control and management studies undertaken in this thesis.

1.2 Distributed Generation and the Microgrid

Distributed Generation (DG) is an approach that employs small-scale technologies to generate electricity close to the end users of power. This has become the driving factor of microgrid operation. DG technologies include Distributed Energy Resources (DERs) along with storage assets. DERs embody both modular conventional generating sources such as diesel, micro turbines, fuel cells, hydrothermal units etc., and the environmental friendly generations such as wind, solar, biogas etc. Apart from the generating sources, storage assets such as batteries, small pumped hydro units, flywheels, super capacitors etc., also contribute to DG technologies. The Department of Energy, US, defines Distributed Generation as "Distributed Generation is the small scale power generation technologies located close to the load being served, capable of lowering costs, improving reliability, reducing emission and expanding energy options".

The best way to realize the emerging potential of DGs is to take a system approach that treats generation, associated loads and controls as an integrated system or Microgrid operation. Thus, extended operation of DG technologies with the necessary controls and communication with the utility grid and the customized loads leads to microgrid operation. In brief, a microgrid is an integrated energy system consisting of interconnected loads and distributed energy resources, which as an integrated system, can operate in parallel with the grid or in an intentional island mode [2].

1.3 Need, Challenges and Solutions of Microgrid Operation

The microgrid can provide a large variety of technical, environmental and socio-economic benefits to the utility and the consumers depending on its operational strategies. The microgrid operation with distributed generations close to the loads eliminates central bulk power generation, which in turn relieves transmission and distribution network costs, saving of fossil fuels, reduction of pollution and greenhouse gases as well as technical advantages like loss reduction, peak shaving, voltage profile and load factor improvements and power quality enhancement. During disturbances, it can disconnect the generation and load from the rest of the system to retain the overall system integrity. It has the potential of improving local reliability that supports the overall system performance. Despite

technological advancements in electrical power grid and practically immature microgrid operation still imposes various technical challenges. The challenges are:

- Since microgrid involves renewable energy resources which are intermittent in nature, continuous supply to the load is uncertain.
- The hybrid energy system operation demands complicated control and management.
- Dominant use of power electronic interfaced DERs that lead to severe voltage and frequency fluctuation in the system due to less inertia.
- The conventional distribution of power is from one end where the protection is relatively simple; in contrast, microgrid operates with many energy sources placed at various places where the coordination of protection devices is tedious.
- The real and reactive power injection and absorption is directly related to frequency and voltage in the system respectively. Higher penetration of DERs will results in voltage rise in the system.
- In case of undesired system faults, it requires fast detection of islanding condition to guarantee safety and reliability of the system.

However, these challenges can be overcome by judicious planning, use of proper design and control techniques in the microgrid operation. Some such solutions to tackle these challenges are:

- Strategic deployment of DERs with respect to their location, size and technology to suit the requirement.
- Proper control techniques to manage the operation of all components in the microgrid i.e. proper scheduling of DERs output to control the voltage and frequency.
- Use of energy storage to balance the load demand and generation, which indirectly smoothen the frequency regulation.
- Proper schemes for protection of system.

1.4 Optimization techniques and problem formulating domains

Optimization is the procedure of finding the optimal solution to a problem. The optimality of a solution is evaluated in terms of an objective. Even though there has been a significant amount of research to deal with a single objective, the real world problem involves multiple objectives, which mostly conflict with each other. Classical optimization is

still a good way to find one best solution in one simulation run but not in handling multi-objective problem as there exists a set of trade-off solution of multiple objectives instead of a single solution. In such case, meta-heuristic algorithms are ideal for dealing with multi-objective optimization problems because of their population search based approach. Moreover, this multi-objective optimization can have two approaches:

i) **Weighted sum approach** – A simple method that would form a composite objective function based on the preference factor assigned to each objective. Optimizing the single composite objective function will result in one solution from the trade-off solution set.

ii) **Pareto based approach** – Ideal multi-objective approach that would treat each objective individually in the optimization procedure and result in a set of Pareto solutions where there would be a provision for decision-making based on the application.

Hence, the second method of optimization procedure is preferred for the advantage of visualizing all possible combination of objective values that exist in the trade-off solution between two conflicting objectives. In case of optimization methods, meta-heuristic algorithms are predominantly applied and they are of two types:

1. Gradient search method (Trajectory based) – Search one solution at one time
2. Population search method – Process a group of solutions at a time.

Between the above methods, the former is a slow process because of single solution search; one such example is Simulated Annealing (SA), Tabu Search (TS) whereas the latter is efficient and fast in finding the optimal solution as it processes a group of solutions in the search process, making it easier in finding the optimal solution. The population-based methods are better in exploring the optimal solutions at a faster rate. Some such Evolutionary and Meta-heuristic algorithms are: Genetic Algorithm (GA), Particle Swarm Optimization (PSO), Ant Colony Optimization (ACO), Ant Bee Colony (ABC), Bacterial Foraging Optimization (BFO) etc.

Thus, the problem of active distribution network planning in this thesis is formulated as a multi-objective problem and load frequency control of a microgrid is treated as a single objective problem. Both the problems are optimized using proposed efficient meta-heuristic algorithms.

Chapter 2

Literature Review

Chapter 2

2 Literature Review

2.1 Distributed Generation (DG) Planning in Distribution Network

The prerequisite of the microgrid operation is the optimal Distributed Generation planning. Distributed generation (often called as decentralized generation, dispersed generation and embedded generation) is a small scale generation connected either in the distribution network or in the sub-transmission network in the range from (1-10 MW). Hence, typical Optimal DG Planning (ODGP) deals with finding the location and sizing of the DG units to be installed in the existing network subject to various operational and investment constraints. Even though the installation of DGs in distribution network offers a variety of benefits, it may also impose some problems and limitations at higher penetration level if they are not placed at proper location with correct penetration level (sizing). The aspects that are influenced by the connection of DG units are as follows [6]: Voltage deviations, Grid losses, Power quality, Fault level, Protection system and Reliability. Therefore, the location and the sizing of DG become a challenging task for active distribution system planning and operation.

Even though there is relatively large research on ODGP [7]-[9] on different perspective related to technical and economic issues of DG operation, for an active distribution network operation planning, little research on DG location and size have to be carried out. The mathematical formulation of DG planning can be attempted as single or multi-objective problem either with single DG or with multiple DG units considering technical and economic constraints. The representative objective functions considered in the DG planning are: 1) minimization of the total power loss of the system; 2) minimization of energy losses; 3) minimization of system average interruption duration index (SAIDI); 4) Cost minimization; 5) Minimization of voltage deviation; 6) Maximization of DG capacity; 7) maximization of profit; 8) maximization of a benefit/cost ratio; and 9) maximization of voltage limit loadability [8]. The solution techniques for ODGP have been evolving and number of approaches have been developed, each with its particular mathematical and computational characteristics. The techniques discussed are classified as one of the three

categories: Conventional methods, intelligent search-based methods and fuzzy set based method. Conventional method includes analytical and numerical approaches.

DG planning has been attempted with several analytical approaches [10]-[15]. Acharya et al. proposed an analytical method, based on the exact loss formula, to optimally site and size a single DG [10]. Lee and Park [11] proposed an analytical method for finding the optimal locations of multiple DGs in combination with Kalman filter algorithm for determining their optimal size. T. Gözel and M. H. Hocaoglu [12] developed an analytical method using a loss sensitivity factor based on the equivalent current injection to find the optimum size and location of a single DG. Hung et al. [13] suggested analytical expressions for finding optimal size and power factor of different types of DGs. The same has been extended in [14] to compute the optimal location and size of multiple DGs for different types of DGs. Tah et al. [15] proposed a novel analytical expression for optimum DG size at each bus by eliminating the use of bus impedance matrix for loss reduction in the system.

In case of numeric approach, there are several methods of optimization adopted in DG planning problem such as gradient approach [16], linear programming [17], sequential quadratic programming [18], Non-linear programming [19]-[23], dynamic programming [24], Ordinal optimization [25]. P. Vovos and J. Bialek [16], proposed a gradient search for the optimal sizing of DGs in meshed networks considering fault level constraints. Keane and Malley [17] proposed a methodology based on linear programming to obtain optimal allocation and sizing of embedded generation considering technical constraints for accommodating maximum DG power penetration on the distribution network. AlHajri et al. [18] applied Sequential Quadratic Programming (SQP) to solve ODGP without considering the fault level constraints. Atwa et al. [19] proposed a methodology to convert discrete probabilistic generation-load model with all possible operating conditions into a deterministic model and solved it using a mixed integer nonlinear programming (MINLP) technique for optimally allocating either only wind DG units or different types of DG units [20] . Porkar et al. [21] employed MINLP for optimal allocation of different types of DG units considering electricity market price fluctuation. Kumar et al. [22] evaluated an ODGP model in hybrid electricity market using MINLP. Similarly, Abri et al. [23], proposed MINLP for optimally placing and sizing the electronically interfaced DG units, with an objective of improving the voltage stability margin. Esmaili et al. [24] proposed a method for optimal placement of DGs

to maximize VSM simultaneously minimizing the grid power losses using the dynamic programming search technique to find the global optimal solution. Jabr and Pal [25] developed an ordinal optimization method for specifying the locations and sizes of multiple DGs such that a tradeoff between loss minimization and DG capacity maximization is achieved. The fuzzy set based methods are mostly used in conjunction either with conventional or heuristic techniques.

Analytical methods are easy to implement and fast to execute. However, their results are only indicative, since they make simplified assumptions including the consideration of only one power system loading snapshot. Among the available numerical methods for ODGP, the most efficient are nonlinear programming, sequential quadratic programming and ordinal optimization methods. Heuristic methods are usually robust and provide near-optimal solutions for large, complex ODGP problems. These methods are comparatively efficient than conventional techniques irrespective of complexity of the problem. Generally, they require high computational effort. However, this limitation is not necessarily critical in DG placement applications.

A set of DG planning methods is proposed using GA presented in [26]-[28]. Gampa et al. [26] proposed a novel sensitivity index based method for optimal placement where the size of DGs is optimized using multi-objective GA considering both technical and investment costs. Ogunjuyigbe et al. [27] proposed a dynamic GA based multi-objective optimization depending on the variability of equipment cost for a tri-objective hybrid system. They also justified the replacement of large diesel generators with small (split) ones to reduce LCC, carbon dioxide emissions and dumped energy by 46%, 82% and 94% respectively. Whereas, Singh et al. [28] evaluated the optimal placement of different DG types in distribution network using a variety of load models using GA. Optimized DG system design improved with regard to security, technical, economic and environmental viewpoints. Muttaqi et al. [29] proposed a cost based DG sizing and placement using PSO technique. An economic approach was implemented to evaluate system reliability. Kowsalya [30] used Bacterial Foraging Optimization Algorithm (BFOA) to find the optimal size of DG whereas loss sensitivity factor is used to identify the optimal locations for installation of DG units with an objective of minimizing network power losses, operational costs and improving voltage stability. Mitra et al. [31] investigated suitable mix of micro turbine and solar PV penetration

in microgrid for optimal operation using Simulated Annealing (SA), with trade-off between high upfront cost of solar PV system and fuel cost of micro turbine system. Prabha and Jayabarathi [32] applied Invasive Weed Optimization (IWO) method to optimally size DG whereas optimal DG placement was based on power loss factor sensitivity approach. IWO resulted in more cost-effective DG configuration. Sultana et al. [33] investigated a complex combinatorial problem of locating and sizing of DG for real power loss/energy loss minimization of electric radial distribution networks. The Krill Herd Algorithm was employed to determine the optimal size and location of DG. Hybrid approach led to greater power loss reduction, better stability index compared to individual conventional and heuristic approaches. Such hybrid algorithms used for DG planning are presented in [34]- [36].

The above reviewed heuristic algorithms are mostly population based and dependent on algorithmic specific parameters and other controlling parameters, which may affect the effectiveness of the algorithm. The difficulty of this parameter selection may increase with modifications and hybridization techniques. Rao et al. [37] proposed a new optimization technique called Teaching-Learning Based Optimization (TLBO), which is free from algorithm specific parameters and has been utilized for single objective optimization problems. Niknam et al. [38] proposed a new multi-objective teaching-learning-based optimization algorithm in order to solve the optimal location of automatic voltage regulators (AVRs) in distribution systems with distributed generators (DGs). Nayak et al. [39] presented a non-domination based sorting multi-objective teaching-learning-based optimization algorithm, for solving the optimal power flow (OPF) problem which is a nonlinear constrained multi-objective optimization problem where the fuel cost, transmission losses and L-index are to be minimized. One of the variants of this parameter less TLBO algorithm is proposed in multi-objective frame for DG planning studies in this thesis.

2.2 Optimal planning of active distribution network in microgrid perspective

The location and size of conventional Distributed Generations connected in the distribution network have to be planned for active management of load. However, continuously increasing demand and depleting fuel-based generation urged the need of including renewable energy source integration in the system. In such situations, optimally planning the favorable combination of energy sources along with their best location and size

is extremely important both in technical and economic terms. This is especially relevant in the presence of inherently intermittent and environment dependent resources such as wind and solar power which introduce significant uncertainty and variability in the system. Apart from this, large-scale integration of renewable sources demands better smart grid technologies to address various challenges ahead of its operation. Thus, dynamically planning the resource mix for optimal and cost effective operation of the active distribution network both in case of grid tied mode and autonomous mode of operation, is required for timely exploration in this area of research.

2.2.1 Planning of grid connected active distribution network

The evolving active distribution network can operate both in the grid-connected mode and in autonomous mode depending on the need. Diligent planning of Distributed Energy Resources for the required mode of operation is a challenging task in the pace of network characteristics changes [41]. The optimal mix and location of renewable and non-renewable DG sources have to be identified for reaping the potential benefits of their connection in the distribution network. In particular, connecting intermittent sources like wind turbine or solar power will lead to various technical challenges to sustain operation of active distribution system [42] in a reliable and secure manner.

So far, DG planning models were reported in two major ways. They are static and dynamic planning models. These planning models can be attempted both with single and multi-objective approaches. In static model, all the investment decisions are made at the starting of the planning horizon [43]. Even though exhaustive work has been done in optimizing the location and sizing of DG units in the distribution network, substantial amount of research addresses this problem by considering dispatchable DG sources [44] such as gas turbine, diesel generator and fuel cell etc., with a single objective [45], [46]. It is also attempted as single objective problems of DG planning with stochastic models that include uncertain power generating sources such as wind and PV [47], [48]. Similarly, static planning models were also attempted in multi-objective frame. Harrison et al. in [49] studied the DNO loss reduction incentives with optimal location and capacities using multi-objective OPF and has been shown that the identified incentive has greater impact on the network deferral reinforcement whereas a multi-objective model using NSGA-II is proposed in [50] for

minimizing monetary cost index, technical and economic risk factors. The authors have used fuzzy domain for modeling various uncertainties such as load, voltage and loading constraints and the electricity price. Though the work attempted DG planning as a multi-objective problem, they have utilized weighted sum multi-objective approach in which two or more objectives are converted to a single composite objective by assigning preference vector to each objective and thereby not serving the actual purpose.

In dynamic planning model, some of the work considered simultaneous investment of both DG and network but the work does not deal with uncertainties associated with the DG planning problem. Maria et al. in [51] proposed a multi-objective framework with two shell process i.e. design and optimal operation of microgrid. Internal process includes optimal management of microgrid using NSGA-II whereas external procedure implements design features through glow-worm swarm optimization. On the other hand, Li guo et al. in [52] presented a multi-objective stochastic optimal planning method for standalone microgrid considering uncertainties by using chance-constrained programming algorithm. Mohammadi et al. in [53] investigated the optimal operation and management of microgrid in a stochastic framework by generating several stochastic scenarios and later reducing and converting them into a deterministic problem. These deterministic problems were solved using new optimization strategy based on Adaptive Modified Firefly Algorithm (AMFA). A two scale dynamic programming is proposed in [54] to avoid conflicts between short term and long term planning benefits pertaining to wind and battery respectively. A dynamic optimization scheme has been presented for optimal energy management of wind-battery hybrid system. The capacity and operation of DGs are optimized in [55] in a microgrid by proposing a new hybrid optimization, that combines Quadratic Programming and PSO. Investments in the microgrid are justified in terms of Net Present value (NPV) and uncertainties are incorporated using fuzzy set theory. Smart energy management system is proposed in [56] to minimize the operational cost of microgrids by optimally coordinating the power production of DG sources and energy storage systems. Though the above discussed work formulated dynamic planning model on multi-objective frame, one way or other it has compromised either multi-objective approach or system dynamics and factoring in uncertainties.

As an effort to bridge the above possibilities, a pareto optimal based multi-objective planning model is proposed for grid connected active distribution network by manifesting all possible system dynamics and uncertainties associated with generation and load.

2.2.2 Autonomous mode of active distribution network operation

The active distribution network either can be in grid-connected mode or independently operated based on the renewable generation capacity and the load demand [57]. In the former mode of operation, the deficit or excess power can be supplied or traded with the readily available main grid. Whereas in the latter mode of operation, the real and reactive power is generated and managed within the network including temporary power exchanges with storage units if it exists. However, planning the operation and management of such an active network with random and intermittent renewable sources coupled with uncertain load in two modes of network operation is tough, and is a complex process due to the goals, constraints and uncertainties. The microgrid operation must be addressed towards challenges like power quality, reliability, supply and demand balancing, environment impact and various economic and stability aspects. Dealing with these challenges in an autonomous mode of operation with renewable sources demands an added effort towards technology handling. To address this problem, use of conventional generation and the storage assets to support its power fluctuation will be an appealing solution improving system reliability. Thus, the optimally planned microgrid operation plays an important role in taking the existing grid operation to a smarter level in so many ways, particularly when electrifying a remote and isolated area.

It is generally accepted that conventional islanding of any microgrid predominantly operates with diesel units, which involves high costs and emission due to high fuel consumption unlike load shedding in unintentional islanding. To bring down the fuel cost of diesel operated islanded microgrid and to reduce the environmental impact, the diesel units are supplemented with renewable power generations such as solar, wind, biogas etc. However, the uncertain generation especially with solar and wind will introduce fluctuation in supply which in turn would lead to unstable operation [58] of the grid, thereby increasing costs for flexible operation of the diesel back up. In such conditions, energy storage systems play a vital role in reducing the overall system cost by smoothening load peaks thereby

overcoming the operating burden of diesel generators and cost constraints. Therefore, ESS can make robust and flexible system operation economical.

Ritwik et al. [59] proposed an ANN based controller for battery storage is based on the required power to be injected from the battery storage in case of power shortage to maintain the grid voltage. The proposed controller is trained off line and tested online with different loading conditions for power quality improvement and stable system for variable test conditions. Jin et al. [60] proposed a compensation control strategy with modified droop and wind power compensation for damping system frequency and power fluctuations. In [61]-[63] computational methods for optimal sizing of an off grid hybrid solar wind electric power generation system have been proposed and optimal configuration of the system has been identified to achieve minimum annualized cost of the system with the presence of battery storage. System reliability is enforced in terms of Loss of Power Supply and its relation with the system configuration has been studied completely by making use of probability density functions by processing weather data. Xinda et al. [64] developed three control algorithms and sizing strategies for batteries to minimize the hourly generation imbalance due to wind generation.

Zhao et al. [65] proposed GA based optimization to optimize the size of real world standalone microgrid at Donghfushan island to achieve minimum life cycle cost and emission simultaneously maximizing the renewable source penetration. Ting et al. [66] examined the operation and control of standalone hybrid power system by implementing controller to each sources so as to extract the maximum from them. Hussain et al. [67] developed a model for autonomous microgrid with optimal mix of DGs and the performance was analyzed through small signal analysis. The unstable operation was also studied with large penetration of wind and solar sources. Various stability aspects of microgrid operation both in the grid connected and standalone mode have been discussed in [68]-[71].

2.3 Load frequency control methods in microgrid

The main variables used to control the operation of power system are voltage, frequency, real and reactive power. The voltage and frequency are regulated by adjusting the reactive and real power respectively in the system. The power frequency control becomes a challenging task if load and source of power generation fluctuate in the system.

Hence, the load frequency control is an important function of modern power system which is dispersed geographically over a large scale and interconnected with multiple generations. This load frequency control equally requires greater attention in case of isolated small-scale microgrid operation. In grid connected microgrid operation, the infinite main grid regulates the frequency deviation due to variations in the load and renewable sources, whereas in case of islanded operation, it involves greater challenge and demands advanced control strategies to balance supply and demand with available generations. In case of islanded operation, there is no grid support for the frequency regulation in the system; it depends solely on the dispatchable sources such as diesel and storage units. These storage units play a vital role in the economic and smooth operation of islanded microgrid with excess renewable sources. Even though there are several research work on the microgrid control and management over the past decade [72]-[73], load frequency control in such an active distribution system still needs improved controls due to strong coupling between real and reactive power in the network operation. This may lead to poor performance of conventional droop control due to inability to control frequency and voltage magnitude [74] independently.

There are several LFC schemes reported in the literature from classical droop controls to various advanced control strategies in the past decades. Those schemes for conventional and distributed generation power system are comprehensively summarized in [75]. Authors [76]-[79] proposed improvements in conventional droop control for load frequency control of microgrids. Guerrero et al. [76] developed a generalized hierarchal droop control for both AC and DC microgrid whereas authors [77]-[79] shown the benefits of various energy storage systems in frequency support of microgrid operation, especially in the autonomous mode with droop control. Apart from this conventional control techniques and methods employing droop characteristics, intelligent algorithms based control techniques are also growing equally in frequency regulation studies in power systems [80]-[83]. Application of inteligent algorithms is not only confined to PI controller tuning applied for conventional generations in frequency regulation studies, but also applied to tune gains of the PI controllers employed in pitch control of wind energy conversion systems [84]. Bevrani et al.[85] proposed an online intelligent technique by combining fuzzy logic and PSO algorithm for frequency regulation in an isolated microgrid. The frequency control has been implemented by tuning PI controller gains for different case studies. Keeping apart various

techniques applied to load frequency control of microgrid, the challenges such as uncertainty in intermittent renewable generation, low inertia associated with power electronic interfaced DERs, dynamics and nonlinear complexities necessitates robust control technique. These techniques helps to get tradeoff between the robust system performance and stability in the closed loop system response against system uncertainties, such type of techniques are discussed in [86]-[89].

In addition to these schemes, model predictive control is slowly getting into control applications of power industry and is also applied to Load Frequency Control (LFC) / Automatic Generation Control (AGC) problem in recent times due to its simple and fast implementation. MPC has proved efficient in the process industry due to its modeling flexibility that involves straightforward design procedure, acceptable computational time and easy constraints handling, it is well received in all control application, and it is widely adopted in industries such as petrochemical industry, electrochemical, power and water management etc.

Although so many variants of MPC have been proposed by the authors for different applications, the classical dynamic matrix control (DMC) of MPC is predominantly applied to the load frequency control problem. Some researches that applied MPC to load frequency control are presented [90]-[95].

To explore the efficiency of intelligent techniques for load frequency control of microgrid, a novel strategy using levy flights and spider monkey optimization algorithm is proposed and an adaptive model predictive control is proposed to overcome the limitations in the MPC for load frequency control of microgrid.

2.4 Motivation

The thesis presented an extensive review on the research topic for planning and control of an active distribution system through a microgrid perspective. Distributed Generation is at the heart of microgrid operation and planning their location and sizing plays a primary objective in any active distribution system operation. There is enough literature available for tackling the problem DG planning: some have used conventional programming while others have attempted population based meta-heuristic optimization methods. Irrespective of the technique used, the unanimous objective of primary DG planning is to

achieve the objective of minimized system loss and improved voltage profile. Keeping this in mind, a variant of an existing optimization algorithm, which is parameter independent, is proposed to improve the objectives.

The next level of planning in a microgrid operation is, its cost management. It is well known that there are several DG technologies like costlier and polluting dispatchable sources such as diesel and gas, and environment friendly technologies such as wind and solar. Planning the optimal and economic operation of DG units to supply the load is the ultimate requirement of microgrid operation. In view of this, a new multi-objective optimization technique is proposed to find the optimal mix of DG units for economic operation of a grid connected distribution system and it has been extended to autonomous operation of active distribution system in the presence of storage units.

While planning the DGs and their economics of operation in a microgrid, the main purpose of microgrid operation should not be ignored i.e. the active management of load which is directly linked with the frequency of operation. Thus, load frequency control of isolated microgrid is also attempted in this thesis with two types of control techniques. The first one uses PI controllers whose gains are tuned with a meta-heuristic technique called levy based spider monkey algorithm and the second one uses model predictive control where fuzzy controller is embedded into it for better adaptive performance of load frequency control in microgrid.

The thesis addresses the overall planning of optimal and economic operation of DGs in the active distribution system and the load frequency control in an isolated microgrid, which needs to be analyzed. These problems are analyzed using the proposed meta-heuristic optimization algorithms.

2.5 Contribution

The contributions made in the thesis are as follows:

- A Multi-objective based Peer enhanced Teaching-Learning Based Optimization (PeMOTLBO) algorithm is proposed to find a set of pareto optimal solutions for planning DG in distribution system. The proposed algorithm is parameter less and has performed better for multi-objective optimization in DG planning compared to conventional multi-objective techniques. Optimal location and size of DG units are

found with minimum active power loss and voltage deviation in the distribution system. A fuzzy set theory approach has been used to find best compromising DG location and size from the set of trade-off solutions.

- New hybrid Grid-based Multi-objective Harmony Search algorithm (GrMHS) is proposed for optimizing the active distribution network operation. In the proposed method, a grid-based strategy is used as a secondary selection criterion in non-dominating sorting procedure of pareto based multi-objective optimization. The harmony search algorithm is employed for optimization purpose. The optimal resource mix of Distributed Energy Resources has been identified for both grid connected and autonomous mode of active distribution system operation. The planning model considered three conflicting objectives viz., i) energy loss ii) voltage deviation and iii) cost of DG operation.
- A novel eagle strategy by combining levy flights with Spider Monkey Optimization Algorithm (SMA) is proposed for load frequency control of an isolated microgrid. The proposed algorithm has been used for tuning gains of the PI controller employed in controllable generation such as diesel unit for load frequency control of an isolated microgrid. The results of the proposed algorithm have been compared with other prominent algorithm such as PSO, Firefly Algorithm (FA), and Harmony Search (HS) algorithm.
- A fuzzy adaptive Model Predictive Control (MPC) has been proposed for load frequency control of isolated microgrid. Rule based fuzzy controller is employed within MPC algorithm to fuzzify the tuning parameter present in the cost function of MPC. The proposed method improved the adaptive performance of the MPC for better frequency control in the microgrid. The results of the proposed method have been compared with PI controller response in the system.

2.6 Thesis Organization

The thesis is organized into seven chapters, with a summary of each chapter given as follows:

Chapter-1 introduces DG and its need in the distribution network operation. It briefly outlines the planning of active distribution network with relevant terms and topics. The

frequency regulation in the system operation is also emphasized. In short, an overview of the problem addressed in this thesis is presented.

Chapter-2 presents a detailed literature survey on the research topic with past and ongoing research. The literature review presents various techniques and approaches of DG placement and sizing in the distribution network followed by elaborate discussion of dynamic planning of optimally placed DGs for economic grid operation. Later, the load frequency control of microgrid is also reviewed with relevant analysis. Following an extensive survey on the topic, the motivation for the proposed research work, contribution, and organization of the thesis are also presented.

Chapter-3 presents the DG modeling and its incorporation in the backward-forward sweep distribution load flow. The formulated objectives and constraints for DG placement and sizing problem are explained. Non-dominated sorting based multi-objective Teaching Learning based Optimization (TLBO) algorithm is discussed and a variant of TLBO called Peer enhanced Multi-objective TLBO (PeMOTLBO) is proposed for optimizing the location and sizing of DGs. Simulation results and discussions of the proposed algorithm are presented. The comparison metrics evaluation to support the superiority of the proposed algorithm is also shown.

Chapter-4 proceeds with the uncertainty modeling of load and generation such as wind and solar power. A new hybrid Grid-based Harmony Search algorithm is proposed by incorporating the grid based strategy in the basic harmony search algorithm. DG planning model to find the optimal mix of DG units is proposed for non-autonomous microgrid operation with three conflicting objectives viz., i) energy loss ii) voltage deviation and iii) cost of DG operation. The same model and algorithm is extended to plan the autonomous operation of active distribution network by enforcing the renewable bus available limits with optimal DG units. The quality of results obtained by the proposed methodology is ascertained with the help of performance metrics evaluation for both the cases.

Chapter-5 presents the load frequency control of an isolated microgrid. First of all, the need and means of the load frequency regulation in a microgrid is explained and a new eagle strategy for optimizing the gains of proportional and integral (PI) controller is proposed and the advantage of the proposed eagle strategy that combines levy flights with spider monkey optimization algorithm is explained. Finally, the results of the proposed method are

compared with other algorithms such as PSO, Firefly Algorithm (FA), and Harmony Search (HS) algorithm and validated.

Chapter-6 explains fuzzy adaptive model predictive control for the load frequency control of an isolated microgrid. The MPC algorithm is simple and more efficient in frequency control without employing PI controllers. The fuzzy tuned model predictive control is proposed with necessary justifications. The results obtained by the proposed method are compared with PI controller and are validated.

Chapter-7 summarizes the salient features of the reported research work in this thesis and suggests the future scope of the work.

2.7 Summary

This chapter presented a detailed and extensive review on planning of active distribution network on multi-objective frame and on the load frequency control of autonomous microgrid operation. The need and reason behind multi-objective problem formulation for DG planning and the limitations involved in various multi-objective approaches were highlighted. The necessity of faster and more efficient controllers in load frequency control of microgrid has been discussed. Finally, the motivation and contribution of the research work have been presented.

Chapter 3

Distribution Generation planning using Peer enhanced Multi-Objective Teaching –Learning based Optimization Algorithm

Chapter 3

3 Distribution Generation planning using Peer enhanced Multi-Objective Teaching –Learning based Optimization Algorithm

3.1 Introduction

This chapter intends to present a new variant of Teaching Learning based Optimization algorithm in multi-objective frame called Peer enhanced Multi-objective Teaching Learning Based Optimization (PeMOTLBO) algorithm for optimizing DG location and sizing in the distribution network. TLBO algorithm is chosen as there is no algorithmic parameter that affects the optimization process of the problem. The problem is attempted with pareto based multi-objective approach as it deals with two conflicting objectives of the planning problem, such as real power loss and voltage deviation. The DG planning problem is subjected to voltage limits and maximum penetration level of DG constraints in distribution network, whereas the decision variables are location and size of the DG units. DGs are modeled as negative load model and considered to be operating at a constant power factor of 0.85 lead. The fuzzy set theory is also applied to choose the best solution from the obtained pareto set.

3.2 Modelling of DG in distribution system load flow

The load flow studies are common procedures applied to get the steady state operating characteristics of the power system, especially the voltage profile in the system. However, the load flow methods used in transmission system viz., Gauss-Seidel and Newton-Raphson and Fast Decoupled methods are not valid in distribution Systems due to the well-known characteristics of an electric distribution system. The characteristics are:

- Radial or weakly meshed structure;
- Multiphase and unbalanced operation;
- Unbalanced distributed load;
- Extremely large number of branches and nodes;
- Wide-ranging resistance and reactance values, low X/R ratio ($\leq$ 1).

There are distribution load flow methods, which can be applied to distribution network for analyzing distribution system planning and operation studies like load scheduling, DG incorporation, demand side management etc. There are different distribution load flow methods available in the literature:

- Direct distribution load flow (DDLF)
- Backward forward sweep distribution load flow(BFS)
- Vector based distribution load flow(VDLF)
- Primitive impedance based distribution load flow
- Current injection based load flow

In the distribution system load flow, first three can be applied only to the radial system whereas the primitive impedance and current injection methods can be applied to both radial and meshed distribution system. In this thesis, Backward Forward Sweep (BFS) distribution load flow is used for the analysis because it is simple and easy to implement and takes less computational time.

3.2.1 Backward and Forward Sweep load flow algorithm (BFS)

The BSF distribution load flow method includes two steps [104]: Backward sweep and the forward sweep.

The backward sweep is based on KCL for finding each branch currents

The forward sweep is based on KVL for finding the voltage for each upstream bus of a line or a transformer branch.

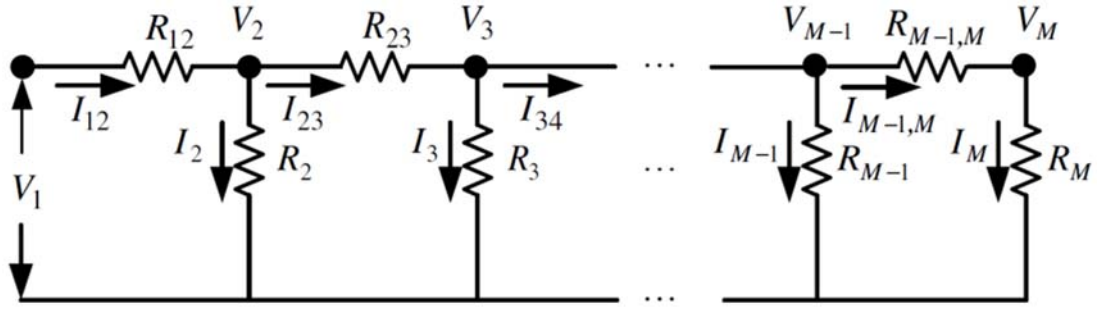

Figure 3.1: A simple resistive network

This method can be explained by above simple network. During backward sweep, line currents are calculated by the equations given below:

Let m=4 nodes

$$I_4 = \frac{V_4}{R_4} \quad (3.1)$$

$$I_{34} = I_4 \quad (3.2)$$

$$I_3 = \frac{V_3}{R_3} \quad (3.3)$$

$$I_{23} = I_{34} + I_3 \quad (3.4)$$

$$I_2 = \frac{V_2}{R_2} \quad (3.5)$$

$$I_{12} = I_{23} + I_2 \quad (3.6)$$

Then in general

$$I_i = \frac{V_i}{R_i} \quad (3.7)$$

$$I_{i,i+1} = I_{i+1,i+2} + I_{i+1} \quad (3.8)$$

The line currents are calculated from last node to first node. So it is known as backward sweep. During forward sweep, voltages are calculated by the equation below:

$$V_2 = V_1 - I_{12}R_{12} \quad (3.9)$$

$$V_3 = V_2 - I_{23}R_{23} \quad (3.10)$$

$$V_4 = V_3 - I_{34}R_{34} \quad (3.11)$$

Then in general

$$V_{i+1} = V_i - I_{i,i+1}R_{i,i+1} \quad (3.12)$$

The voltages are calculated from second node to last node. So it is known as forward sweep. For a typical 6-bus radial distribution system shown in Figure 3.2.

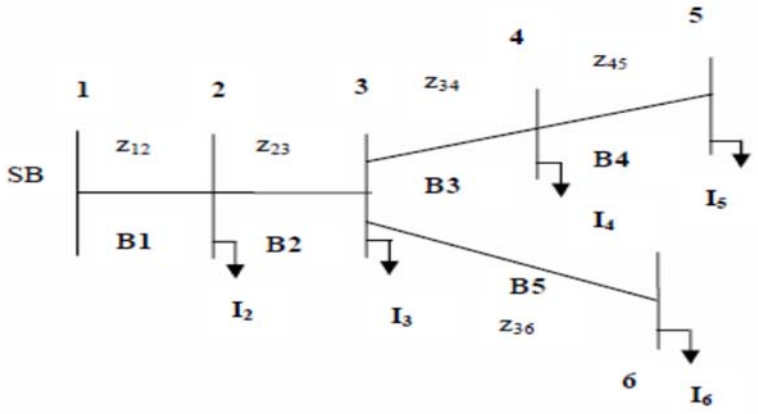

Figure 3.2: Typical 6-bus radial distribution system

Assuming a flat voltage profile as initial voltages, during backward sweep

$$\left.\begin{aligned} I_{36}&=I_6\\ I_{45}&=I_5\\ I_{34}&=I_{45}-I_4\\ I_{23}&=I_{34}+I_{36}-I_3\\ I_{12}&=I_{23}-I_2 \end{aligned}\right\} \quad (3.13)$$

The above equations can be written in general form as

$$J(k) = \sum_{m=adjl(q)} J(m) - I(q) \quad (3.14)$$

Where J (k) =branch current in line k. I (q) =current injection at bus-q.

During forward sweep, the voltages are calculated from equation (3.12). Backward and Forward sweeps are repeated until convergence is achieved.

3.2.2 DG as negative PQ model

The DGs can be classified into four types based on the real and reactive power injections and absorption. In this chapter, DG is considered as capable of injecting real and reactive power to the distribution network and the operating power factor is taken as 0.85 lead [98]. To incorporate the generation in the distribution load flow, it is considered as negative load at a particular bus. Thus, the DG is modeled as negative PQ in the load flow.

3.3 Proposed Peer enhanced Multi-Objective Teaching-Learning Based Optimization (PeMOTLBO) Algorithm

The proposed optimization method is based on the fact that along with influence of a teacher, learners also put in effort in improving the output in a class. A group of learners constitutes the population in basic TLBO. The different design variables in TLBO are analogous to different subjects offered to learners and the result is analogous to the fitness. The teacher is considered as the most learned person, the best solution so far is analogous to the Teacher in TLBO. The process of TLBO is divided into two parts. The “Teacher Phase” means learning from the teacher and the “Learner Phase” means learning through the interaction among learners. The implementation of TLBO algorithm is as follows [37]:

- ***Initialization***

Population X is randomly initialized by a search space bounded by matrix of N rows and D columns. The *jth* parameter of the *ith* learner is assigned values randomly using the equation

$$x_{(i,j)}^{0} = x_j^{min} + rand * \left(x_j^{max} - x_j^{min}\right) \tag{3.15}$$

N: number of learners in a class i.e. "class size".

D: number of courses offered to the learners.

G: maximum number of iterations.

'rand' represents a uniformly distributed random variable within the range (0, 1), x_j^{min} and x_j^{max} represent the minimum and maximum value for *jth* parameter. The parameters of *ith* learner for the generation g are given by

$$X_{(i)}^{g} = \left[x_{(i,1)}^{g}, x_{(i,2)}^{g}, x_{(i,3)}^{g}, \dots\dots, x_{(i,j)}^{g}, \dots, x_{(i,D)}^{g}\right] \tag{3.16}$$

The objective values at a given generation form a column vector. In dual objective scenario, two objective values are present for the same row vector. The two objectives (a and b) can be evaluated as:

$$\begin{bmatrix} Ya_i^g \\ Yb_i^g \end{bmatrix} = \begin{bmatrix} fa\left(X_{(i)}^{g}\right) \\ fb\left(X_{(i)}^{g}\right) \end{bmatrix} \tag{3.17}$$

For all the equations used in the algorithm, $i = 1,2,3 \dots N$ and $g = 1,2,3, \dots., G$. The random distribution followed by all the *rand* values is the uniform distribution.

- ***Teacher Phase***

The mean parameter M^g of each subject of the learners in the class at generation g is given as:

$$M^g = \begin{bmatrix} mean\left(\left[x_{(1,1)}^{g}, \dots., x_{(i,2)}^{g}, \dots, x_{(N,1)}^{g}\right]\right) \\ mean\left(\left[x_{(1,j)}^{g}, \dots., x_{(i,j)}^{g}, \dots, x_{(N,j)}^{g}\right]\right) \\ mean\left(\left[x_{(1,D)}^{g}, \dots., x_{(i,D)}^{g}, \dots, x_{(N,D)}^{g}\right]\right) \end{bmatrix}^T \tag{3.18}$$

This is effectively given as:

$$M^g = \left[m_1^g, m_2^g, \dots\dots, m_j^g, \dots, m_D^g\right] \tag{3.19}$$

The learner with the minimum objective function value is considered as the teacher. The teacher phase makes the algorithm proceed by shifting the mean of the learners towards its teacher. To obtain a new set of improved learners, a random weighted differential vector is formed from the current mean and the desired mean parameters and added to the existing population of learners.

$$Xnew_{(i)}^g = \left[x_{(i)}^g + rand * \left(X_{teacher}^g - M^g\right)\right] \tag{3.20}$$

The superior learners in the matrix $Xnew$ replace the inferior learners in the matrix X using the non-dominated sorting algorithm [29].

- ***Proposed Modification in MOTLBO algorithm***

The modification is done in this phase (Teacher phase) of MOTLBO based on the fact that along with teacher, learners also put in effort in improving the mean result of class. This will improve the convergence in getting good optimal solutions.

$$Xnew_{(i)}^g = \left[x_{(i)}^g + rand * \left(X_{teacher}^g - T_F M^g\right) + +rand * \left(x_{(i)}^g - M^g\right)\right] \tag{3.21}$$

- ***Learner phase***

In this phase, the process of mutual interaction tends to increase the knowledge of the learner. For a given learner $X_{(i)}^g$, another learner $X_{(r)}^g$ is randomly selected $(i \neq r)$. The ith parameter of the matrix $Xnew$ in the learner phase is given as:

$$Xnew_{(i)}^g = \begin{cases} X_{(i)}^g + rand * \left(X_{(i)}^g - X_{(r)}^g\right) & if (Y_i^g < Y_r^g) \\ X_{(i)}^g + rand * \left(X_{(r)}^g - X_{(i)}^g\right) & otherwise \end{cases} \tag{3.22}$$

The PeMOTLBO algorithm, due to the multi-objective requirements, adapts to the scenario by having multiple $Xnew$ matrices in the learner phase, one for each objective. So, the learner phase operations for a dual objective problem are as shown in equations below.

$$Xnew_{(i)}^{g}\Big|_{a} = \begin{Bmatrix} X_{(i)}^{g}+rand*\left(X_{(i)}^{g}-X_{(r)}^{g}\right) & if\left(Ya_{i}^{g}<Ya_{r}^{g}\right) \\ X_{(i)}^{g}+rand*\left(X_{(i)}^{g}-X_{(r)}^{g}\right) & otherwise \end{Bmatrix} \quad (3.23)$$

$$Xnew_{(i)}^{g}\Big|_{b} = \begin{Bmatrix} X_{(i)}^{g}+rand*\left(X_{(i)}^{g}-X_{(r)}^{g}\right) & if\left(Yb_{i}^{g}<Yb_{r}^{g}\right) \\ X_{(i)}^{g}+rand*\left(X_{(r)}^{g}-X_{(i)}^{g}\right) & otherwise \end{Bmatrix} \quad (3.24)$$

The X and $Xnew$ matrices are passed together to the non-dominated sorting algorithm and only the best learners are selected for the next iteration. The algorithm is terminated after G iterations. Final set of learners represent the pareto optimal solutions.

- ***Best compromise solution based on fuzzy set theory***

For the purpose of decision-making, a best compromise solution is computed using a technique based on fuzzy set theory.

$$\mu_i = \begin{cases} 1, & F_i = F_i^{min} \\ \frac{F_i^{max}-F_i}{F_i^{max}-F_i^{min}}, & F_i^{min} < F_i < F_i^{max} \\ 0, & F_i^{max} = F_i \end{cases} \quad (3.25)$$

The above equation gives a measure of the degree of satisfaction for each objective function for a particular solution. The corresponding membership function for the non-dominated solution k is calculated as follows:

$$\mu^k = \frac{\sum_{i=1}^{No}\mu_i^{ko}}{\sum_{k=1}^{M}\sum_{i=1}^{No}\mu_i^{k}} \quad (3.26)$$

Where

M: Number of Pareto solutions; No: Number of objectives.

The best compromise solution is the one achieving the maximum member ship function.

3.4 Problem formulation

The pareto-based multi-objective technique is used to find trade-off solutions among conflicting objectives. In this chapter, the conflicting objectives considered are active power loss and voltage deviation. The active power loss is reduced with increase in DG size but it may raise the voltage which in turn increase the voltage deviation. Thus , DG planning is formulated as multi-objective problem with location and size of DGs as decision variables.

$$Min\ f1 = (p_{loss}) \tag{3.27}$$

$$Min\ f2 = \sum_{i=1}^{n}(V_i - 1)^2 \tag{3.28}$$

Subject to

$$0 \leq P_{DG} \leq P_{DG}^{max} \tag{3.29}$$

$$V_{imin} \leq V_i \leq V_{imax} \tag{3.30}$$

Where, p_{loss} is the total real power loss in the system, n is the total number of buses, V_i is the voltage magnitude at bus i. P_{DG} is the real power of DG and P_{DG}^{max} is the maximum power of DG. P_{DG}^{max} is 1.2 MW for IEEE 33-bus system and IEEE 69 bus system whereas 2 MW for Indian 85-bus systems [105] to account for higher loss in the system.

3.5 Simulation results and discussions on the test systems

The proposed PeMOTLBO algorithm has been tested on IEEE 33-bus system, IEEE 69-bus system and Indian 85-bus system. The line data and bus data of these systems are given in Appendix. The single line diagrams of these systems are also shown in Appendix. In all cases, negative PQ model is considered for DG and assumed to be working at a power factor of 0.85 lead. The results of proposed method have been compared with prominent multi-objective technique called Non-dominated Sorting Genetic Algorithm (NSGA-II) and basic multi-objective TLBO (MOTLBO). The superiority of the proposed PeMOTLBO has been validated. Various control parameters used in proposed PeMOTLBO and NSGA-II algorithm are given in Table 3.1. For ease of comparison the same population size and iterations are considered in NSGA-II, MOTLBO and PeMOTLBO algorithms. The proposed algorithm for DERs planning model is coded using MATLAB programming and all the simulations are carried out on a personal computer with an i5 processor, speed of 2.53GHz and memory of 4GB RAM.

Table 3.1 Control parameters for TLBO and NSGA-II algorithms

TLBO [37]	NSGA-II [40]
Population size=30 Maximum no. of iterations=150 Max. runs=30	Population size=30 Maximum no. of iterations=150 Max. runs=30 Cross over probability-0.9 Mutation probability-0.1

Figure 3.3, Figure 3.4 and Figure 3.5 shows the improvement in voltage profile with increase in DG units in the IEEE 33-bus, IEEE 69-bus system and Indian 85-bus system respectively. It is observed that the voltage at the buses tends to increase with the increase in penetration level of DG power in the systems considered. The maximum penetration of each DG is considered to be same for respective system. In case of four DG, average voltage profile of the system is reached nearly to the sub-station's voltage i.e., 1p.u.

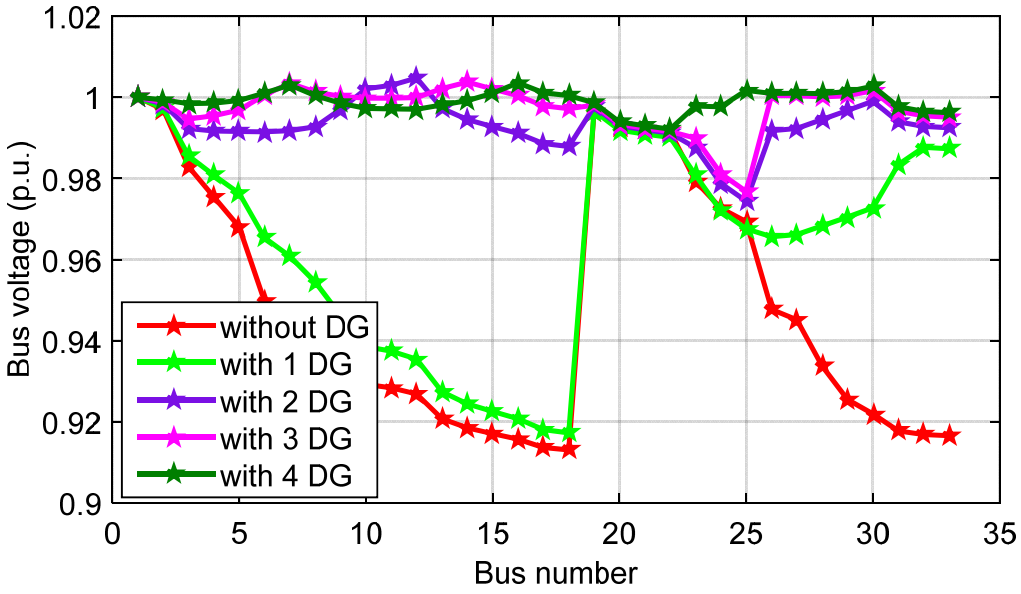

Figure 3.3: IEEE 33-bus system: Voltage profile of the system for different DG case

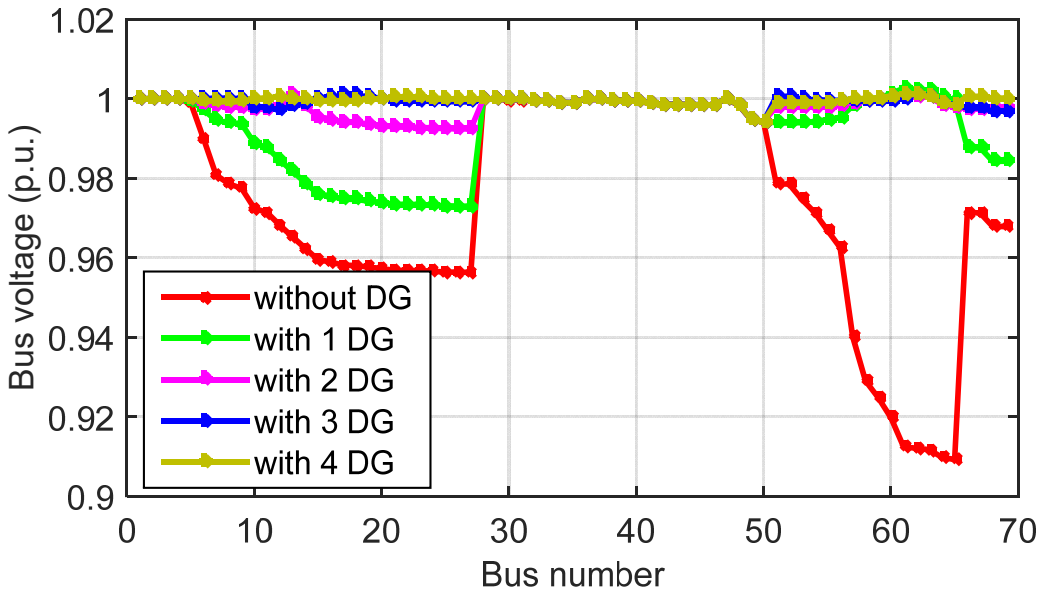

Figure 3.4: IEEE 69-bus system: Voltage profile of the system for different DG case

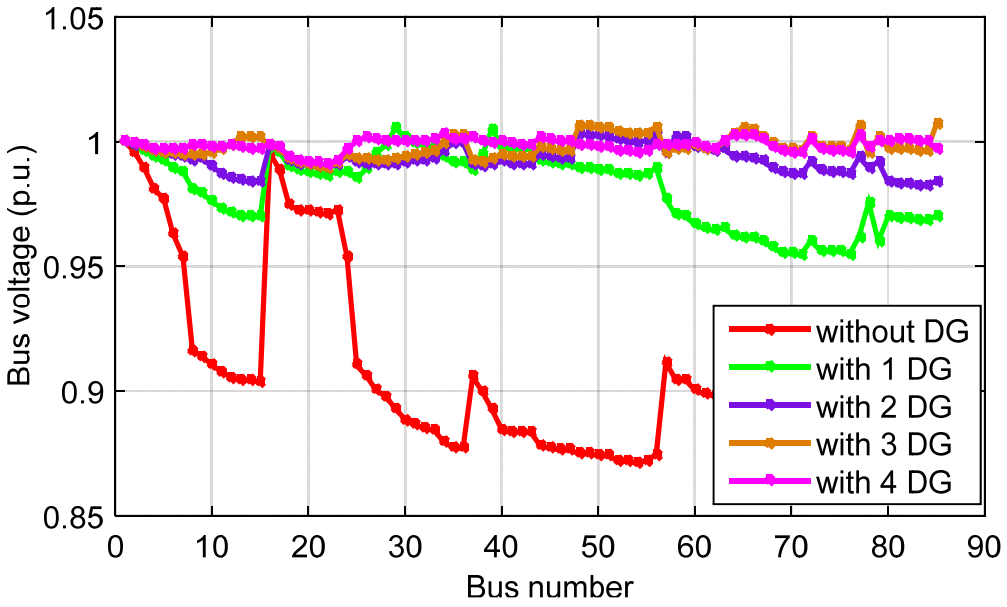

Figure 3.5: Indian 85-bus system: Voltage profile of the system for different DG case.

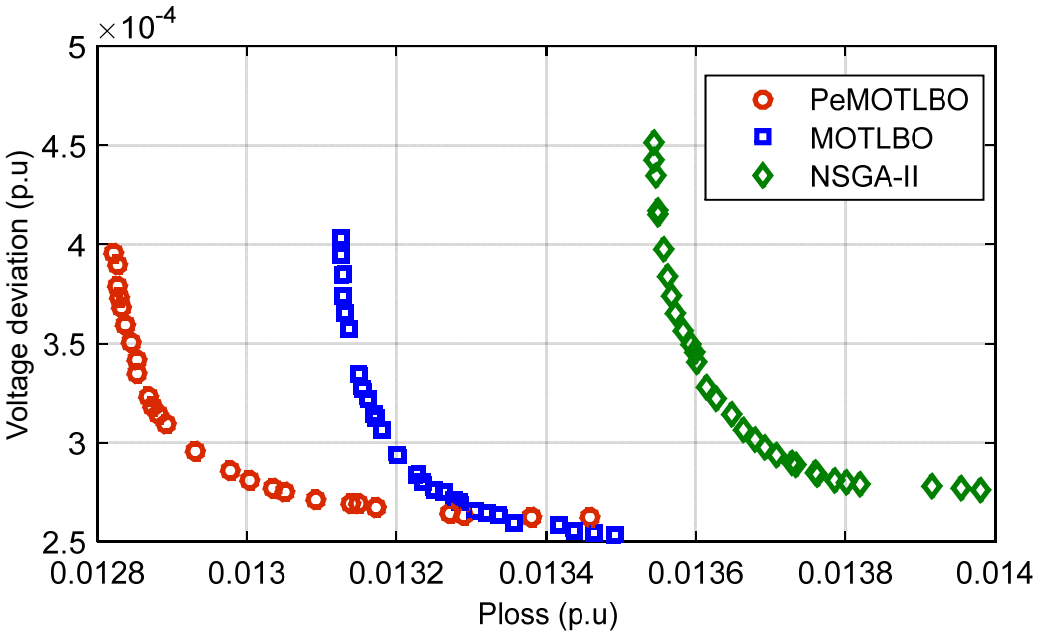

Figure 3.6: IEEE 33- bus system: Pareto optimal fronts of PeMOTLBO, MOTLBO and NSGA-II

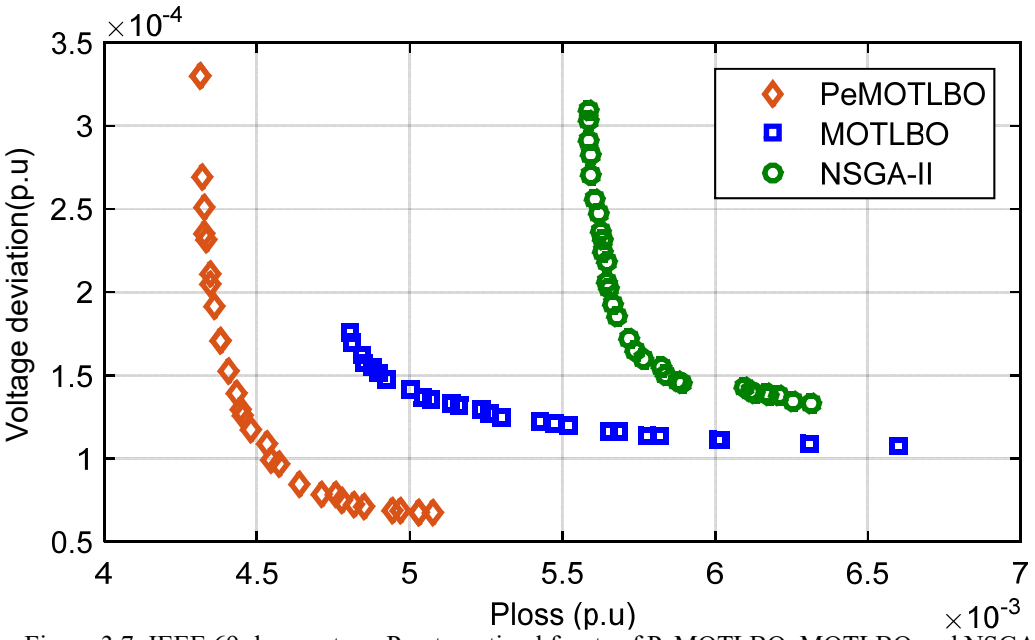

Figure 3.7: IEEE 69- bus system: Pareto optimal fronts of PeMOTLBO, MOTLBO and NSGA-II

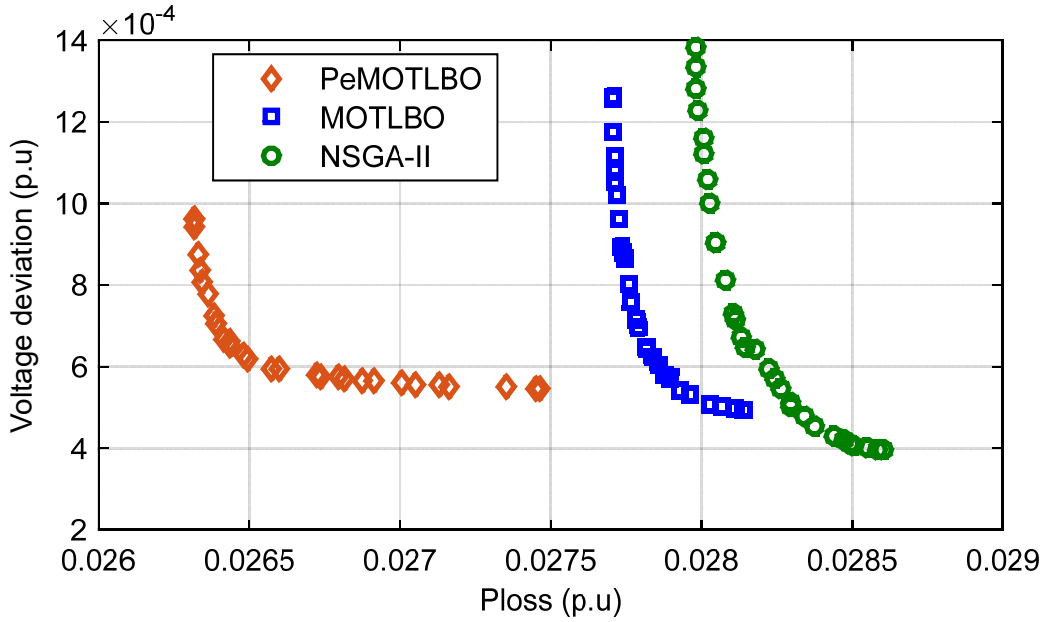

Figure 3.8: Indian 85-Bus system: Pareto optimal fronts of PeMOTLBO, MOTLBO and NSGA-II

The variation in voltage profile and the losses have been studied by increasing DG from one unit to four units. Table 3.2 shows the comparative study of proposed PeMOTLBO algorithm for different DG cases for IEEE 33-bus system. The locations and size of DGs for various DG numbers have been optimized by proposed PEMOTLBO algorithm and it is shown in Table 3.2. It is observed that with two DGs of capacity 2.20083 MW at buses 30

and 12, the system gives better voltage profile of 0.9744 p.u. with loss reduction of 79.2%. However, connecting 1 MW or 2 MW at one or two places with any DG technology imposes difficulty as they generate power on a small scale. Therefore, it is better to go for a reasonable number of DG units with limited size, which may reduce the cost. For analysis purpose, the system is tested by connecting 3 DGs and 4 DGs and there is considerable reduction in total real power loss and further improvement in voltage profile. Similarly in Table 3.3, it is observed that with one DG of capacity 1.9534 MW at bus 61, the IEEE 69-bus system gives better voltage profile of 0.9730p.u with loss reduction of 89.3% and Table 3.4 shows the comparative study for Indian 85-bus system where with one DG of capacity 2 MW at bus 28 gives a voltage profile of 0.9551 and with loss reduced to 73.1%. IEEE 69-bus system and Indian 85-bus system are also analyzed for up to four DG cases. The pareto optimal solutions of PeMOTLBO, MOTLBO and NSGA-II for four DG case have been compared and it is shown in Figure 3.6, Figure 3.7 and Figure 3.8 for IEEE 33-bus system, IEEE 69-bus system and Indian 85-bus system respectively. It is perceived that the pareto front of PeMOTLBO dominates the base algorithm MOTLBO and NSGA-II. This shows the superiority of the proposed algorithm in terms of both better objectives and diversity among the solutions within the optimal fronts. Among the 30 pareto optimal solutions obtained, one solution with the best compromise between the two functions is explored by using fuzzy set theory approach from the pareto front. Based on its output, the solutions are selected and tabulated in Table 3.5, Table 3.6 and Table 3.7 for comparison with NSGA-II and MOTLBO methods.

Table 3.2 IEEE 33-Bus system: Comparison of proposed PeMOTLBO results without and with DG

Performance Quality	Without DG	With 1 DG	With 2 DG	With 3 DG	With 4 DG
DG location (Bus number)	-	31	30,12	30,14,7	7,30,16,25
DG size (MW)	-	1.2	1.2 1.0083	1.0241 0.5268 0.9965	0.8563 1.0050 0.4802 0.7426
P_{loss}(p.u)	0.2027	0.1129	0.0422	0.0298	0.0128
% loss reduction	-	44.3	79.2	85.3	93.6
Worst voltage (p.u)	0.9131	0.9173	0.9744	0.9768	0.9922
Best voltage (p.u)	1.0000	1.0000	1.0048	1.0038	1.0036
Voltage deviation(p.u)	0.1171	0.0650	0.0024	0.0011	0.0003

Table 3.3 IEEE 69-Bus system: Comparison of proposed PeMOTLBO results without and with DGs

Performance Quality	Without DG	With 1 DG	With 2 DG	With 3 DG	With 4DG
DG location (Bus number)	-	61	13,61	51,17,62	21,67,61,12
DG size (MW)	-	1.9534	0.8068 1.7787	0.6207 0.4871 1.7073	0.3130 0.2994 1.7547 0.3007
P_{loss}(p.u)	0.2247	0.0240	0.0097	0.0077	0.0048
% loss reduction	-	89.3	95.7	96.6	97.9
Worst voltage (p.u)	0.9092	0.9730	0.9924	0.9943	0.9943
Best voltage (p.u)	1.0000	1.0026	1.0010	1.0011	1.0012
Voltage deviation(p.u)	0.0992	0.0113	0.0004	0.0001	0.0001

Table 3.4 Indian 85-Bus system: Comparison of proposed PeMOTLBO results without and with DGs

Performance Quality	Without DG	With 1 DG	With 2 DG	With 3 DG	With 4DG
DG location (Bus number)	-	28	48,58	77,85,48	64,34,26,82
DG size (MW)	-	2	0.8230 1.6266	0.9443 0.5755 0.8431	0.7661 0.7010 0.6656 0.3868
P_{loss}(p.u)	0.3163	0.0851	0.0458	0.0398	0.0269
% loss reduction	-	73.1	85.5	87.4	91.5
Worst voltage (p.u)	0.8713	0.9551	0.9826	0.9897	0.9907
Best voltage (p.u)	1.0000	1.0062	1.0030	1.0068	1.0029
Voltage deviation(p.u)	0.1287	0.0538	0.0039	0.0024	0.0008

Table 3.5 IEEE 33-bus system: Comparison of proposed PeMOTLBO with MOTLBO and NSGA-II for 4 DG case

Method	DG location (bus number) and size (MW)				Worst voltage (p.u)	P_{loss} (p.u)
NSGA-II [40]	31	14	8	25	0.9178	0.0151
	0.9178	0.4688	0.8602	0.8361		
MOTLBO [37]	8	14	30	25	0.9921	0.0132
	0.6511	0.5070	1.0508	0.7565		
Proposed PeMOTLBO	7	30	16	25	0.9922	0.0129
	0.8563	1.0050	0.4802	0.7426		

Table 3.6 IEEE 69-bus system: Comparison of proposed PeMOTLBO with MOTLBO and NSGA-II for 4 DG case

Method	DG location (bus number) and size (MW)				Worst voltage (p.u)	P_{loss} (p.u)
NSGA-II [40]	61	50	51	25	0.9944	0.0057
	1.7304	0.7916	0.7202	0.3928		
MOTLBO [37]	49	15	26	61	0.9965	0.0053
	0.8441	0.5013	0.0926	1.8261		
Proposed PeMOTLBO	21	67	61	12	0.9943	0.0048
	0.3130	0.2994	1.7547	0.3007		

Table 3.7 Indian 85-Bus system: Comparison of proposed PeMOTLBO with MOTLBO and NSGA-II for 4 DG case

Method	DG location (bus number) and size (MW)				Worst voltage (p.u)	P_{loss} (p.u)
NSGA-II [40]	12	19	68	34	0.9941	0.0281
	0.6252	0.4173	0.8060	0.9151		
MOTLBO [37]	79	8	34	80	0.9898	0.0278
	0.5625	0.9378	0.7791	0.3421		
Proposed PeMOTLBO	64	34	26	82	0.9907	0.0269
	0.7661	0.7010	0.6656	0.3868		

3.5.1 Performance Metrics Comparison of proposed PeMOTLBO with NSGA-II

In any multi-objective optimization, the basic goals to be achieved are i) To find solutions close to the pareto optimal and ii) To identify a solution as diverse as possible in the non-dominated front. The performance of the proposed algorithm is evaluated with two metrics (one evaluating the progress towards the true pareto-optimal front and the other evaluating the spread of solutions) that tests both the goals. True pareto front for most of the engineering problems are not defined, the better pareto solutions set on comparison is considered as true pareto front. In this thesis, set coverage metric for first goal and spacing metric for second have been considered. To compare the proposed PeMOTLBO method with robust NSGA-II, both the algorithms are executed for 30 independent runs. Box plot is used to show the quality of results obtained with these metrics.

3.5.1.1 Set coverage metric

This metric can be used to get an idea of the relative spread of solutions between two sets of solution vectors A and B. The set coverage metric $C(A,B)$ calculates the proportion of solutions in B, which are weakly dominated by solutions of A:

$$C(A,B) = \frac{|\{b \in B \exists a \in A : a \preccurlyeq b\}|}{|B|} \tag{3.31}$$

Since the domination operator is not a symmetric operator $C(A,B)$ is not necessarily equal to 1- $C(B,A)$. Thus, it is necessary to calculate both $C(A,B)$ and $C(B,A)$ to calculate how many solutions of A are covered by B and vice-versa.

Box plot: For a pair of $C(A,B)$ there are 30 C-metric values for 30 independent runs. This box plot can be used to visualize the distribution of C-metric values. The upper and lower end of the box corresponds to 75th and 25th percentiles and central portion is the median. Figure 3.9, Figure 3.10 and Figure 3.11 are the box plot of C-metric values for IEEE 33-bus, IEEE 69-bus and Indian 85-bus systems respectively. The left boxes in the box plot correspond to average distribution of C-metric values of proposed method i.e. Ic (PeMOTLBO, NSGA-II) where C-metric values of PeMOTLBO are not weakly dominated by NSGA-II and it shows the probability of PeMOTLBO dominating NSGA-II is more, which shows the superiority of proposed algorithm. Table 3.8 reveals that there is significant difference of average coverage metric values (Ic) between PeMOTLBO and NSGA-II in all the systems considered.

Table 3.8 C-Metric: Mean value, standard deviation of proposed PeMOTLBO and NSGA-II

Test systems	Methods	Mean	Standard deviation
IEEE 33-Bus system	**Proposed PeMOTLBO**	0.7211	0.3982
	NSGA-II [40]	0.1833	0.3758
IEEE 69- Bus system	**Proposed PeMOTLBO**	0.7744	0.3984
	NSGA-II [40]	0.1267	0.2970
Indian 85-Bus system	**Proposed PeMOTLBO**	0.6067	0.3572
	NSGA-II [40]	0.1233	0.2811

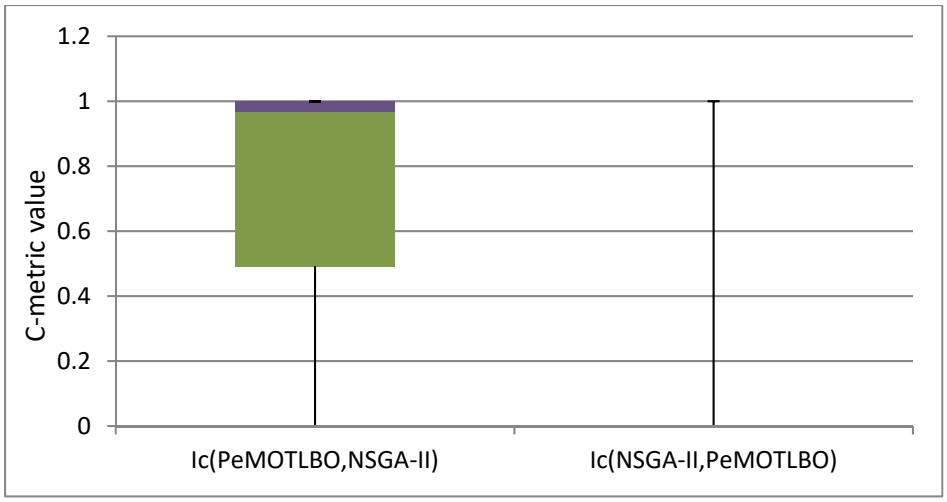

Figure 3.9: IEEE 33-bus system - Box plot of C-metric value

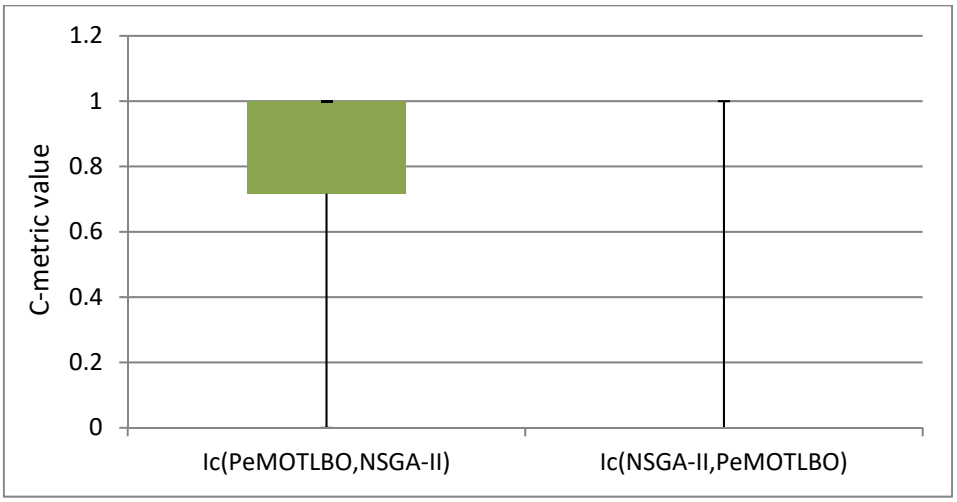

Figure 3.10: IEEE 69 -bus system - Box plot of C-metric value

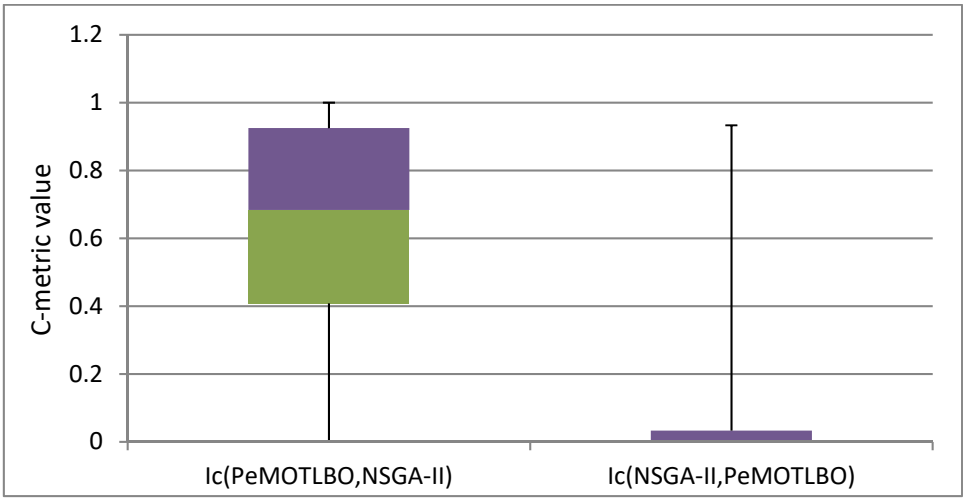

Figure 3.11: Indian 85-bus system - Box plot of C-metric value

3.5.1.2 Spacing metric

This metric is to find the diversity among the non-dominated solutions. This measures the relative distance between consecutive solutions in the obtained non-dominated set.

$$S = \sqrt{\frac{1}{|Q|}\sum_{I=1}^{|Q|}\left(d_i - \bar{d}\right)^2} \tag{3.32}$$

Where $d_i = min_{k\in Q \wedge k\neq i}\sum_{m=1}^{M}\left|f_m^i - f_m^k\right|$ and $\bar{d}$ is the mean value of the above distance measure $\bar{d} = \sum_{i=1}^{|Q|} d_i/|Q|$. The distance is the minimum value of the sum of the absolute difference in objective function values between the i^{th} solution and any other solution in the obtained non-dominated set. If S value is zero, it shows that all the non-dominated solutions in the pareto front are equidistantly spaced. Figure 3.12, Figure 3.13 and Figure 3.14 show the distribution of space metric values for IEEE 33-bus system, IEEE 69-bus system and Indian 85-bus systems respectively and the difference noted is highly significant in favor of the proposed PeMOTLBO method. The spread of space metric values is close to the zero in case of proposed method which implies, the solutions in the pareto obtained are equidistantly placed with each other. The comparison of s-metric values of proposed PeMOTLBO and NSGA-II methods are tabulated in Table 3.9.

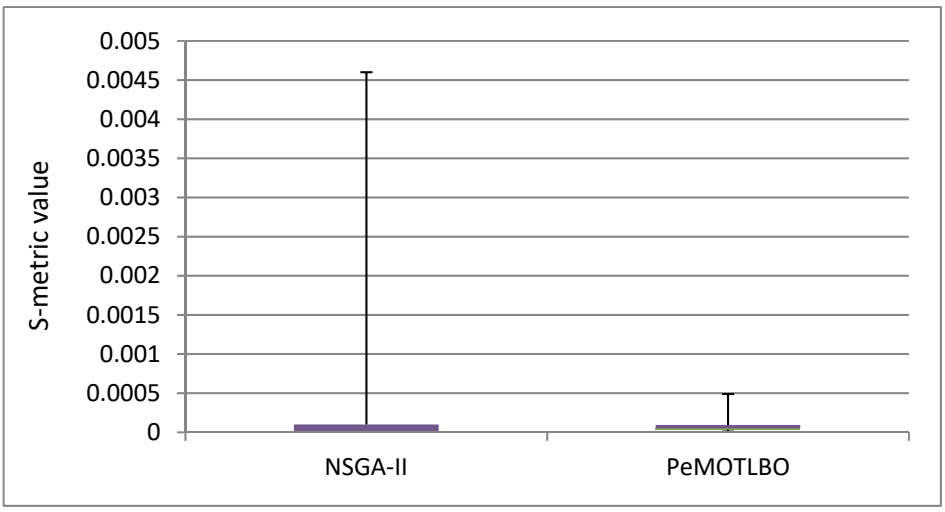

Figure 3.12: IEEE 33-bus system- Box plot of S-metric values

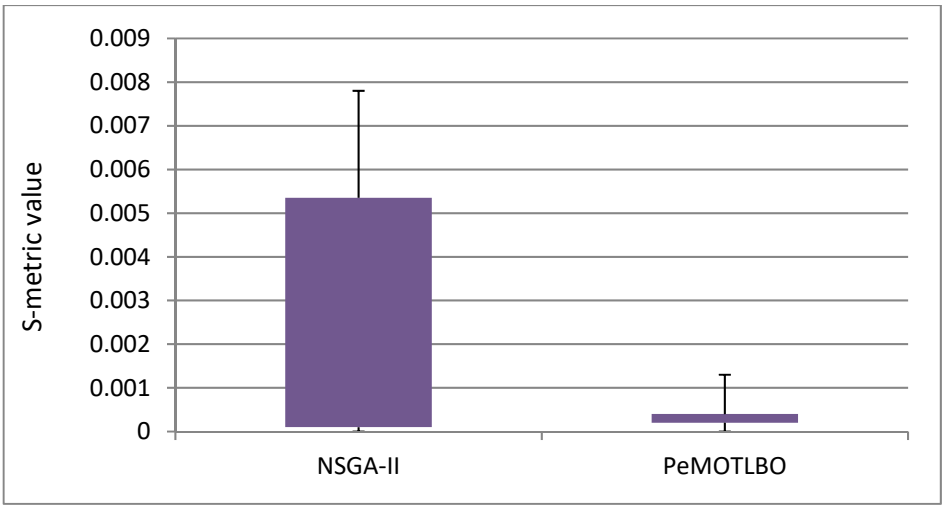

Figure 3.13: IEEE 69-bus system- Box plot of S-metric values

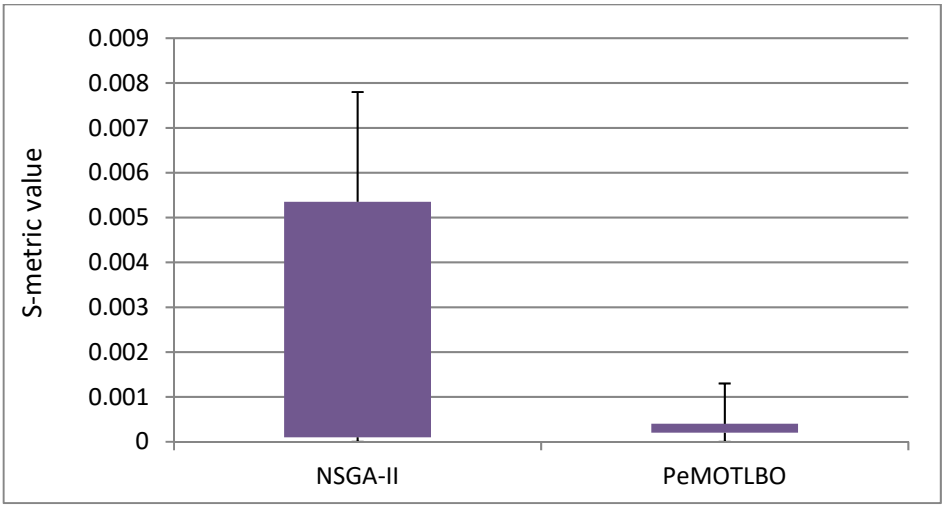

Figure 3.14: Indian 85-bus system- Box plot of S-metric values

Table 3.9 S-Metric: Mean vale, standard deviation of Proposed PeMOTLBO and NSGA-II

Test systems	Methods	Mean	Standard deviation
IEEE 33-Bus system	**Proposed PeMOTLBO**	$9.945*10^{-5}$	$1.2099*10^{-4}$
	NSGA-II [40]	$7.5987*10^{-4}$	0.0014
IEEE 69-Bus system	**Proposed PeMOTLBO**	$9.5077*10^{-6}$	$1.1202*10^{-5}$
	NSGA-II [40]	$5.2652*10^{-4}$	$7.8914*10^{-4}$
Indian 85-Bus system	**Proposed PeMOTLBO**	$3.1151*10^{-4}$	$2.8314*10^{-4}$
	NSGA-II [40]	0.0019	0.0028

3.6 Summary

In conclusion, to consolidate the contribution made, this chapter attempted to answer the problem of optimal placement and sizing of DG units on distribution systems as multi-objective problem with new algorithm. A new variant of TLBO algorithm has been proposed for optimization purpose. The proposed peer enhanced teaching-learning based optimization (PeMOTLBO) is employed to find a set of pareto optimal solutions for planning of DG in a distribution system and fuzzy set theory approach has been used to find the best compromising DG location and size. The effectiveness of the proposed method is tested on IEEE 33-bus, IEEE 69-bus distribution system and Indian 85-bus distribution system. The pareto front obtained by the proposed PeMOTLBO has been compared with basic MOTLBO and NSGA-II and a qualitative comparison is also made with well-known NSGA-II method. The comparison shown the superiority of the proposed algorithm in terms of both better objectives and diversity among the solutions in the optimal fronts obtained. Two performance metrics have been evaluated to ascertain two goals of the multi-objective optimization and the proposed technique exhibited better metric value compared to NSGA-II.

Chapter 4

Optimal Planning of Active Distribution Network Operation with hybrid Distributed Energy Resources using Grid-based Multi-Objective Harmony Search Algorithm

Chapter 4

4 Optimal Planning of Active Distribution Network Operation with hybrid Distributed Energy Resources using Grid-based Multi-Objective Harmony Search Algorithm

4.1 Introduction

In this chapter, an efficient Grid-based Multi-objective Harmony Search (GrMHS) algorithm is proposed for planning and operation of Distributed Generation (DG) in active distribution network. This grid based multi-objective algorithms establishes coordinate system (grid) with dimension of number of considered objectives for plotting the locations of objective values in the objective plane. These DG technologies include both dispatchable and non-dispatchable (renewable) distributed energy resources. The optimal mix of these DERs and location of renewable and non-renewable DG sources has to be identified to make use of the potential benefits of their connection in the distribution network. Particularly, when connecting intermittent sources like wind and solar will lead to various technical challenges to sustain the reliable and secured operation of distribution system. The location and size of fuel based distributed generation are optimized using proposed grid based harmony search algorithm where a grid-based strategy has been embedded in multi-objective optimization as a secondary selection criterion instead of crowding distance. The proposed algorithm is tested for two and three objective cases of DERs planning in distribution network. The planning model identifies the optimal mix of renewable and dispatchable DGs by minimizing three conflicting objectives viz., i) Energy loss, ii) Voltage deviation and iii) Cost of DG integration in the distribution network. Moreover, the proposed model serves to be more realistic for planning as it considered all uncertainties associated with load, electricity price, wind speed and solar irradiance. This chapter also analysed the limitation on locating the renewable sources in the autonomous active distribution network operation. This has been enforced by adding constraints on the bus limits for renewable source connection. The autonomous operation of active distribution network operation is analysed with additional

battery storage sources connected to the system to support the loads, as there is no grid support in the autonomous system operation.

4.2 Proposed Grid based Multi-Objective Harmony Search (GrMHS) Algorithm

Harmony Search (HS) algorithm is a Meta heuristic optimization algorithm inspired from the improvisation process of music in search of perfect harmony [96]. HS algorithm is simple, converges faster and more efficient in searching optimal solution among other heuristic algorithms. On the other side, a grid-based dominance strategy has been proposed as secondary selection criterion in multi-objective formulation using GA [97] and it is claimed to be better in terms of convergence and diversity of solutions when compared to NSGA-II and SPEA (Strength Pareto Evolutionary Algorithm) techniques. Since multi-objective form of harmony search algorithm is found to be better when compared with NSGA-II [98] for DG planning problem, the idea of applying grid based dominance strategy in multi-objective optimisation using harmony search algorithm is attempted and Grid based Multi-objective Harmony Search (GrMHS) algorithm is proposed for DG planning in this chapter. The results are found promising in terms of better optimal solutions. Before entering the procedural steps of proposed GrMHS algorithm, a few necessary definitions and concepts are introduced below:

4.2.1 Definitions and concepts

In GrMHS, grid coordinates are used to locate individuals in the objective space. To set the grid structure of k^{th} objective, minimum and maximum values of k^{th} objective are found in the entire population P and it is denoted as $P_m^{\min}$and $P_m^{\max}$ respectively. Then, the lower and upper limits of the grid in the kth objective are determined as follows:

$$ll_k = P_m^{\min} - (P_m^{\max} - P_m^{\min}) / (2 * div) \quad (4.1)$$

$$ul_k = P_m^{\max} + (P_m^{\max} - P_m^{\min}) / (2 * div) \quad (4.2)$$

Where div refers to the number of divisions of the objective space (generally user defined). If there are M objectives, then objective space will be divided into div^M hyper boxes. Thus, the width w_k of hyper box in the k^{th} objective can be given as:

$$w_k = (ul_k - ll_k) / div \tag{4.3}$$

The grid coordinates of individual in the k^{th} objective is calculated as:

$$G_k(x) = \lfloor (f_k(x) - ll_k) / w_k \rfloor \tag{4.4}$$

Where $\lfloor . \rfloor$ denotes the floor function, $G_k(x)$ is the grid coordinates of individual x in the k^{th} objective and $f_k(x)$ is the actual objective value in the k^{th} objective.

Grid dominance: Let $x, y \in P, x \prec_{grid} y :\Leftrightarrow$

$$\forall i \in (1,2,....,M) : G_i(x) \le G_i(y) \wedge$$
$$\forall j \in (1,2,....,M) : G_j(x) \le G_j(y) \tag{4.5}$$

Where $x \prec_{grid} y$ denotes that x grid-dominates y , M is the number of objectives.

Grid difference: Let $x, y \in P$, the grid difference between them is denoted as

$$GD(x, y) = \sum_{k=1}^{M} |G_k(x) - G_k(y)| \tag{4.6}$$

4.2.2 Fitness calculation

Unlike single secondary selection criterion, in NSGA-II, for evolving populations to have an optimum value, GrMHS considers three grid-based criteria to select individual with better fitness. They are grid ranking (GR), grid crowding distance (GCD) and the grid coordinate point distance (GCPD). GR and GCPD are used to evaluate convergence of the pareto solutions while GCD is concerned with the diversity of individuals within the pareto front.

GR is defined as the summation of its grid coordinates in each objective

$$GR(x) = \sum_{k=1}^{M} G_k(x) \tag{4.7}$$

Density estimation of solutions is taken care of by the GCD by considering the distribution of neighbours of a solution and it is given by

$$GCD(x) = \sum_{y \in N(x)} (M - GD(x, y)) \tag{4.8}$$

Where $N(x)$ is the set of neighbours of x and solution y is regarded as neighbour of solution x if grid difference, $GD(x,y) < M$.

The Euclidian distance between an individual and the best corner solution of its hyper box is called GCPD and it is calculated as follows:

$$GCPD(x) = \sqrt{\sum_{k=1}^{M} \left(\left(F_k(x) - (lb_k + G_k(x) \times d_k) \right) / d_k \right)^2} \tag{4.9}$$

4.2.3 Framework of proposed Grid based Multi-Objective Harmony Search (GrMHS) algorithm

The framework of the proposed GrMHS algorithm is explained in the following steps:

Step 1: Input algorithm parameters such as the Harmony Memory Considering Rate (HMCR), distance bandwidth (bw) and Pitch Adjusting Rate (PAR) and limits on decision variables.

Step 2: Initialization of randomly generated population.

$$P \leftarrow Initialize \quad (P)_{N*D}$$

Where, N-Population size; D-Number of decision variable.

Step 3: Evaluate the objectives for the initialized population

Step 4: While termination criteria is not met **do**

Step 5: Harmony search improvisation process on the decision variables.

For all p $\in P$
For all d $\in D$
Generate random number rand ()
If rand () < HMCR
select a solution x_i from the existing population
If rand () < PAR
$x_i^{new} = x_i + rand \ () * bw$
End if
else
x_i^{new} is randomly generated
End if
End for
End for
P^{new} is new population

Step 6: Intermediate population formation

$$P' \leftarrow P \bigcup P^{new}$$

Step 7: Environmental selection (P') /* Detailed procedure can be referred in [97]*/

Step 8: end while */* *Step 4* */*

Step 9: Return final population P i.e. pareto optimal solutions

Step 10: Fuzzy set theory is used to select the best solution from the pareto solutions.

$$\mu_i = \begin{cases} 1 & F_i = F_i^{\min} \\ \dfrac{F_i^{\max} - F_i}{F_i^{\max} - F_i^{\min}} & F_i^{\min} < F_i < F_i^{\max} \\ 0 & F_i = F_i^{\max} \end{cases} \tag{4.10}$$

Where, μ_i gives the degree of satisfaction of each objective function.

$$\mu^{k} = \frac{\sum_{i=1}^{NO} \mu_i^{k}}{\sum_{k=1}^{M} \sum_{i=1}^{NO} \mu_i^{k}} \tag{4.11}$$

The best solution is the one with maximum membership function.

4.3 Modeling of generation and load: uncertainties and certainties

The uncertainty models of renewable resources and load are modeled using probability density function (pdf) based on five year wind speed and solar irradiance data [99]. For the ease of computation, each year of the planning period (five years) is divided into four seasons with each season represented by any day within the season presuming similar weather conditions throughout the season. From each season, a typical day's probability distribution of hourly wind speed and solar irradiance is generated using Weibull and beta probability density function respectively. The day representing each season is again divided into 24-hour time segments. So, each year contains 96 time segments (24 hours per day, 1day per season and 4 seasons per year) and for each year, every time segment has to process 90 wind speeds and irradiance data (30 days per month and 3 months per season). For each time segment the mean and standard deviation of those data is calculated and from them the beta and Weibull probability density functions are generated for each hour. These continuous pdfs generated at each segment are further divided into different states to evaluate the power available from each state and summed up to get the total power extracted from wind and solar at the particular hour. The load profile is assumed to follow IEEE-Reliability

Test System profile [106]. The cost of power ($/MW) purchased from the main grid is assumed constant and hence, it depends only on the amount of load supplied from the main grid. The sections that follow present the detailed modeling and processing of probability density functions.

4.3.1 Wind speed modeling

There are various methods to model the wind speed behavior but very often, the recommended expression for wind speed modeling is the Weibull probability density function, which is based on the comparison of actual wind speed profiles at different sites. The wind speed profile estimated using Weibull pdf $(f_w(v))$ is given by

$$f_w(v) = \frac{k}{c}\left(\frac{v}{c}\right)^{k-1} \exp\left[-\left(\frac{v}{c}\right)^{k}\right] \tag{4.12}$$

Where, k is called the shape factor and c is called the scale factor. If k=2 is considered, the corresponding pdf is called Rayleigh pdf. In this work, since the pdf has been built for each time segment, scale and shape factor have to be calculated from the mean ($\bar{u}$) and standard deviation (σ) of wind speed data at each time segment. The expressions for k and c are as follows:

$$k = \left(\frac{\sigma}{\bar{u}}\right)^{-1.086} \tag{4.13}$$

$$c = 1.12\bar{u} \tag{4.14}$$

4.3.2 Solar irradiance modeling

The random phenomenon of solar irradiance data is described using Beta probability density function, which is given by the following:

$$f_b(s) = \begin{cases} \dfrac{\Gamma(\alpha+\beta)}{\Gamma(\alpha)\Gamma(\beta)} * s^{(\alpha-1)} * (1-s)^{(\beta-1)} & ,0 \le s \le 1,\ \alpha \ge 0,\ \beta \ge 0 \\ 0 & ,otherwise \end{cases} \tag{4.15}$$

To calculate the parameters of the Beta distribution function, the mean (μ) and standard deviation (σ) of the random variable i.e. solar irradiance s are utilized as follows:

$$\beta = (1-\mu) * \left(\frac{\mu * (\mu+1)}{\sigma^2} - 1\right) \tag{4.16}$$

$$\alpha = \frac{\mu * \beta}{1 - \mu} \tag{4.17}$$

These Weibull and Beta probability distribution functions evaluated at each time segments are utilized to calculate the power available from wind and solar respectively.

4.3.3 Calculation of power output of the wind turbine and PV module

In order to incorporate the output power of wind-based DG and solar DG units in the planning problem formulation, the continuous pdf generated at each hour has been divided into states (periods), where in each state the solar irradiance and wind speed have been within certain limits. In other words, for each time segment there will be a number of states. In this work, the step is adjusted to be 1m/s for wind speed and 0.1kW/m^2 for solar irradiance since more number of steps will increase complexity in computation while fewer numbers of steps affects accuracy. In this section, the output power of the wind turbine and PV module corresponding to each state will be calculated using the wind turbine power performance curve and PV characteristics respectively. For the sake of simplicity, the average value of each state is utilized to calculate the output power for this state (e.g. for the wind speed, if the 2nd state has the limits 1 m/s and 2 m/s, hence, the average value of this state (va2) =1.5 m/s).

The probability of the wind speed and solar irradiance of DG units for each state during any specific hour is calculated using the following:

$$P_v\{G_w\} = \int_{V_{w1}}^{V_{w2}} f_w(v).dv \tag{4.18}$$

$$P_s\{G_y\} = \int_{S_{y1}}^{S_{y2}} f_b(s).ds \tag{4.19}$$

The hourly average output power of a PV module or a wind turbine is the summation of the power produced at all possible states for this hour multiplied by the corresponding probability of each state. Once the average output power is calculated for each time segment, the average output power is calculated for the typical day in a season and hence, the output of the entire planning period.

4.3.3.1 Calculation of power output of wind turbine

The output power of the wind turbine depends on the wind speed of the site, as well as the parameters of the power performance curve. Therefore, once Weibull pdf is generated for a time segment; the output power during the different states of this segment can be calculated using the following equation.

$$P_w(v_{aw}) = \begin{cases} 0 & 0 \le v_{aw} \le v_{ci} \\ P_{rated} * \dfrac{(v_{aw} - v_{ci})}{(v_r - v_{ci})} & v_{ci} \le v_{aw} \le v_r \\ P_{rated} & v_r \le v_{aw} \le v_{co} \\ 0 & v_{co} \le v_{aw} \end{cases} \tag{4.20}$$

4.3.3.2 Calculation of power output of PV module

The output power of the PV module is dependent on the solar irradiance and ambient temperature of the site as well as the characteristics of the module itself. Depending upon the required amount of solar power penetration, the number of modules are added to the PV panel. Here it is 16000 modules for 1.2 MW of power. The output power during each state in the generated beta pdf is calculated using the following equations:

$$T_{Cy} = T_A + s_{ay}\left(\frac{N_{OT} - 20}{0.8}\right) \tag{4.21}$$

$$I_y = s_{ay}\left\lfloor I_{sc} + K_i(T_{Cy} - 25)\right\rfloor \tag{4.22}$$

$$V_y = V_{oc} - K_v * T_{Cy} \tag{4.23}$$

$$P_{Sy}(s_{ay}) = N * FF * V_y * I_y \tag{4.24}$$

$$FF = \frac{V_{MPP} * I_{MPP}}{V_{oc} * I_{sc}} \tag{4.25}$$

4.3.4 Battery storage model

Lithium Ion battery is considered in this work as frequent switching from charging and discharging does not impose any limitation. At any time, the state of the battery is related to the previous state of the battery irrespective of discharging and charging of the battery. The battery is charged up to SOC^{max} only when the total generation from the renewable sources is greater than the load in the systems and it is mathematically written as:

$$Ebat\,(t) = Ebat\,(t-1) + \left(\left(nw * Pw(t) + ns * Ps(t)\right) - Pload\,(t)\right) * \eta_{ch} \tag{4.26}$$

On the other hand, when the load is greater than the available energy generated, the battery will discharge provided its State of Charge (SOC) is greater than SOC^{min} and is given by:

$$Ebat\ (t) = Ebat\ (t-1) + \left(Pload\ (t) - \left(nw * Pw(t) + ns * Ps(t)\right)\right) * \eta_{disch} \qquad (4.27)$$

Where, $Ebat\ (t)$ and $Ebat(t-1)$ are the available battery capacity at time t and (t-1). The charging and discharging efficiency of the battery are 0.85 and 0.95 respectively.

4.3.5 Load and price modeling

Daily load curve is modelled for each season using the typical demand level factor (DLF) as a percentage of the particular peak load at each bus. The planning period is considered to be 5 years and it is assumed to be a certain percentage of load growth α_g every year. The demand level at every hour of the planning period is modeled as:

$$S^{D}_{i,t,h} = S^{D}_{i,base} * DLF_{i,t,h} * \left(1+\alpha_g\right)^t \qquad (4.28)$$

Where, $DLF_{i,t,h}$ is demand level factor for a typical daily load at every bus in year t. $S^{D}_{i,base}$ is the base load at each bus. The electricity price changes with market operation, which in turn change with the demand level so it is assumed that the electricity price follows the changes in the demand level.

4.4 Problem formulation

This section presents the formulation of the distributed generation planning problem for optimizing three conflicting objectives in an active distribution network. The processing of season wise data and modeling of wind turbine and solar panel can be looked up in [48]. DGs are modelled as a negative load [100]. It can be inferred from section 4.3 that each time segment represents 90h (30 days per month*3 months per season) so, the objective functions and constraints are formulated as follows:

$$F_1 = \sum_{y=1}^{ny} \sum_{h=1}^{96} \left(\sum_{i=1}^{nl} P_{loss} \right) * 90 \qquad (4.29)$$

$$F_2 = \sum_{i=1}^{n} \left(V_i - 1\right)^2 \qquad (4.30)$$

$$F_3 = \left(\sum_{y=1}^{ny} \left(\sum_{h=1}^{96} f_{DE}(P_{DE}) + C_e(p) + OM(p_{DE}) \right) + OM(ren) \right) + C_{inv} \tag{4.31}$$

Where,

$$f_{DE}(P_{DE}) = C_{gasoil} * (a.P_{DE}^{\ 2} + b.P_{DE} + c) \tag{4.32}$$

$$OM_i(P_{DE}) = k_{OMi} * P_{DE} \tag{4.33}$$

$$OM(ren) = K_{WT} * C_{WT} + K_{PV} * C_{PV} + K_{Bat} * C_{Bat} \tag{4.34}$$

$$C_e(p) = \sum_{e=1}^{m} \sum_{i=1}^{ndg} \mu_{ei} * C_{ei} * P_{ei} \tag{4.35}$$

$$C_{inv} = \sum_{i=1}^{ndg} CI_i * CAP_i \tag{4.36}$$

Equality Constraints:

$$P_{load} = P_{diesel} + P_{wind} + P_{pv} \pm P_{bat} \tag{4.37}$$

In-equality constraints:

$$0 \le P_{DG} \le P_{DG}^{\max} \tag{4.38}$$

$$V_{i\min} \le V_i \le V_{i\max} \tag{4.39}$$

Table 4.1 Cost associated with various DER types

DER type	Initial Investment ($/kW)	Annual M&O cost ($/kW)	Emission cost ($/kg)			
			NOx	CO_2	CO	SO_2
DE	500	-	0.28	0.013	0.022	0.131
WT	1600	50	-			
PV	6000	35	-			

4.5 Optimal operation strategy for grid connected and autonomous mode operation of active distribution network

4.5.1 Optimal operation strategy for grid connected mode

The operation strategy procedure for identifying optimum solution in grid-connected mode of operation is depicted in the form of flowchart is shown in Figure 4.1. The cost associated with each DG technology has been presented in Table 4.1.

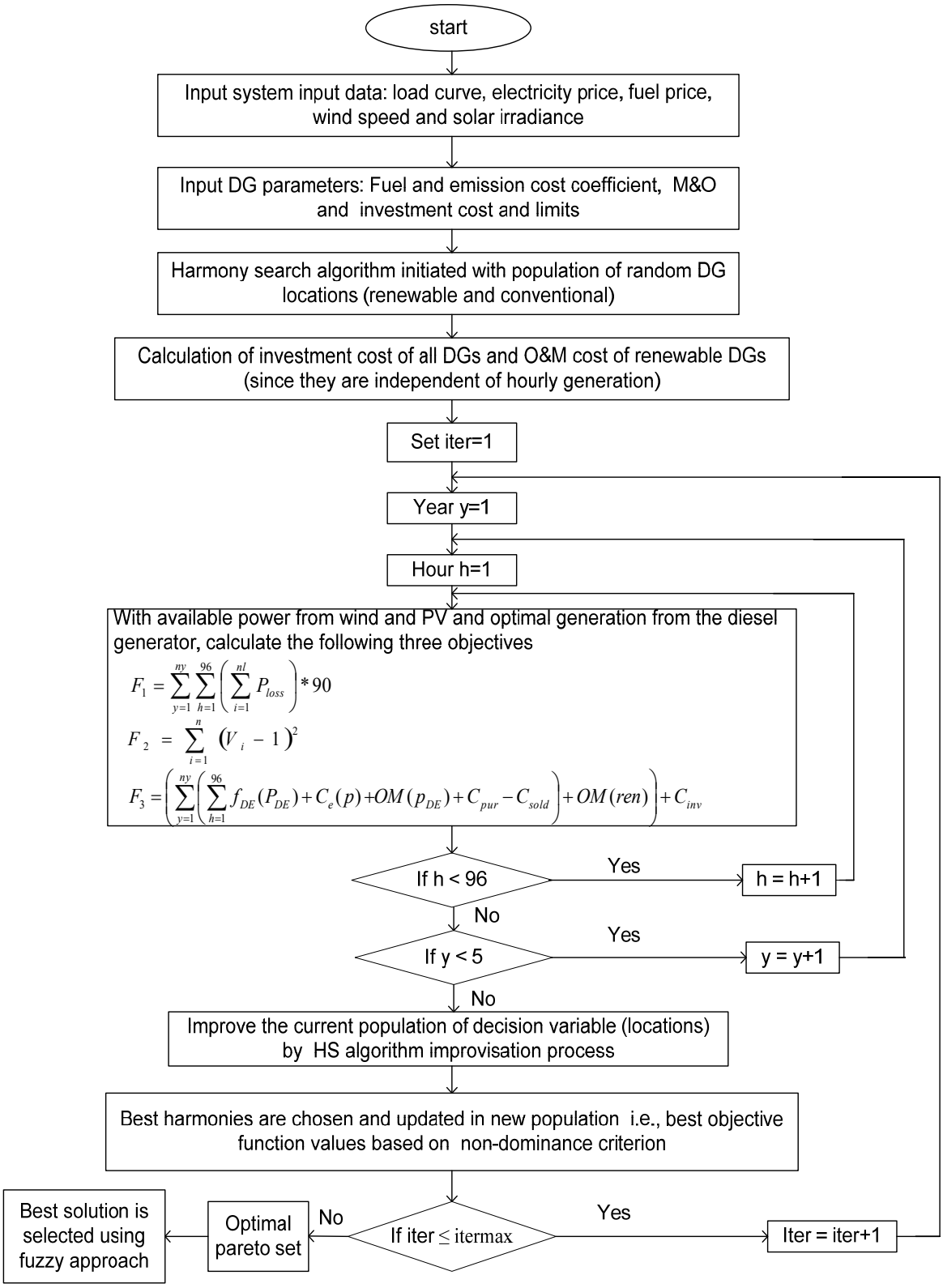

Figure 4.1: The proposed planning strategy for grid connected mode of operation

4.5.2 Optimal operation strategy for autonomous mode

The proposed planning strategy is explained in the flowchart depicted in Figure 4.2 It is clearly perceived from the flowchart that the diesel generator is least preferred to supply the load as its power generating cost is very high due to fuel consumption.

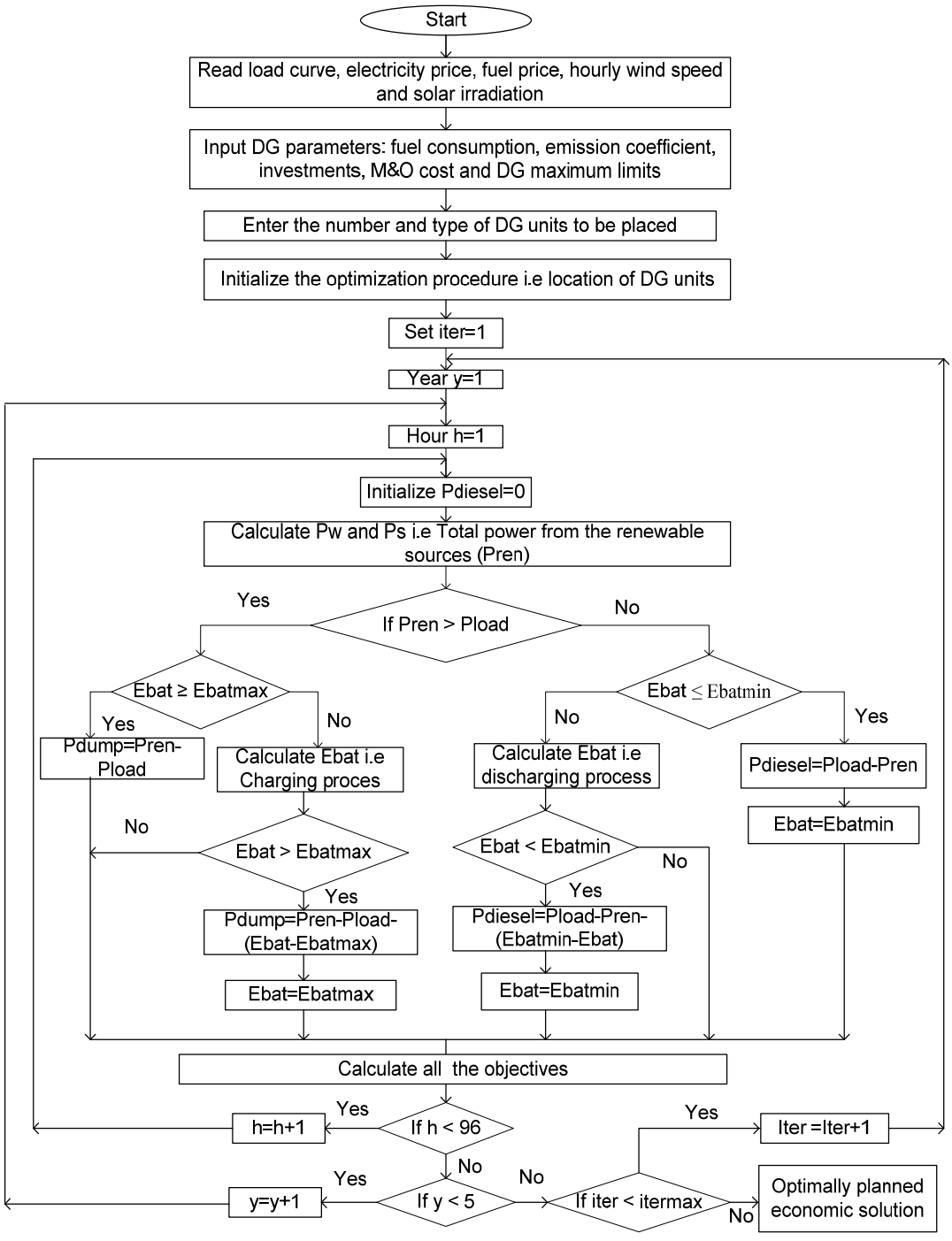

Figure 4.2: The proposed planning and operational strategy for autonomous mode of operation

4.6 Simulation results and discussion

In this section, the active distribution network planning is analyzed for two cases: i) Two objectives: Minimization of active power loss and voltage deviation and ii) Three objectives: Minimization of real power loss, voltage deviation and total cost of DG integration. The proposed GrMHS algorithm is tested on IEEE 33-bus system, IEEE 69-bus system and Indian 85-bus radial distribution system. The proposed algorithm for DERs planning is coded using MATLAB programming and all the simulations are carried out on a personal computer with an i5 processor, speed of 2.53GHz and memory of 4GB RAM. The proposed GrMHS algorithm is executed with 30 populations for a maximum of 100 iterations for all the cases.

4.6.1 Two objectives: Minimization of active power loss and voltage deviation

The proposed GrMHS algorithm is applied for minimizing two conflicting objectives such as active power loss and voltage deviation (similar to section 3.4). For this case, DG is modelled as negative load and assumed to supply real and reactive power to the distribution network. The power factor of DG is assumed as 0.85 lead.

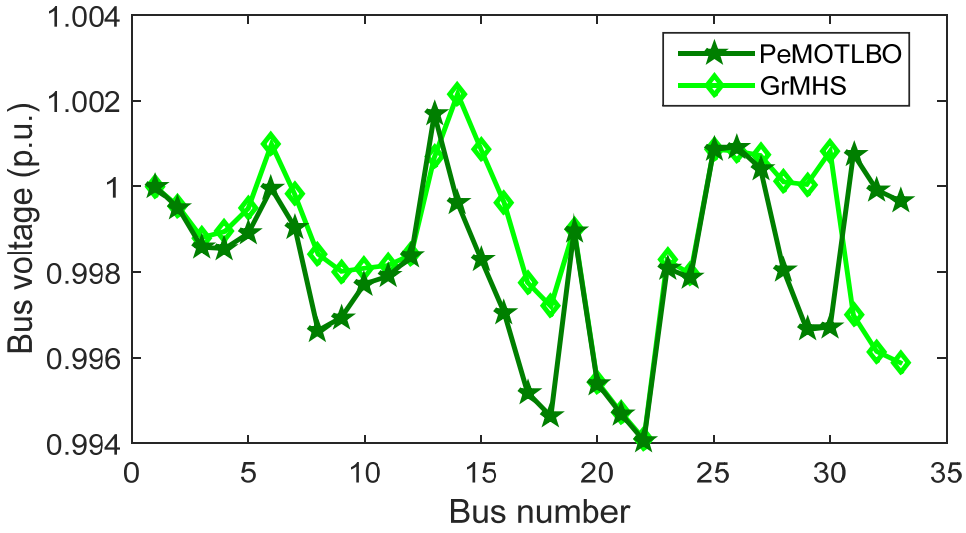

Figure 4.3: IEEE 33-bus system: Comparison of voltage profile with the proposed GrMHS and PeMOTLBO

The effectiveness of the proposed algorithm is demonstrated with IEEE 33-bus system, IEEE 69-bus system and Indian 85-bus distribution respectively. The computation time for the proposed algorithm is also less and it is almost half of the time taken by the PeMOTLBO algorithm proposed in the chapter 3.

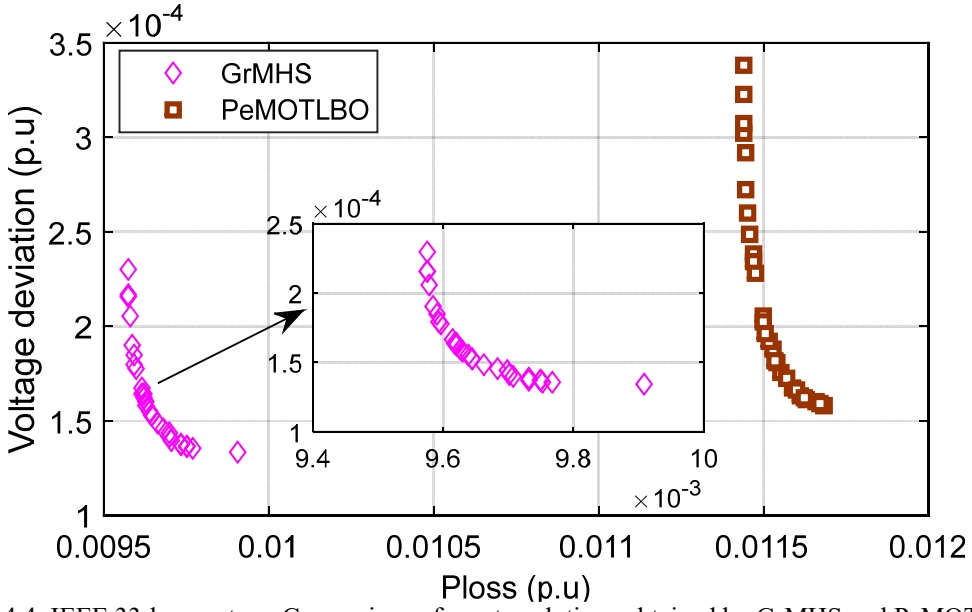

Figure 4.4: IEEE 33-bus system: Comparison of pareto solutions obtained by GrMHS and PeMOTLBO

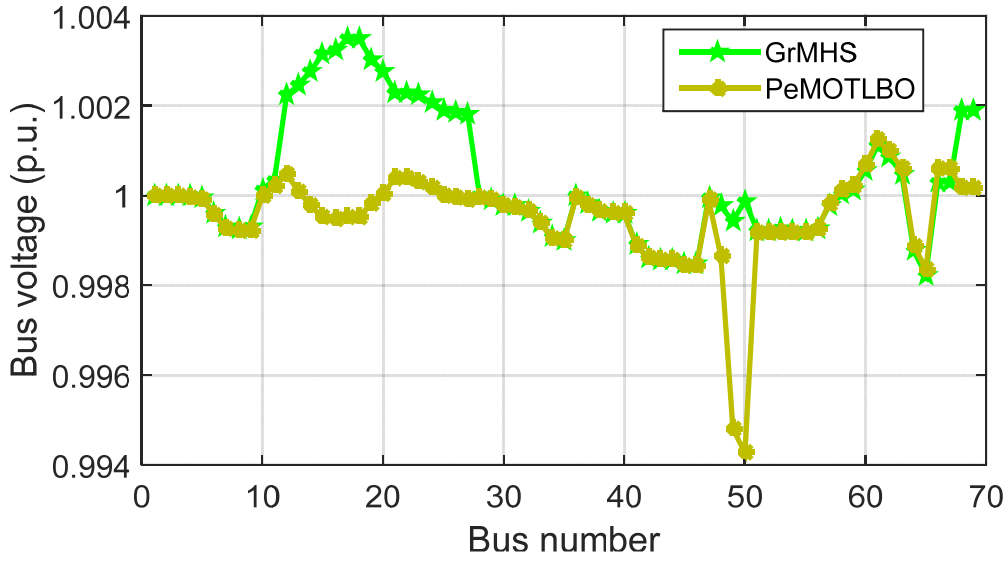

Figure 4.5: IEEE 69-bus system: Comparison of voltage profile with GrMHS and PeMOTLBO

The comparison of voltage profile and the pareto solutions between voltage deviation and active power loss are shown in Figure 4.3 and Figure 4.4 respectively, for IEEE 33-bus system. Similarly, the same for IEEE 69-bus system and Indian 85-bus system are shown in Figure 4.5, Figure 4.6 and Figure 4.7, Figure 4.8 respectively. The consolidation and comparison of results for all the three systems are shown in Table 4.2. The optimal location and size obtained by proposed algorithm is giving better active power loss reduction.

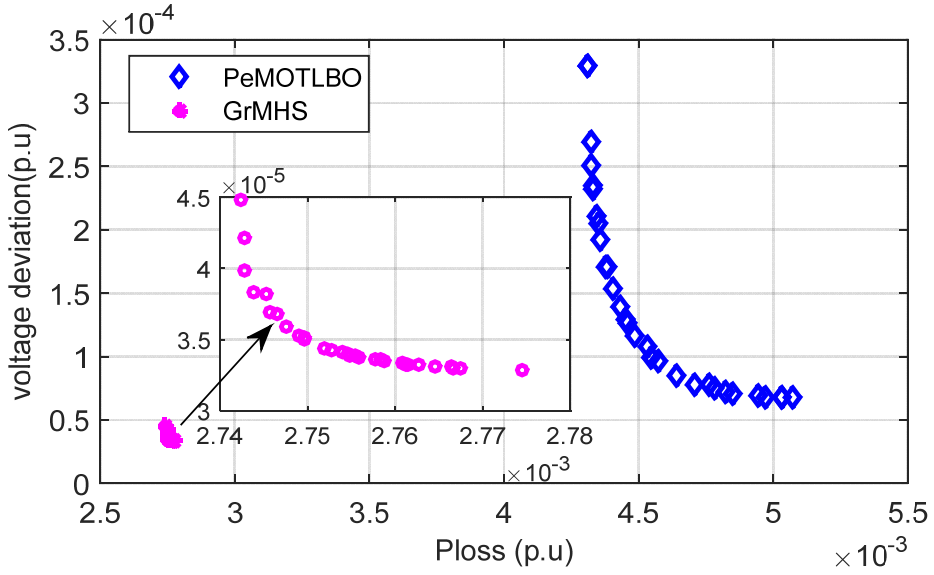

Figure 4.6: IEEE 69-bus system: Comparison of pareto solutions obtained by GrMHS and PeMOTLBO

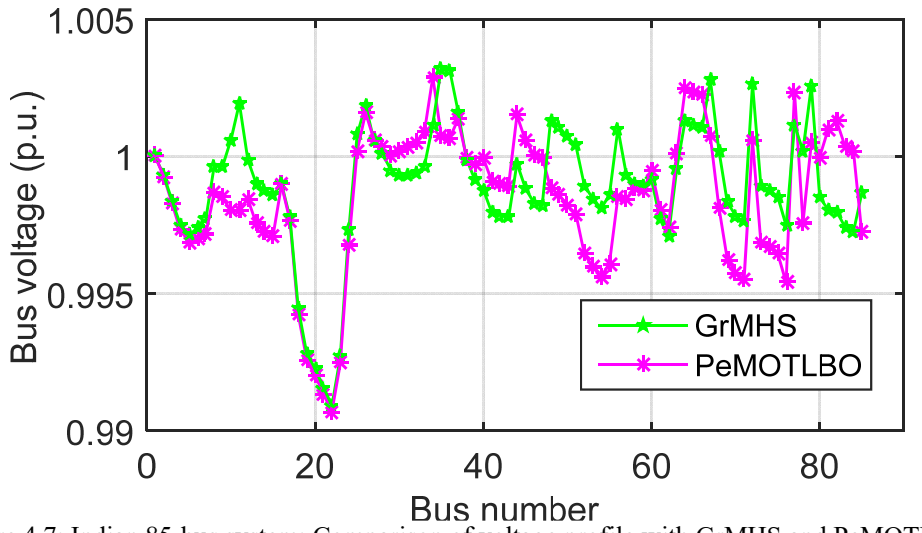

Figure 4.7: Indian 85-bus system: Comparison of voltage profile with GrMHS and PeMOTLBO

Table 4.2 Consolidation and comparison of results for two objectives case

		IEEE 33-bus system				IEEE 69-bus system				Indian 85-bus system			
		Proposed GrMHS		PeMOTLBO		**Proposed GrMHS**		PeMOTLBO		**Proposed GrMHS**		PeMOTLBO	
Location (Bus number)	Size (MW)	14	0.5791	7	0.8563	11	0.5248	21	0.3130	26	0.6415	64	0.7661
		30	0.9874	30	1.0050	50	0.7610	67	0.2994	35	0.6391	34	0.7010
		6	0.8168	16	0.4802	18	0.3944	61	1.7547	67	0.6831	26	0.6656
		25	0.7411	25	0.7426	61	1.7498	12	0.3007	11	0.5716	82	0.3868
Real power loss (p.u.)		0.00963		0.0129		0.002742		0.0048		0.0262		0.0269	
Voltage deviation		0.0002		0.0003		0.3525e-4		0.0001		0.0006		0.0008	
Worst voltage (p.u.)		0.9941		0.9922		0.9984		0.9943		0.9909		0.9907	
CPU time (s)		17.477		34.567		22.706		89.22		38.53		131.8803	

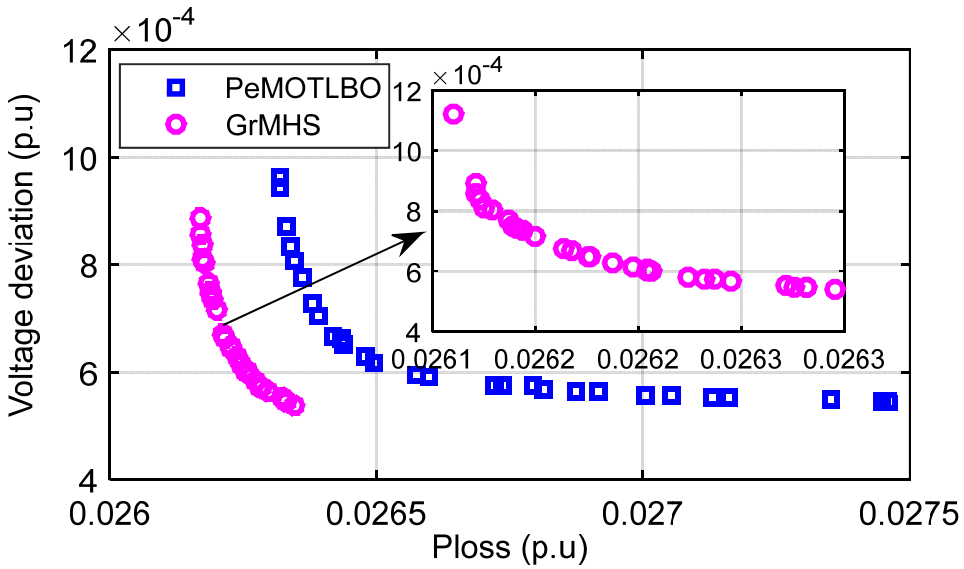

Figure 4.8: Indian 85-bus system: Comparison of pareto solutions obtained by GrMHS and PeMOTLBO

4.6.2 Three objectives: Grid connected mode of operation with hybrid DERs

The planning of grid connected active distribution network is studied with three objectives: 1. Energy loss 2. Voltage deviation 3. Cost of DG integration in this section. These objectives are conflicting with each other. So they are formulated multi-objective problem. As the IEEE 33-bus and IEEE 69-bus systems have nearly the same load and active power loss and behave in a similar manner as reported in the previous DG planning studies, the performance of the proposed GrMHS algorithm in this planning model is evaluated with IEEE 33-bus system and Indian 85-bus distribution system shown in Appendix. The DG technologies include both dispatchable and non-dispatchables (renewable sources) DERs. Daily load profile is assumed to follow the load curve of IEEE-RTS system [106] for 5 years with 5% of annual load growth for both the system. To avoid computational complexity, one-day profile of load and generation has been taken from each season. Thus, only 96 time segments are processed for one year where each time segment corresponds to 90 hours approximately in all season [48]. Connecting distributed generations to the grid connected distribution network will transform them to operate as non-autonomous mode of a microgrid. The various DGs considered here are wind turbine, solar and diesel generator. Figure 4.9 shows the load variation of IEEE 33-bus system in the first year of the planning horizon

along with typical generation profile of each DER. The hourly profile of wind speed and solar radiation data for five years have been accessed from [99].

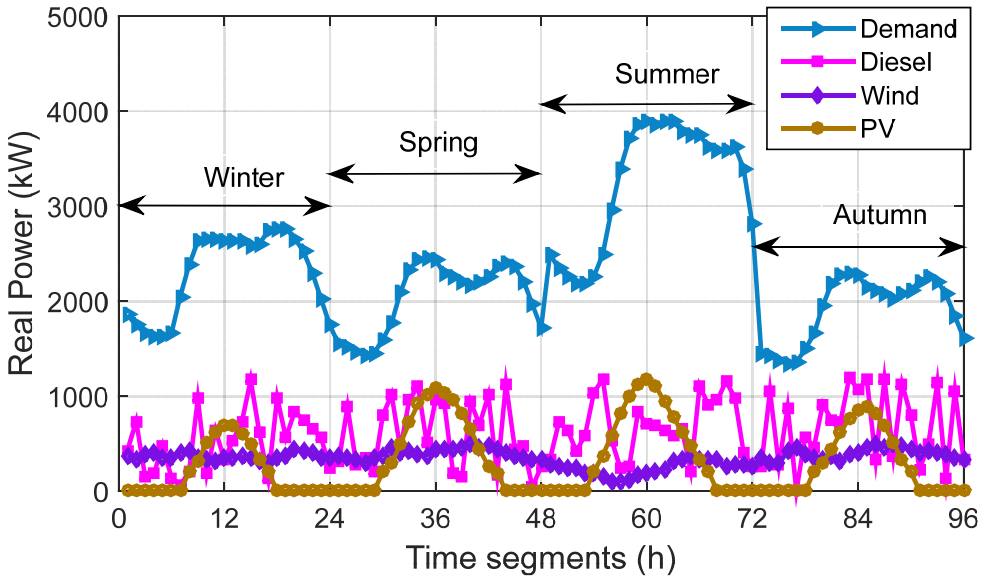

Figure 4.9: Yearly profile of Load and generations of various DERS

4.6.2.1 IEEE 33-bus system

This system is assumed to be connected to the main grid (grid connected micro-grid operation) with hourly load variation and DG sources. Since the planning period is considered as 5 years, the objective functions such as energy loss, costs are evaluated for the whole planning period in iterative process. By doing so, the aggregated demand and energy loss of the system are obtained as (113.18+j70.073) GVA and (4638.1+j3093.7) MVA respectively when there is no DG connected in the system. Four combinatorial scenarios were analysed with different DG type to validate the objective values. The number of DGs is fixed as three as their total ratings are equal to the base demand. Figure 4.10 shows the voltage profile of the IEEE 33-bus system obtained by the proposed GrMHS algorithm for different combinations of DGs in the system. It is observed that even though the number of DGs is same, there is variation in the voltage profile of the system with respect to the DG type. A better voltage profile is noticed obviously for 3 diesel generators case as it is the only controllable generation among all three DG types. Figure 4.11 shows the seasonal variation of total energy loss of the system for various combinations of the DGs. It is perceived that the energy loss reduction is significant if all three DGs are diesel generators and there is

reasonable energy loss reduction where all three are DG technologies. However, if DGs are either PV or wind technologies, the energy loss reduction is not any better than in cases involving diesel generators.

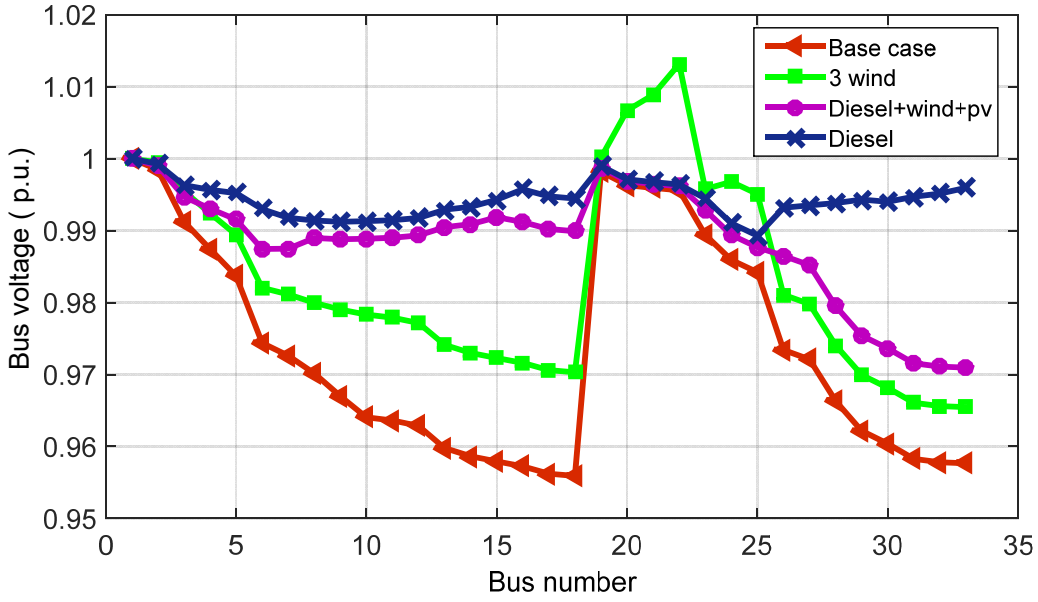

Figure 4.10: IEEE 33-bus system: Bus voltage variation for different DG combinations.

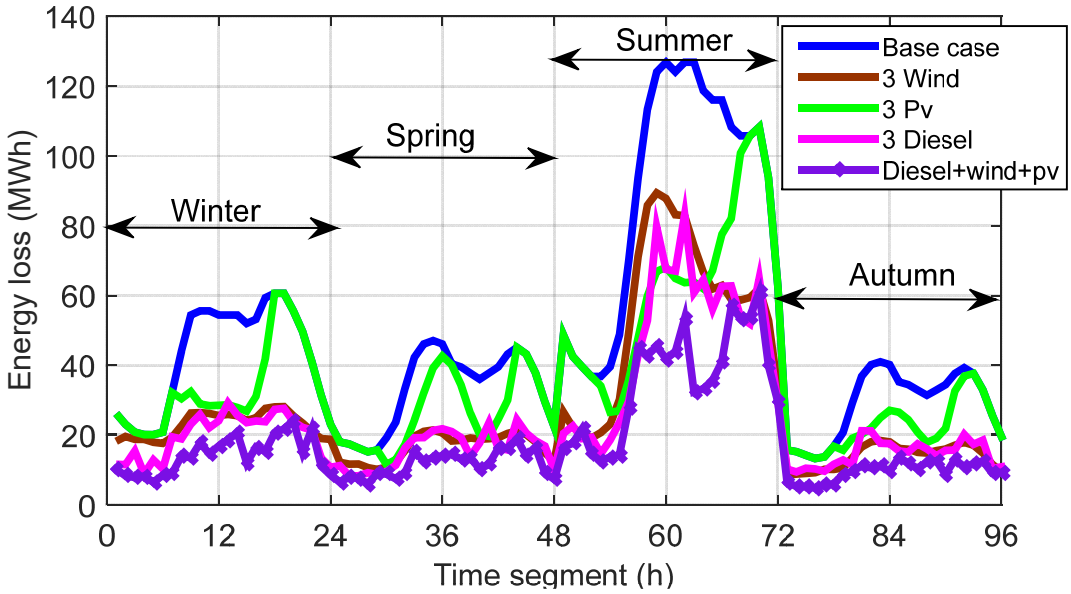

Figure 4.11: IEEE 33-bus system: Seasonal energy loss variation for all DG combinations

Figure 4.12 shows the comparison of the pareto solutions found by GrMHS with basic MOHS and NSGA-II technique. For validating the superiority of the proposed grid based multi-objective harmony search algorithm over basic MOHS and NSGA-II method, all three

diesel generator case has been compared in Figure 4.12. It is evident from the figure that efficient searching has been done by the proposed GrMHS over MOHS and NSGA-II to find out better optimal solutions with respect to all objectives. The spread of the solutions is found to be wide in case of GrMHS.

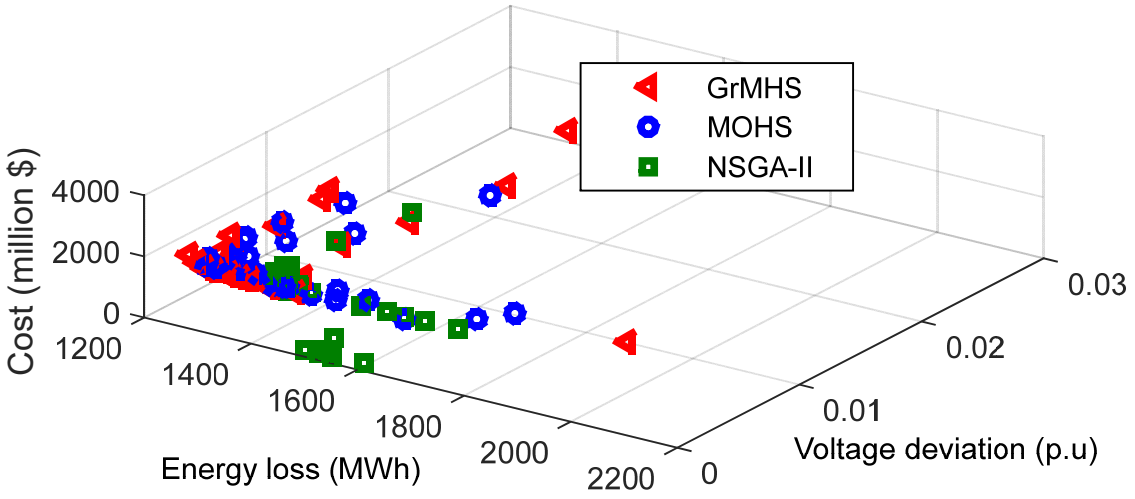

Figure 4.12: IEEE 33-bus system: Comparison of pareto solutions of Proposed GrMHS with MOHS and NSGA-II

The consolidated result of the planning problem using GrMHS in IEEE 33-bus system for different combinations of DG has been summarized and compared with MOHS and NSGA-II, which is shown in Table 4.3. It shows that, despite hourly variation in the power output of renewable resources, the total power contributed by each renewable resource such as wind and solar in the entire planning period is fixed based on modelled wind speed and solar irradiance for five years. Therefore, whatever power available from them is utilized and only the firm generation from diesel is altered. It is ascertained from the table that among all four combinations of DGs, if all 3 DGs are diesel, an appreciable energy loss reduction around 72.13% is achieved with a voltage deviation of 0.00032 p.u but the cost is found to be 2006.33 million$ which is predominantly very high compared to other cases. On the other hand, if all 3 DGs are renewable, being either wind or solar power, the percentage of loss reductions and voltage deviations are about 45.19%, 34.04% and 0.0012 p.u 0.03023 p.u respectively and the cost involved is about 11.1507 million$ for wind and 22.2914 million$ for solar, far cheaper compared diesel based DG.

Table 4.3 IEEE 33-bus system: Validation and comparison for optimal mix of dispatchable and non-dispatchable DG units

Parameter	Without DG	**Proposed GrMHS**				MOHS[98]				NSGA-II [40]			
		Diesel	Wind	PV	Diesel-Wind-PV	Diesel	Wind	PV	Diesel-Wind-PV	Diesel	Wind	PV	Diesel-Wind-PV
Contribution of DGs over 5 years Size (location) GWh (bus no.)	-	24.713 (24)	18.209 (28)	13.373 (30)	27.139 (30)	25.723 (10)	18.209 (31)	13.374 (30)	26.555 (30)	25.912 (30)	18.209 (15)	13.373 (24)	28.261 (28)
	-	26.458 (30)	18.209 (33)	13.374 (13)	18.209 (15)	26.823 (24)	18.209 (29)	13.374 (13)	18.209 (15)	26.968 (03)	18.209 (32)	13.373 (27)	18.209 (13)
	-	26.385 (12)	18.209 (16)	13.374 (24)	13.374 (26)	25.244 (30)	18.209 (16)	13.374 (24)	13.374 (06)	25.846 (08)	18.209 (27)	13.373 (12)	13.374 (30)
Total energy loss (MWh)	4638.1	1293.06	2546.8	3059.1	1607.96	1307.39	2560.01	3059.1	1649.62	1438.11	2480.49	3181.79	1782.71
Energy loss reduction (%)	-	**72.13**	**45.19**	**34.04**	**65.33**	**71.81**	**44.81**	**34.04**	**64.43**	**68.99**	**46.52**	**31.39**	**61.56**
Voltage dev. (p.u)	0.0302	0.00032	0.0012	0.0302	0.0001	0.0004	0.0013	0.0302	0.0006	0.0005	0.0018	0.0302	0.0005
Cost of DG integration (Million $)	-	**2006.33**	**11.150**	**22.291**	**688.747**	**2033.16**	**11.15**	**22.29**	**732.80**	2006.9	**11.15**	**22.291**	**677.94**
Total generation (GWh)	-	77.556	54.63	40.12	58.733	77.79	54.63	40.12	58.14	78.725	54.63	40.12	59.84
Total demand supplied from grid (GWh)	113.18	35.624	58.55	73.06	54.45	35.39	58.55	73.06	55.04	34.46	58.55	73.06	53.34

The results reveal that the optimal renewable resource mix with firm power generation is necessary for obtaining the optimal operation with considerable energy loss reduction and the cost. For instance, if all DG technology is considered, the loss reduction is found to be 65.33% with voltage deviation of 0.00018 p.u. and the total cost is around 688.7479 million$ which is reasonable when compared to other cases. Similar analyses have been carried out with NSGA-II technique and MOHS for the purpose of comparison. It is found to be performing in a similar fashion like GrMHS for all cases but the objective values are found to be inferior to GrMHS.

4.6.2.2 Indian 85-bus system

Indian 85-bus distribution system with a base demand of (2.54703+j2.622) MVA has been modified by incorporating daily load variation using IEEE RTS system [106] over 5 years with an annual load growth of 5%. Thus, the total demand and energy loss of the system over 5 years is found to be (78.307+j79.889) GVA and (7141.5+j4486.8) MVA respectively. Renewable DGs modelling is adopted in the same way as that of the IEEE 33-bus system. Figure 4.13 shows the voltage profile of the Indian 85-bus system for all DGs combination. It shows the effect of connecting the renewable resources and firm generating source such as diesel on voltage profile in the system. The voltage profile in the system found better in case of diesel generator. Figure 4.14 presents the seasonal energy loss variation of the system for different DGs combinations.

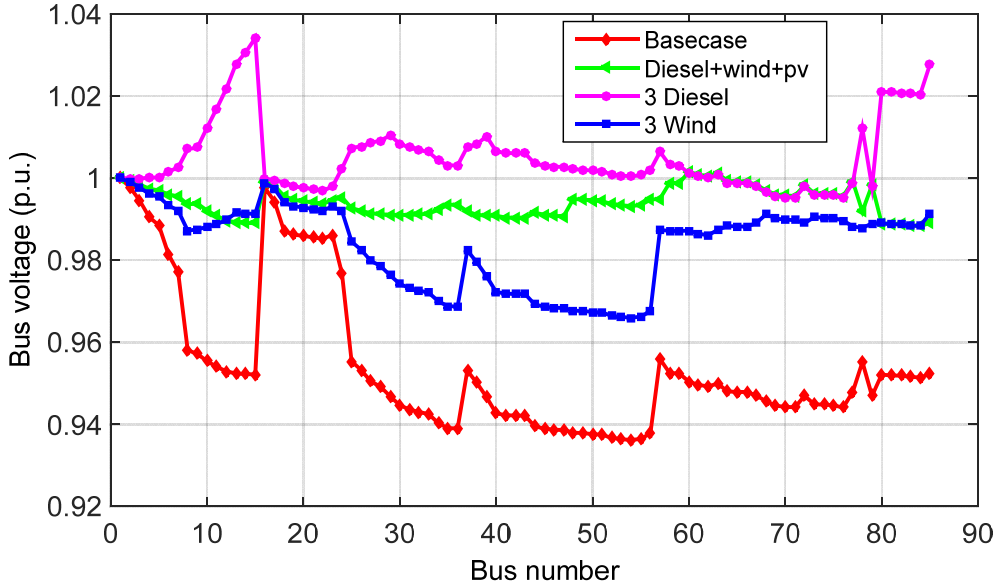

Figure 4.13: Indian-85 bus system: Voltage variation at all buses for different DG combination.

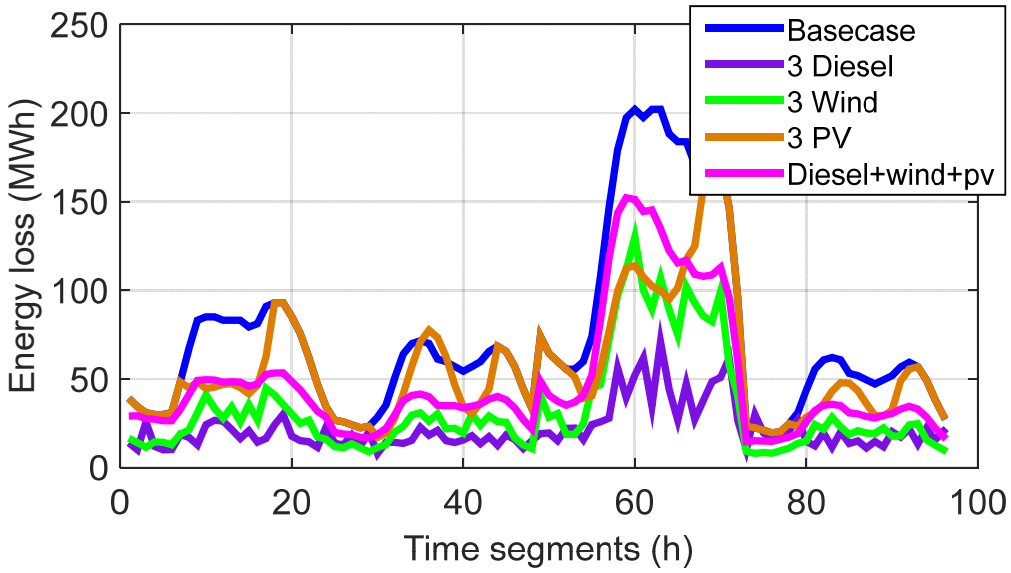

Figure 4.14: Indian-85 bus system: Seasonal energy loss variation for all DG combinations

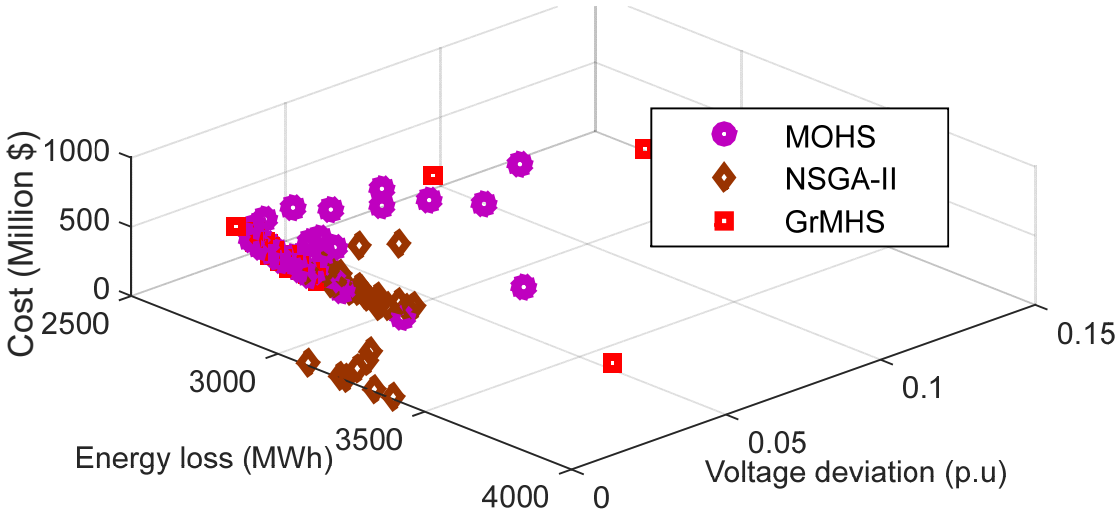

Figure 4.15: Indian 85-bus system: Comparison of pareto solutions of Proposed GrMHS with MOHS and NSGA-II

Figure 4.15 shows the comparison of the pareto solutions obtained by GrMHS with MOHS and NSGA-II technique for Indian 85-bus system for all DG cases. Moreover, the pareto solution obtained by NSGA-II techniques are with two fronts, which introduces ambiguity in the decision making process. In this system, the pareto optimal front obtained by GrMHS method is little close to the basic MOHS method but the best solution given by proposed method is superior to two other methods.

Table 4.4 Indian 85-bus system: Validation and comparison for optimal mix of dispatchable and non-dispatchable DG units

Parameter	Without DG	**Proposed GrMHS**				MOHS[98]				NSGA-II[40]			
		Diesel	Wind	PV	Diesel-Wind-PV	Diesel	Wind	PV	Diesel-Wind-PV	Diesel	Wind	PV	Diesel-Wind-PV
Contribution of DGs over 5 years Size (location) GWh (bus no.)	-	25.129 (63)	18.209 (68)	13.374 9 (33)	27.431 (33)	25.169 (60)	18.209 (29)	13.374 (33)	26.395 (32)	26.139 (34)	18.209 (68)	13.374 (63)	27.147 (58)
	-	26.946 (32)	18.209 (49)	13.374 (60)	18.209 (67)	25.898 (10)	18.209 (48)	13.374 (60)	18.209 (67)	26.558 (09)	18.209 (30)	13.374 (39)	18.209 (53)
	-	24.934 (08)	18.209 (28)	13.374 (07)	13.374 (57)	25.989 (34)	18.209 (67)	13.374 (07)	13.3734 (09)	25.896 (65)	18.209 (48)	13.374 (80)	13.374 (12)
Total energy loss (MWh)	7141.5	1850.43	4311.4	5186.5	2820.79	1889.31	4323.73	5186.5	2860.71	1909.35	4390.76	5344.52	3089.28
Energy loss reduction (%)	-	**74.09**	**39.63**	**27.38**	**60.51**	**73.55**	**39.46**	**27.38**	**59.94**	**73.26**	**38.52**	**25.16**	**56.74**
Voltage dev. (p.u)	1.0245	0.0080	0.0104	0.2031	0.00365	0.00343	0.01043	0.2030	0.00461	0.0019	0.0094	0.2031	0.0009
Cost of DG integration (Million $)	-	**2006.06**	**11.122**	**22.262**	**624.721**	**1977.82**	**11.123**	**22.262**	**675.161**	**2080.32**	**11.123**	**22.263**	**677.24**
Total generation (MWh)	-	77.01	54.628	40.121	59.01	77.0575	54.6282	40.121	57.9783	78.5943	54.6282	40.1217	58.730
Total demand supplied from grid (GWh)	78.307	1.06	23.678	38.185	19.297	1.2495	23.6788	38.185	20.3287	-0.2873	23.679	38.185	19.577

Table 4.4 provides the comparative results of the proposed model in Indian 85-bus system for all DG combinations. It is interpreted from the table that when the system is operating only with diesel, it is almost operating close to the autonomous mode operation of the microgrid as the power generated is found to be 98.34% of demand. This results in 74.09% energy loss reduction from the base case with a voltage deviation of 0.0080p.u. which due to cost constraints of around 2006.06 million$, resulted in the need for renewable resource mix with diesel technology. Since this system's demand is less when compared to other above discussed systems, the contribution from renewable energy seems to be high and has reduced the amount of power purchased from the main grid. Even then, only with renewable DGs, it failed to boost up the percentage of loss reduction and improve voltage deviation in the system. Thus, a mix of DG technology is quite preferred for better optimal operation in the system. For example, one diesel, one wind turbine and one PV in the system resulted in 60.52% loss reduction with voltage deviation of 0.00365p.u and a cost of 624.721 million$. The same analysis has been undertaken by using MOHS and NSGA-II technique to validate the results obtained by GrMHS algorithm. It is clear from Table 4.4 that the objective values are superior in GrMHS compared to MOHS and NSGA-II technique.

4.6.3 Three objectives: Autonomous mode of operation with hybrid DERs

The proposed operation strategy has been implemented in IEEE 33-bus distribution test system and Indian85-bus distribution system using proposed GrMHS algorithm. For both the systems, load profile has been assumed to follow IEEE-RTS system load curve [106] with 5% annual load growth throughout the planning period of 5 years. The systems are installed with 3 diesel generators of 1.2 MW, each capable of meeting the total demand in the system and the renewable resources such as wind and solar generations of each 2 MW and 1.2 MW respectively. The impact of excess renewable resources penetration in the system is analyzed for economic and stable autonomous operation of the active distribution system. Li-ion battery of 2 MW rating is assumed to be fully charged. Initially, with Depth of Discharge (DOD), 15% of its rating is considered and is allowed to charge only when there is excess renewable generation after meeting the load demand at particular hour. The maximum charging efficiency of the battery is considered 0.95.

4.6.3.1 IEEE 33-bus system

The base case load of this system is (3.72+j2.3) MVA and is assumed as peak load of the system. The sum of hourly demand over 5 years is found to be (113.18+j70.07) GVA with total energy loss of (4638.1+j3093.7) MVA. This system is studied for its standalone microgrid operation with DERs with no constraints on renewable sources location and the impact on the objective functions is observed by enforcing available renewable source bus limits. 16 buses have been assumed and are included as a constraint for solar and wind turbine placement. The assumed bus limits for this system are [7 8 9 10 11 12 13 14 26 27 28 30 31 32 33].

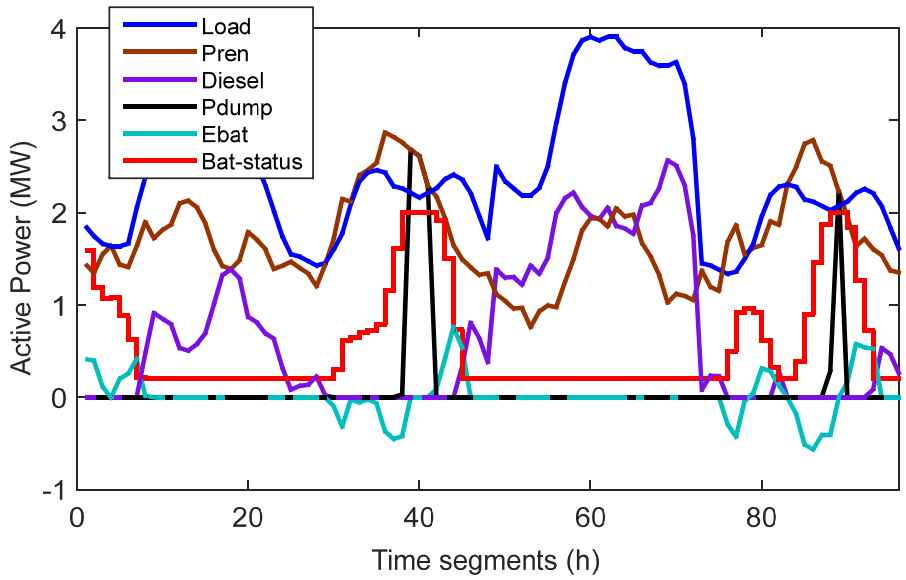

Figure 4.16: IEEE 33-bus system: Variation of load and generation at first year of planning horizon for 9 DERs case

Figure 4.16 shows the load and generations in the system during starting year of planning period for 9 DERs case. The existence of dumped energy in the system is clearly visible when there is excess renewable power generation after meeting load. At the same time, it should be noted that the diesel and battery are not supplying any power to the system as total load being supplied by renewable sources. When the available renewable source bus limits are enforced on the system, the energy loss in the system is increased due to unsuitable location of the renewable sources. This comparison is shown in Figure 4.17. The comparison of voltage profile in the system with and without renewable bus available limits is shown in Figure 4.18.

Figure 4.19 shows the comparison of the pareto optimal solutions of the objective functions before and after enforcing renewable bus limits. It is noticed that the pareto solutions obtained when there are no bus limits enforced is giving better solution when compared to the solution obtained when it is subject to bus limits constraint. When the bus limits are imposed on the system, the solutions are superimposed with each other, thereby making no provision for decision-making.

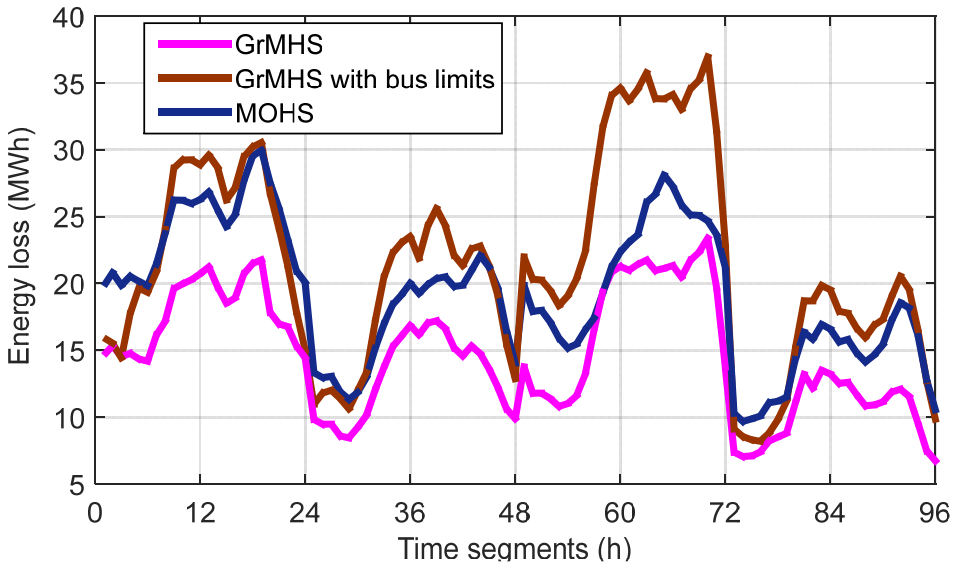

Figure 4.17: IEEE 33-bus system: Comparison of Energy loss for 9DERs case

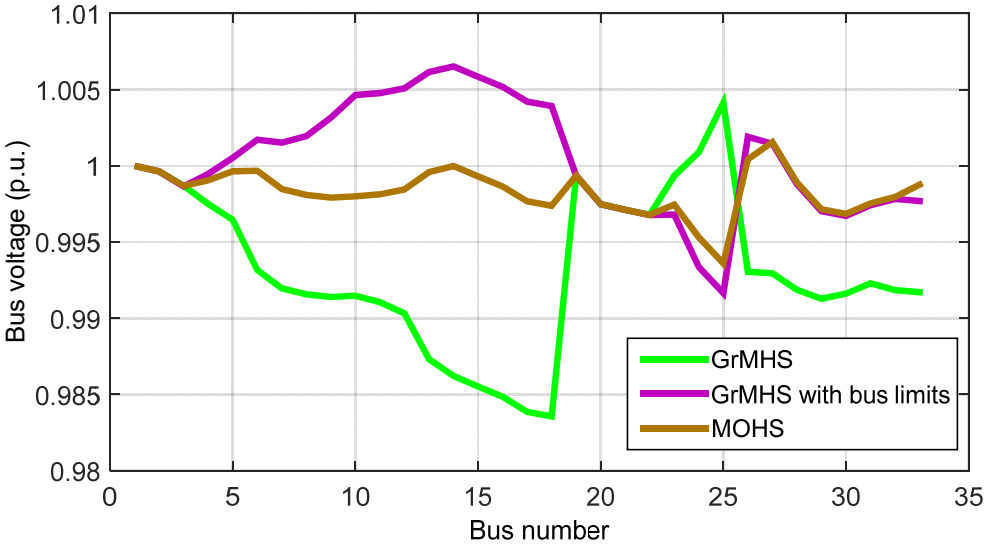

Figure 4.18: IEEE 33-bus system: Comparison of voltage profile for 9DERs case

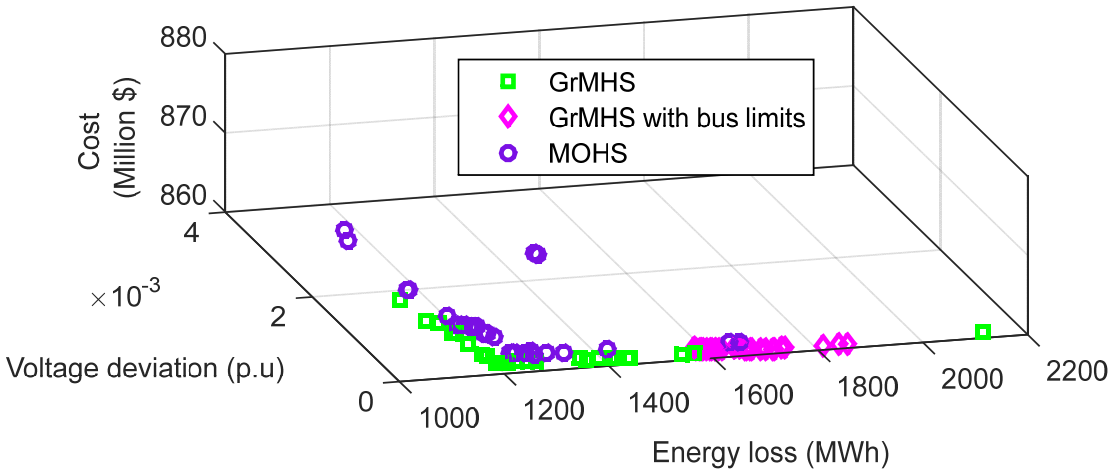

Figure 4.19: IEEE 33-bus system: Comparison of pareto solutions of proposed GrMHS with MOHS

Table 4.5 IEEE 33-bus system: System Performance with various DERs combinations and renewable source bus limits

Total no. of DERs / DERs Type	**Proposed GrMHS**						MOHS [98]			
	Without bus limits				With renewable bus limits		Without bus limits			
	6 DERs		9 DERs		6DERs	9 DERs	6 DERs		9 DERs	
	Loc.	Size (MWh)	Loc.	Size (MWh)	Loc.	Loc.	Loc.	Size (MWh)	Loc.	Size (MWh)
Diesel	7	564.0	8	218.54	27	24	5	564.0	29	218.6
	30	271.7	30	99.21	24	30	32	271.7	7	99.21
	25	66.30	25	10.057	30	10	9	66.30	25	10.06
Wind	24	202.33	25	202.33	13	28	15	202.3	14	202.3
			15	202.33		14			25	202.3
			32	202.33		32			8	202.3
			6	202.33		7			31	202.3
PV	3	148.6	19	148.6	7	7	24	148.6	3	148.6
Battery	23	1.8	5	22.60	3	4	3	1.8	6	22.59
Total energy loss (MWh)	**828**		**1188**		**981**	**1672.2**	**954.0**		**1250.9**	
Voltage deviation (p.u)	2.164e-4		0.0002		4.22e-4	0.0004	2.5126e-4		0.0002	
Cost (Million $)	2685.6		859.94		2685.6	859.94	2685.6		859.94	
Pdumped (MWh)	0		125.84		0	125.84	0		125.84	
Battery charged power (MWh)	0		-23.79		0	-23.79	0		-23.79	

*Loc. – Location

Table 4.5 shows the comparison of system performance in autonomous mode operation of IEEE 33-bus system for two different DERs combination. One case considers less RES and another excess RES. Since power generation by wind is relatively of less cost when compared to PV, increase in renewable source integration is considered only for wind. When

the wind turbine is considered excess in the system, the overall cost is decreased from 2685.6 million$ to 859.94 million$ but energy loss over planning horizon increased from 828 MWh to 1188 MWh while maintaining better voltage deviation in both the cases. As the battery is assumed to be charged only when there is excess renewable power generation after supplying load, battery charging is made possible only in case of excess wind turbines. On the other hand, if excess wind turbines are connected, the amount of dumped energy i.e energy generated but not used is increased in the system. To avoid these discrepencies, enough batteries can be accomodated and operated optimally with a limitted number of wind turbines. To incorporate the practicality, renewable bus limits are enforced in this thesis and due to fixed number of units and assumed uniform wind speed and solar irradiation at all buses, the optimal location alone disturbed as the generation is scheduled based on the load in the system. Thus, from Table 4.5 it is seen that if location constraints are included, the system losses increased from 1188 MWh to 1672.2 MWh in case of 9 DERs with 4 wind turbines, even with same generation due to non-optimally located renewable sources.

4.6.3.2 Indian 85-bus system

An Indian 85-bus distribution network with a maximum demand of (2.5703+j2.622) MVA with a base distribution line loss of (316.7+j198.7) kVA is also considered for autonomous operation with DERs. The total demand over 5 years is found to be (78.307.18+j79.889) GVA with total energy loss of (7141.5+j4486.6) MVA for this system. The constraint for solar and wind resource integration is enforced by considering 28 bus location for their connections for this system. The assumed bus limits for this system are [8 9 10 11 12 13 14 15 25 78 80 81 82 85 57 58 59 60 61 62 44 45 46 47 24 38 83 84].

Figure 4.20 shows the variation of load on the Indian 85-bus system and various source of generation for 9 DERs case. It is observed that the battery reaches its maximum charged state when there is excess energy available from the renewable sources due to less demand in the system. It clearly depicts the increase in dumped energy in the system when there is excess renewable power generation after supplying load. The energy loss profile obtained by GrMHS algorithm before and after enforcing bus limits has been shown in Figure 4.21. Imposing the renewable source bus available limits has worsened the system loss as shown in Figure 4.21. The Figure 4.22 shows comparison of pareto optimal solutions of the objective functions before and after enforcing renewable bus limits. It is noticed that

the pareto solutions are better when they are not subjected to any bus limits constraint. The voltage profile of Indian 85-bus system without renewable bus available limits is compared with enforced bus limits in Figure 4.23.

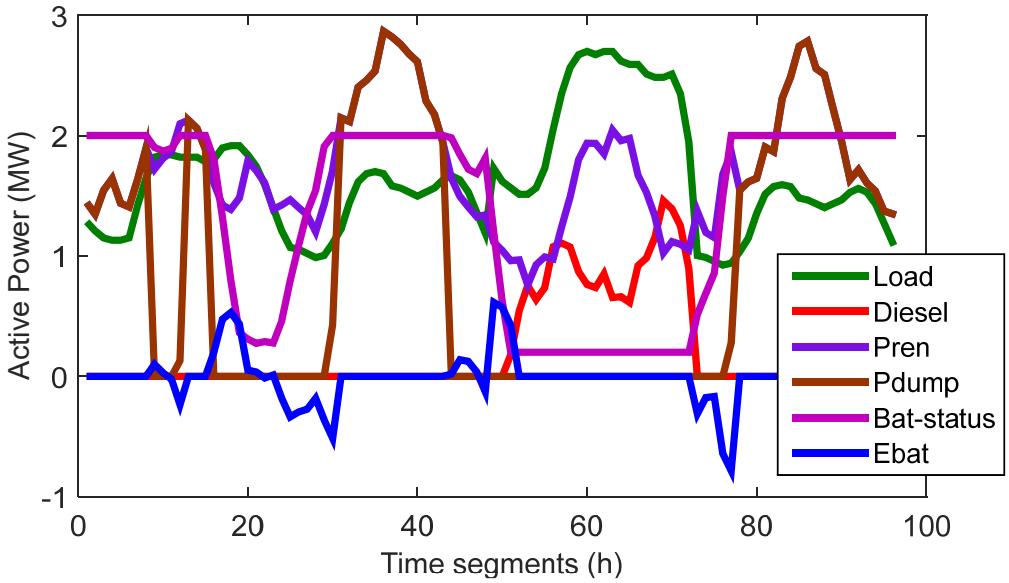

Figure 4.20: Indian 85-bus system: Variation of load and generation for 9 DERs case

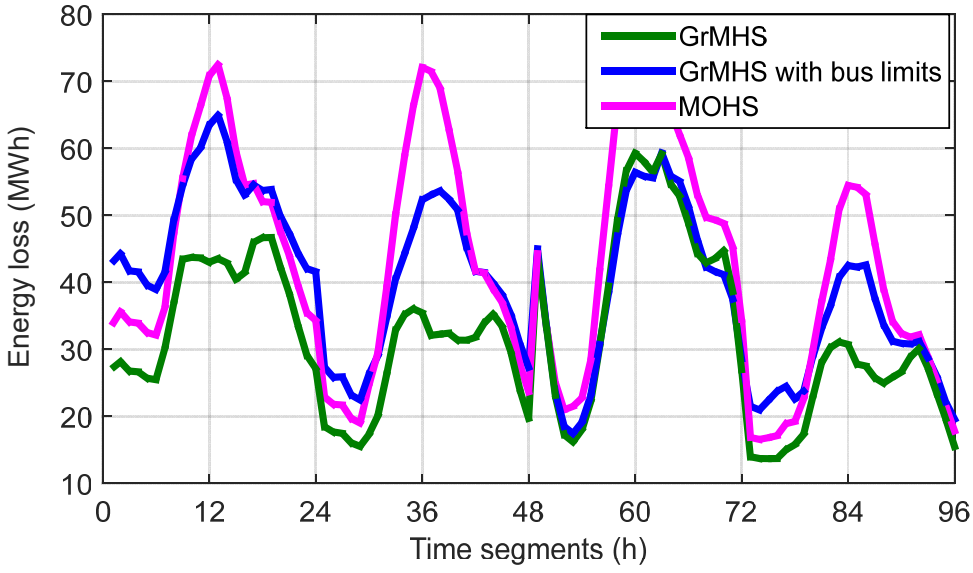

Figure 4.21: Indian 85-bus system: Comparison of Energy loss for 9DERs case

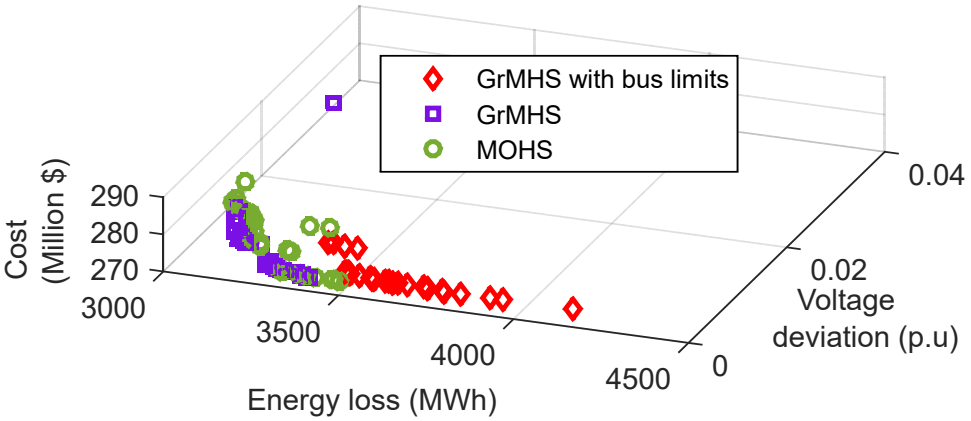

Figure 4.22: Indian 85-bus system: Comparison of pareto optimal solutions of proposed GrMHS with MOHS

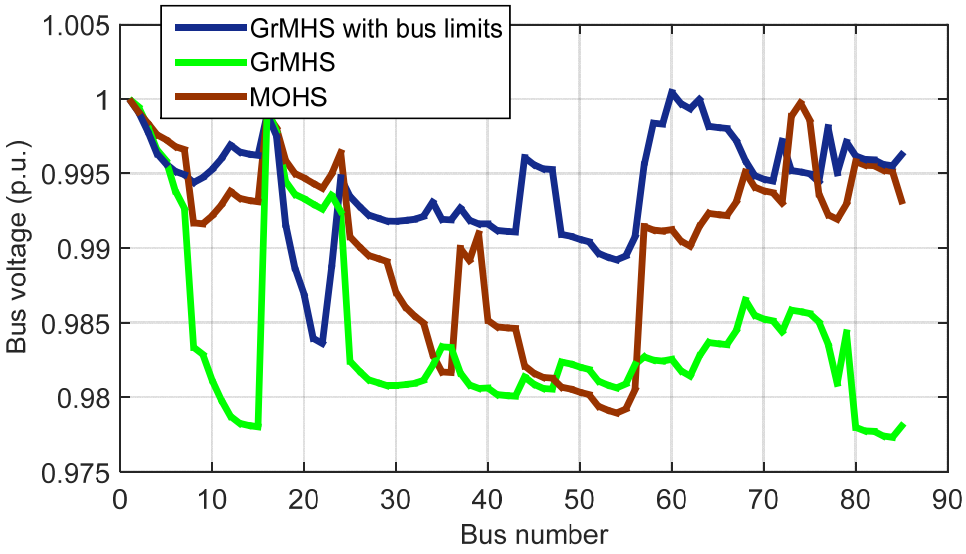

Figure 4.23: Indian 85-bus system: Comparison of voltage profile for 9DERs case

Even though same operational strategy has been adopted for Indian 85-bus system as that of IEEE 33-bus system, it is observed from Table 4.6 that due to less load on the system, the amount of dumped energy i.e. wasted energy is 624.0282 MWh in 5 years. The total cost is reduced from 1339 million$ to 272.825 million$ due to excess wind turbine integration in the system at the cost of increase in system energy loss from 1764 MWh to 3038.73 MWh.

The voltage deviation also increased in the system with increase in the wind turbine in the system. As there is less demand in the system, simply increasing the number of wind turbines has resulted in tremendous increase in the amount of dumped energy in the system. While it has avoided the operation of diesel generators, thereby reducing the operating fuel cost. When the renewable bus limits are imposed, there is much increase in the system energy loss with same amount of generation as that of the case with no bus constraints.

Table 4.6 Indian 85-bus system: System performance with various DERs combination and renewable source bus limits

Total no. of DERs / DERs Type	**Proposed GrMHS**						MOHS [98]			
	Without bus limits				With renewable bus limits		Without bus limits			
	6DERs		9DERs		6DERs	9DERs	6DERs		9DERs	
	Loc.	Size (MWh)	Loc.	Size (MWh)	Loc.	Loc.	Loc.	Size (MWh)	Loc.	Size (MWh)
Diesel	29	424.7	29	105.81	29	31	29	424.7	30	105.81
	60	81.0	64	6.793	64	70	64	81.0	71	6.793
	52	1.7	51	0	52	11	53	1.7	77	0
Wind	68	202.33	67	202.33	60	12	68	202.33	35	202.33
			35	202.33		44			26	202.33
			3	202.33		60			11	202.33
			12	202.33		25			67	202.33
PV	6	148.6	4	148.6	8	24	9	148.6	5	148.6
Battery	8	1.8	2	16.25	25	1	25	1.8	1	16.25
Total energy loss (MWh)	**1764.0**		**3038.733**		**1836**	**3503.24**	**1791**		**3327.58**	
Voltage deviation (p.u)	0.0019		0.0117		0.0031	0.0021	0.0019		0.0010	
Cost (Million $)	1339		272.83		1339	272.83	1339.0		272.825	
Pdumped (MWh)	0		**624.0282**		0	**624.028**	0		**624.0282**	
Battery charged power (MWh)	0		-19.65		0	-19.65	0		-19.65	

*loc. - Location

4.6.4 Performance metrics comparison of proposed GrMHS algorithm with MOHS and NSGA-II

The performance of the proposed algorithm is compared with two metrics (i) Set coverage metric (ii) Space metric (one evaluating the progress towards the pareto-optimal front and the other evaluating the spread of solutions) that tests both the goals. These metrics

evaluation and the comparative study using box plot are followed in similar way as that in chapter 3. Proposed GrMHS method is compared with NSGA-II and MOHS methods by executing each of them independently 25 times.

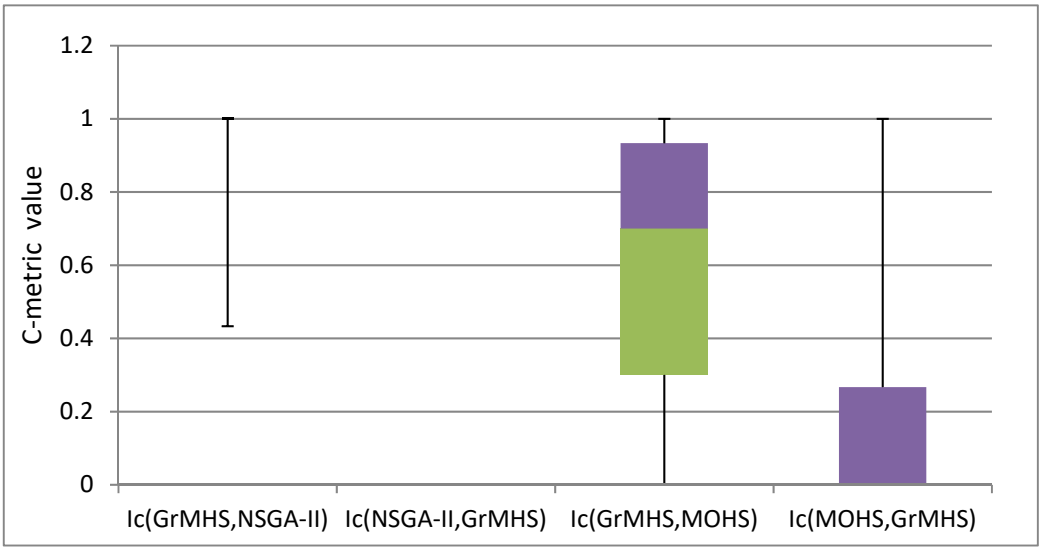

Figure 4.24: IEEE 33-bus system – Comparison of C-metric values obtained with proposed GrMHS

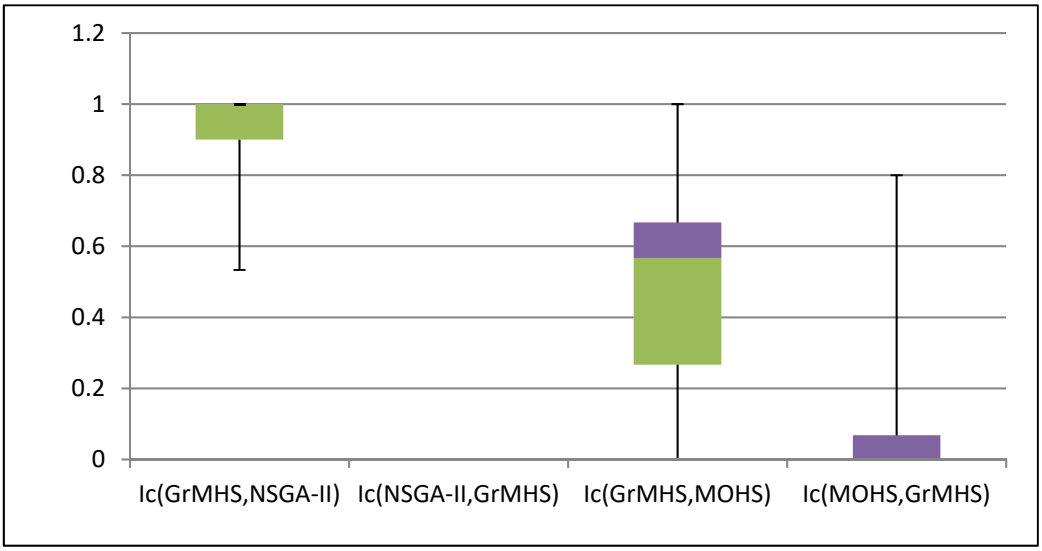

Figure 4.25: Indian 85-bus system – Comparison of C-metric values obtained with proposed GrMHS

The box plot for distribution of coverage metric (I_c) values obtained by proposed GrMHS algorithm has been compared individually with NSGA-II and MOHS methods. The comparison of plots prove the superiority of proposed GrMHS algorithm is shown in Figure

4.24 and Figure 4.25 respectively for IEEE 33-bus system and Indian 85-bus system respectively. It is clearly understood from the graph that the convergence by proposed GrMHS is better when compared to MOHS and NSGA-II.

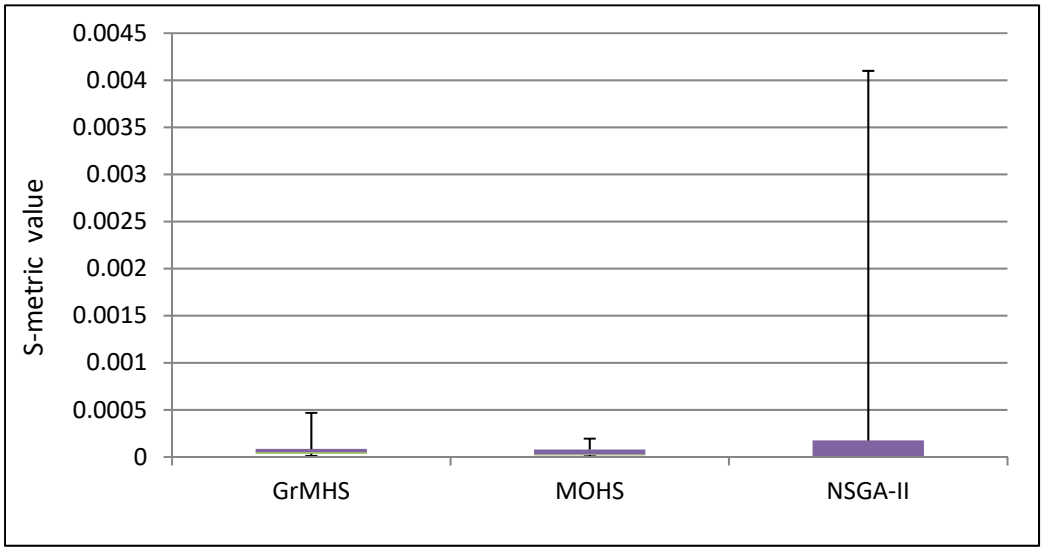

Figure 4.26: IEEE 33-bus system – Comparison of S-metric values obtained with proposed GrMHS

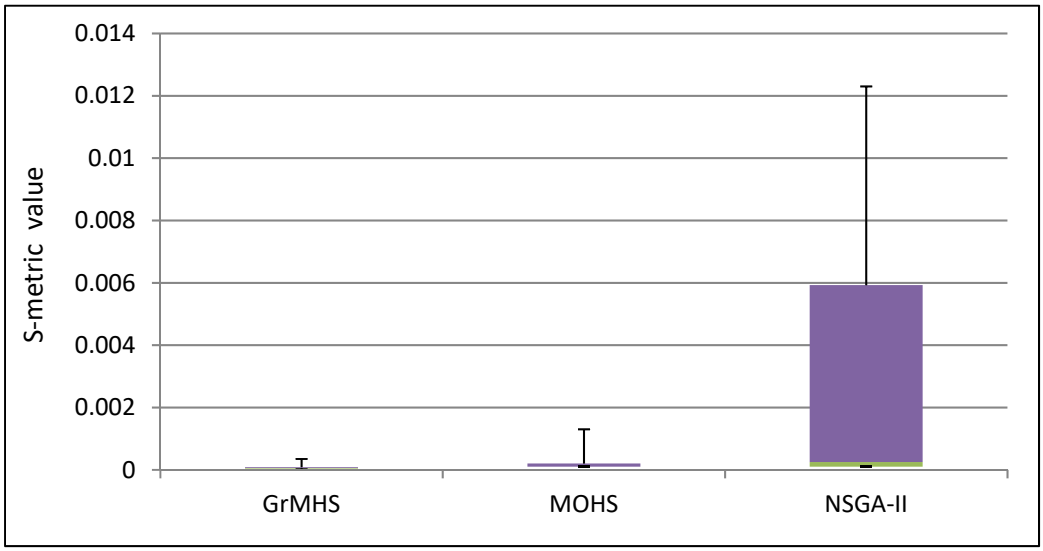

Figure 4.27: Indian 85-bus system – Comparison of S-metric values obtained with proposed GrMHS

Figure 4.26 and Figure 4.27 shows the comparison of S-metric values obtained by GrMHS method with MOHS and NSGA-II for IEEE 33-bus system and Indian 85-bus system respectively. The plots depict that the solutions obtained by GrMHS and MOHS are

equidistantly placed when compared to NSGA-II and MOHS methods as the S-metric values obtained by GrMHS method is close to zero compared to MOHS and NSGA-II method. This ensures better diversity among the solutions in the pareto front.

4.7 Summary

In this chapter, a novel multi-objective algorithm called Grid based Multi-objective Harmony Search algorithm (GrMHS) has been proposed for active distribution network operation planning. A secondary selection criterion i.e. grid setting strategy in objective space is embedded in harmony search algorithm for better performance in multi-objective frame. Optimal resource mix of renewable and fuel based DGs have been identified for economic and efficient operation of active distribution network. It has been analyzed for both grid-connected and autonomous mode of operation with energy storage systems. The limit on location of renewable DGs is also incorporated in the formulation to assess its impact on system energy losses and the voltage profile.

Chapter 5

Load Frequency Control of an Autonomous Microgrid using Levy based Spider Monkey Algorithm

Chapter 5

5 Load Frequency Control of an Isolated Microgrid using Levy based Spider Monkey Algorithm

5.1 Introduction

Frequency and voltage controls are the two main challenges in microgrid operation in grid connected mode and autonomous mode due to the presence of uncertain renewable sources and negligible inertia. Since economic microgrid operation relies on fluctuating renewable sources such as wind and solar, the task of maintaining frequency within the limits for smooth operation of microgrid demands advanced controller action. Keeping this in mind, this chapter proposes eagle strategy where a panoptic exploration to search space has been accomplished for optimizing the gains of PI controller employed in controllable generating units in the islanded microgrid. In the proposed strategy, the search process is of two fold i.e., coarse search by levy flights and an intensive local search by spider monkey algorithm. The proposed strategy has been tested on a typical microgrid test system and its effectiveness is validated with performance index Integral Time Squared Error (ITSE).

5.2 Proposed Eagle strategy using Levy flights with Spider Monkey Optimization Algorithm

Eagle strategy is a methodology rather than algorithm is inspired from the foraging behavior of eagle where eagle search for prey in free random manner. Once the prey is found, it will intensify its hunting process by chasing the prey. Eagle strategy was first developed by Yang et al.[101]. The two main components of eagle hunting strategy include:

i. A coarse global search with enough randomness so as to explore a diverse search space and

ii. Intensive local search using any efficient algorithm.

In this chapter, this strategy first explores the search space globally using levy flight random walk whose step length is not fixed which ensures promising solutions and then an intensive local search is carried out with efficient spider monkey optimization algorithm. This strategy has explored a vast search space to find an optimal solution.

5.2.1 Levy Flights

Random walk whose step length follows a non-Gaussian distribution such as levy distribution is called levy flights.

It is often given in terms of simple power law $L(s) \sim |s|^{-1-\beta}$ where $0<\beta\leq 2$ is levy index. Mathematically, a simple version of levy distribution is given by [102]:

$$L(s,\gamma,\mu)=\begin{cases}\sqrt{\frac{\gamma}{2\pi}}\exp\left[-\frac{\gamma}{2(s-\mu)}\right]\frac{1}{(s-\mu)^{3/2}} & if \quad 0<\mu<s<\infty \\ 0 & if \quad s\leq 0\end{cases} \tag{5. 1}$$

Where μ is shift parameter, $\gamma > 0$ is scale parameter. This is the special case of generalized levy distribution.

In general, levy distribution should be defined in terms of Fourier transform:

$$F(k) = \exp[-\alpha|k|^{\beta}] \qquad 0 < \beta \leq 2 \tag{5.2}$$

Where, α is the scale parameter in range (0, 1). Inverse of the above Fourier transform is not possible except for few special cases when $\beta = 2$ corresponds to Gaussian distribution and $\beta = 1$ corresponds to Cauchy distribution.

In general, the inverse integral is given by

$$L(s) = \frac{1}{\pi}\int_0^{\infty}\cos(ks)\exp[-\alpha|k|^{\beta}]dk \tag{5.3}$$

It can be estimated only when $s \to \infty$

$$L(s) = \frac{\alpha\beta\,\Gamma(\beta)\sin(\pi\beta)/2}{\pi|s|^{1+\beta}} \tag{5.4}$$

The gamma function $\Gamma(z)$ is given by

$$\Gamma(z) = \int_0^{\infty} t^{z-1}e^{-t}dt \tag{5.5}$$

Where z is an integer. Levy flights are more efficient than Brownian random walk in exploring the unknown, large-scale search space. This is due to its variance $\sigma^2(t) \sim t^{3-\beta}$ which increases much faster than the linear relationship $\sigma^2(t) \sim t$ of Brownian walk.

Implementation of levy walk:

There are two steps in generation of random walk with levy flights: choice of random direction that is drawn from normal distribution and generation of random steps, which obeys levy distribution. The latter is achieved by efficient Mantegna algorithm and step length is given by:

$$step = \frac{u}{|v|^{1/\beta}} \tag{5. 6}$$

Where u and v are drawn from normal distribution.

$$u \sim N(0, \sigma_u^2) \quad ; \quad v \sim N(0, \sigma_v^2) \tag{5.7}$$

Where,

$$\sigma_u = \left\{ \frac{\Gamma(1+\beta)\sin\left(\frac{\pi\beta}{2}\right)}{\Gamma[(1+\beta)/2]\beta 2^{(\beta-1)/2}} \right\}^{1/\beta} \quad ; \quad \sigma_v = 1 \tag{5.8}$$

5.2.2 Spider Monkey Optimization (SMO) Algorithm

Spider Monkey Optimization algorithm proposed by JC Bansal et al. [103] is a recently emerging algorithm in the family of nature inspired Meta heuristic algorithms. This algorithm is inspired from the foraging behavior of spider monkeys, which follow certain fission-fusion social structure (FFSS) for their effective foraging action.

Features of Fission Fusion Social Structure:

- Initially spider monkeys survive in single group with 30-60 monkeys and are led by a female leader (global leader) who is responsible for all sorts of decision-making.
- In the foraging process, the group keeps being divided into smaller sub-groups until the group members reach a minimum of 3-5 members in different directions each lead by individual female leaders (local leaders).
- At the end of foraging process all groups are combined together as single group to share the food. This type of foraging movement will increase the effective search for food without foraging competition. The SMO algorithm is inspired from this social structure behavior and it involves the following seven steps:

Step 1: Initialization of population

Populations of P spider monkeys are initialized with D dimensional vectors.

$$SpM(i,j) = SpM(i,j) + rand() * (SpM_{\max j} - SpM_{\min j}) \quad (5.9)$$

Where, $i = 1,2,3 \ldots\ldots P$, $j = 1,2,3 \ldots\ldots D$. $SpM_{\max j}$ and $SpM_{\min j}$ are the maximum and minimum limits on the corresponding j^{th} decision variable.

Step 2: Local Leader Phase (LLP)

The position of each member of each group is updated based on the local leader experience and other group member's knowledge

$$SpMnew(i,j) = SpM(i,j) + rand() * (LL_{kj} - SpM_{ij}) + rand[-1,1] * (SpM_{rj} - SpM_{ij}) \quad (5.10)$$

Where, $SpM(i,j)$ is the j^{th} decision variable of i^{th} SpM (spider monkey). LL_{kj} is the j^{th} decision variable of the local leader in k^{th} group. SpM_{rj} is the j^{th} decision variable of randomly chosen r^{th} spider monkey from the k^{th} group where $r \neq i$.

Step 3: Global Leader Phase (GLP)

Based on the experience of the global leader and other members of local group, the position of SpM is modified.

$$SpMnew(i,j) = SpM(i,j) + rand() * (GL_j - SpM_{ij}) + rand[-1,1] * (SpM_{rj} - SpM_{ij}) \quad (5.11)$$

Where, GL_j is the j^{th} decision variable of the global leader and the j^{th} variable is randomly chosen from (1, 2, 3…D). The position update is done with the help of probabilities p_i.

$$p_i = 0.9 * \frac{fitness_i}{fitness_{\max}} + 0.1 \quad (5.12)$$

Step 4: Global Leader Learning Phase (GLLP)

Greedy selection is applied on the new population and existing population and a population of size P is selected. The position with best fitness within updated population is

considered as new global leader position. Meanwhile if the position of global leader has not changed for certain number of iterations (Global Leader Limit) then, the global limit count is incremented by one.

Step 5: Local Leader Learning Phase

In this phase, the local leaders in each group are updated in a similar fashion as that of the global leader by applying greedy selection by comparing the group members of existing and new population. The one with best fitness is updated as local leader of that particular group and if it is not updating its position for local leader limit, then local leader count is incremented by one.

Step 6: Local leader decision Phase

Suppose the local leader count reaches the local leader limit, then all the members of the group are either randomly initialized or updated with the help of global leader and local leaders.

$$SpMnew(i,j) = SpM(i,j) + rand() * (GL_j - SpM_{ij}) + rand() * (SpM_{ij} - LL_{kj}) \quad (5.13)$$

Step 7: Global leader decision Phase

In this phase, the global limit count is checked for its threshold global leader limit, if it hits the threshold, then global leader will divide the group into two, then three and so on till it reaches the minimum members requirement in the group. Once the maximum number of groups are formed and the position of global leader is not updated, sub groups are combined to form a single group by the global leader.

Eagle strategy: Levy flights with Spider Monkey Optimization Algorithm

1. *Initialize population, X*
2. *Evaluate objective function f(X)*
3. *While (iter<itermax)*
   - *3.1 Coarse global search by levy flights*
     - *Stepsize=0.01*step*(step-best) /*using equation 5.6*/*
     - *X=X+α*stepsize*
     - *Evaluate the objective function /* using equation 5.14*/*
     - *Update population with better fitness*
   - *3.2 Intensive local search by SMO algorithm*
     - *Updated population in (3.1) undergoes all seven phases of SMO algorithm*
     - *Global and local leaders are updated*

   iter=iter+1
4. *Processing of results and validation*

5.3 Problem formulation

In conventional power systems, the secondary control is required to regulate the frequency by tracking the power mismatch between generation and load. In traditional practice, it is done by conventional PI controllers. For effective frequency regulation in case of change in operating conditions, the PI controller gains have to be tuned properly to achieve the desired performance. This chapter proposed Levy based Spider Monkey Algorithm (Levy-SMA) to tune the PI gains for better performance in tracking the power deviations to zero and to test the effectiveness of the proposed algorithm, it has been evaluated and compared with performance metric Integral Time Squared Error (ITSE) value and given by the following equations:

$$ITSE = \int_{0}^{Tsim} t * |\Delta f|^2 \, dt \tag{5.14}$$

Subject to:

$$\left.\begin{aligned} K_{p,\min} \le Kp \le K_{p,\max} \\ K_{i,\min} \le K_i \le K_{i,\max} \end{aligned}\right\} \text{ PI controllers} \tag{5.15}$$

Where $K_{p,\min}$, $K_{i,\min}$ and $K_{p,\max}$, $K_{i,\max}$ are the minimum and maximum values of PI controller gains. $|\Delta f|$ and $Tsim$ are the absolute values of the frequency deviation and total simulation time respectively. The optimization problem is formulated as minimization problem with ITSE as objective function by optimizing K_p and K_i values as the decision variables.

5.4 Simulation results and discussion

This section presents the simulation and discussion on various cases considered for load frequency control of as isolated microgrid. The proposed strategy has been tested on typical microgrid test system shown in Figure 5.1. Frequency control model of the systems is developed in SIMULINK/MATLAB. The cases include the load and generation variation and parametric variation in the system. The sampling period for all cases of simulation is taken as 0.01sec.

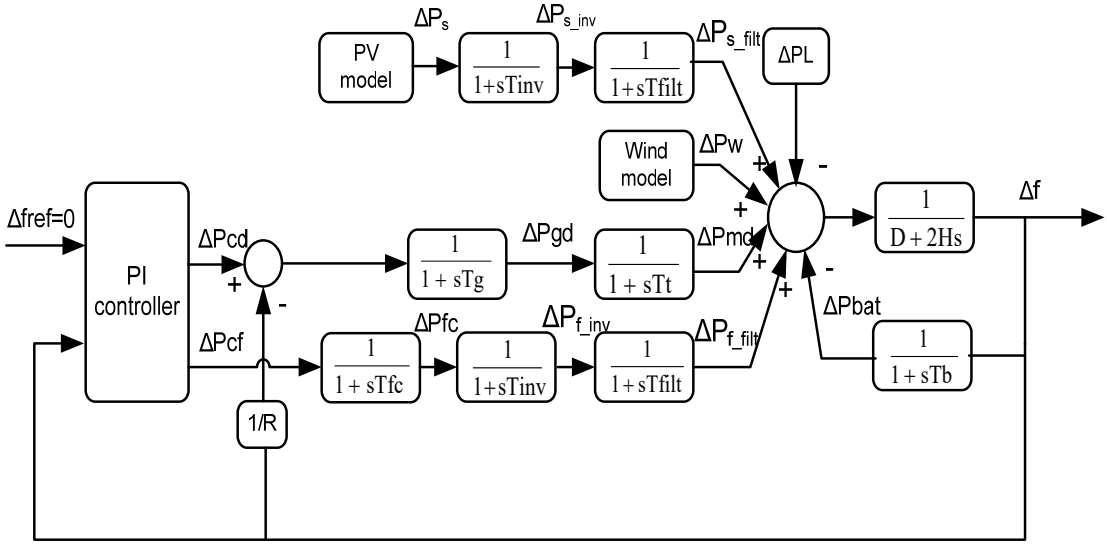

Figure 5.1: Frequency control model of an isolated microgrid with PI controller

Case-1: Base case system response with all DERs

The load frequency control of a microgrid with all sources such as PV, Wind, fuel cell, diesel and battery storage is simulated in this case. This case presents the frequency deviation response of the system with step of 0.02p.u. load change and solar power change i.e. ΔPs taken as 0.2p.u. The mean wind velocity for this case is taken as 7m/s. The frequency regulation is achieved by tuning PI controller gains which are optimized by the proposed algorithm. PI controllers are placed only for the controllable units i.e., diesel units and fuel cell. There are two PI controllers for this system and the corresponding gains are K_{p1}, K_{i1} and K_{p2}, K_{i2} respectively for diesel unit and fuel cell. Figure 5.2 shows the comparison of system response for case-1.

It is clearly understood that the system response with k_p and k_i values obtained by the proposed strategy shows better results when compared to other algorithms. The simulation is carried out with other prominent algorithms such as PSO, Firefly algorithm, Harmony Search algorithm and Spider Monkey Algorithms and the comparison of results validated the superiority of the proposed algorithm. Figure 5.3 shows the comparison of the convergence plot obtained by proposed algorithm with other algorithms. The ITSE value obtained by the proposed algorithm is small and it shows better convergence with less number of iterations whereas other algorithms exhibit premature convergence.

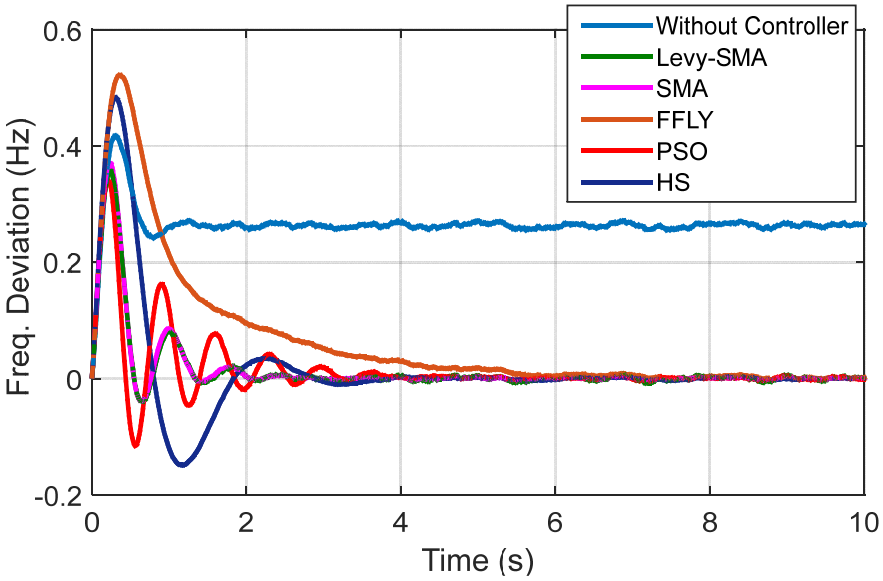

Figure 5.2: Case-1: System response with all micro sources

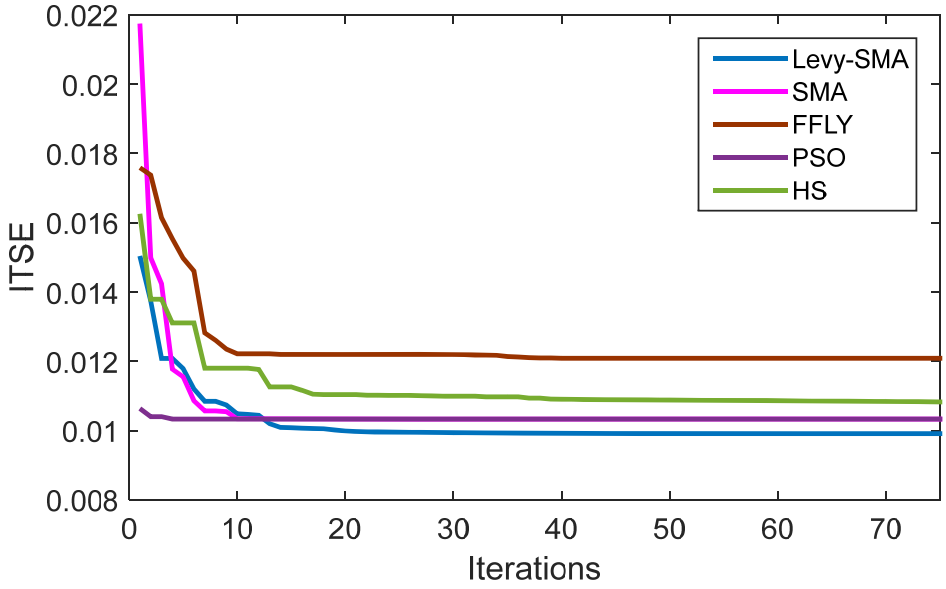

Figure 5.3: Case-1: Comparison of convergence plot

Table 5.1 Performance metric ITSE value for case-1

Algorithms	PI gains				Performance metric (ITSE)
	K_{p1}	K_{i1}	K_{p2}	K_{i2}	
Proposed Levy-SMA	0.6356	5.0000	4.6589	5.0000	0.00991
SMA	0.3349	5.0000	5.0000	5.0000	0.01033
PSO	4.4925	5.0000	5.0000	5.0000	0.01484
HS Algorithm	0.3509	5.0000	5.0000	4.8480	0.04335
Firefly Algorithm	3.0265	5.0000	4.0738	4.0248	0.1158

Table 5.1 provides the consolidated optimized values of K_p and K_i values of PI controllers obtained by each individual algorithm. ITSE values obtained by the proposed algorithm are found to be better when compared to other algorithms.

Case -2: System response with dispatchable DERs

This case studies the frequency regulation in the system when there are only dispatchable units like diesel unit, fuel cell and battery in the system. The load change is taken as 0.02p.u. Here two cases have been examined for frequency control, one with Diesel Engine Generator (DEG) alone and the other including fuel cell contribution in the frequency control. It can be understood that the frequency deviation is considerably reduced with fuel cell participation in the frequency control loop. The system response obtained by the proposed algorithm is compared with other algorithms as shown in Figure 5.4 and the corresponding ITSE values are tabulated in Table 5.2. The contribution of fuel cell in frequency regulation is shown in Figure 5.5.

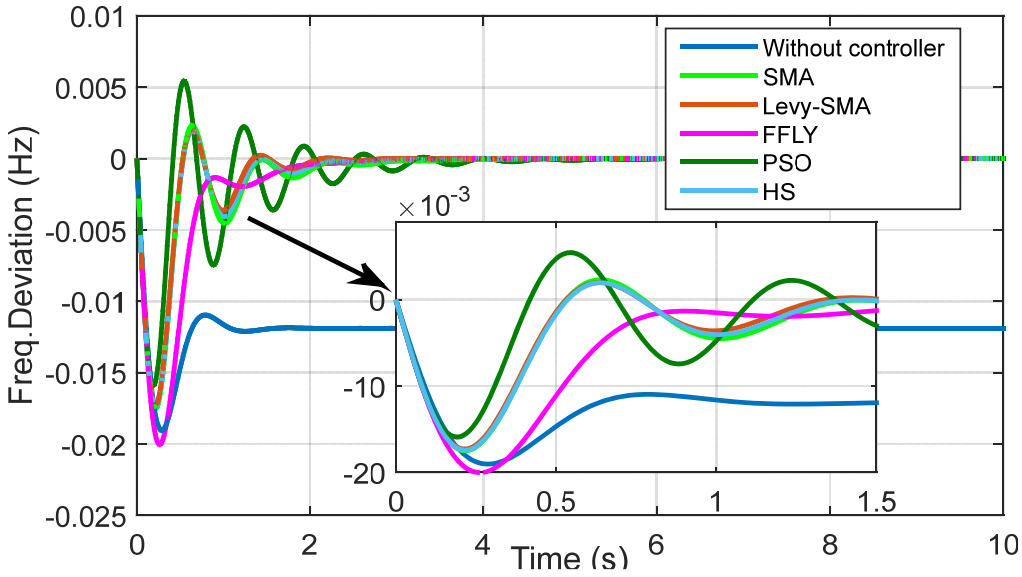

Figure 5.4: Frequency deviation response with dispatchable sources

Table 5.2 Performance metric ITSE value for case-2

Algorithms	PI gains				Performance metric (ITSE)
	K_{p1}	K_{i1}	K_{p2}	K_{i2}	
Proposed Levy-SMA	0.5508	5.0000	4.6573	5.0000	2.039*e-5
SMA	3.5120	4.2121	2.6975	4.3328	2.546*e-5
PSO	4.8661	5.0000	5	5.0000	2.981*e-5
HS Algorithm	1.1496	3.9802	4	5.0000	2.256*e-5
Firefly Algorithm	1.5657	5.0000	4.4981	5.0000	4.327*e-5

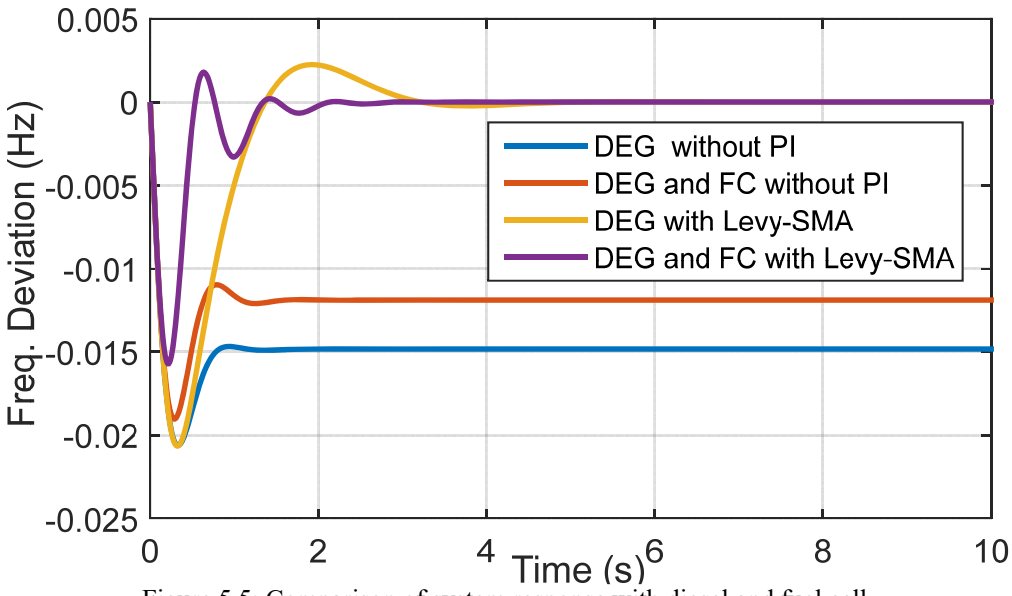

Figure 5.5: Comparison of system response with diesel and fuel cell

Case-3: System response with series of step load variation

In this case, the response of the system is obtained for series step changes in the load. This case demonstrates the robustness of the proposed algorithm for successive changes that exist in the system. The load changes are implemented with subsequent increase and decrease in the value of ΔP_L as shown in Figure 5.6. The system response obtained for this case has been shown in Figure 5.7 and it compares the response obtained by other algorithm. The evaluating performance index values are also compared and tabulated in Table 5.3.

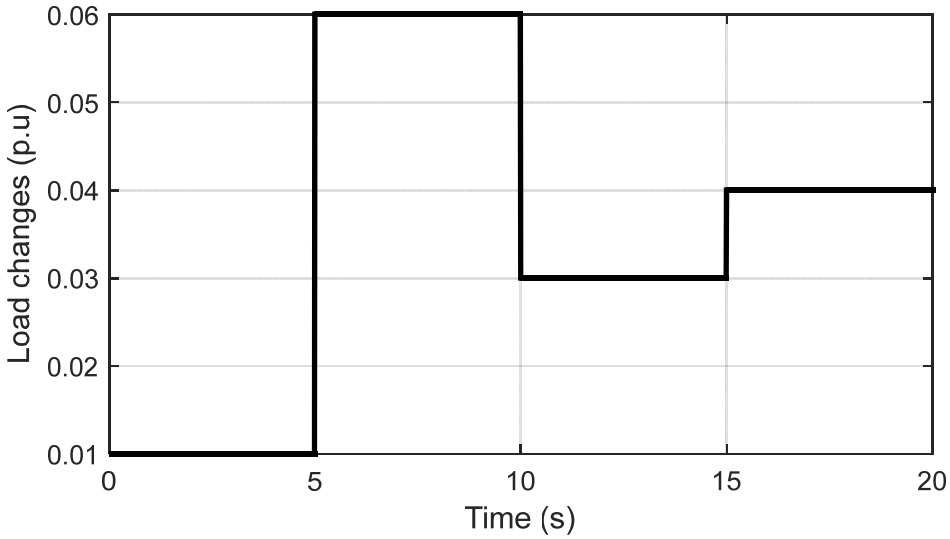

Figure 5.6: Step load variation

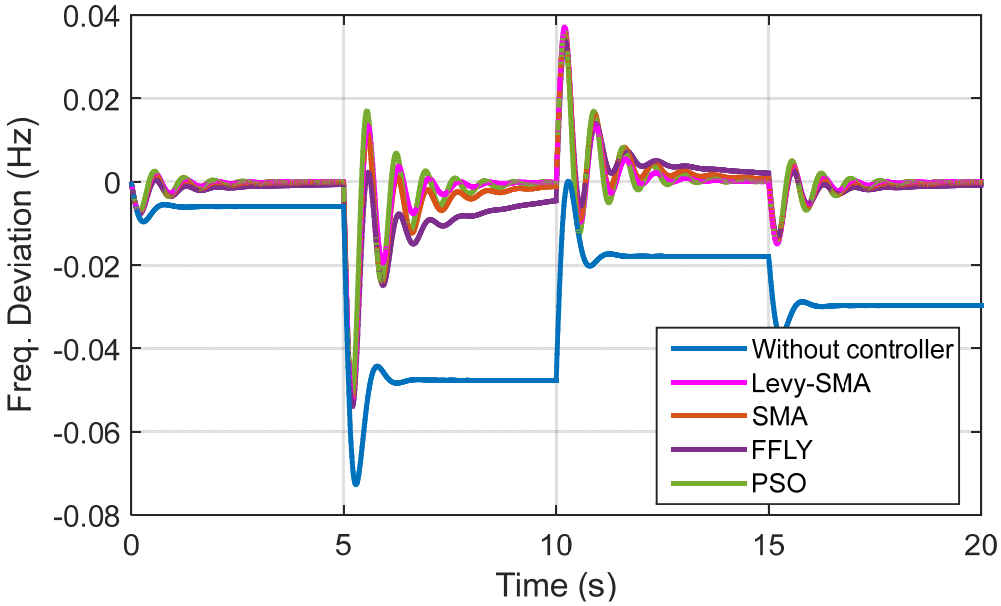

Figure 5.7: Comparison of frequency deviation response for multiple load steps

Table 5.3 Performance metric ITSE value for case-3

Algorithms	PI gains				Performance metric (ITSE)
	K_{p1}	K_{i1}	K_{p2}	K_{i2}	
Proposed Levy-SMA	3.1946	5.0000	5.0000	5.0000	0.0083
SMA	5.0000	3.5846	4.0706	3.5935	0.0090
PSO	5.0000	5.0000	5.0000	4.1999	0.0085
Firefly Algorithm	3.1822	5.0000	4.9910	4.9073	0.01122

Case-4: System response with wind perturbation of 2m/s

This case presents the system response for sudden wind perturbations of 2m/s from its mean wind velocity that exists for 6s in the system. The wind gust component of magnitude 2m/s is introduced for 6s in the wind velocity and the mean velocity of the wind is taken as 6.5m/s. The change in solar power is maintained constant at 0.05p.u. and load change of 0.02p.u. The system response by the proposed levy-SMA and the comparison with other algorithms are shown in Figure 5.8. The performance metric, integral time squared error (ITSE) is evaluated for all algorithm and compared in Table 5.4. The table shows that the value of ITSE is better in case of proposed algorithm.

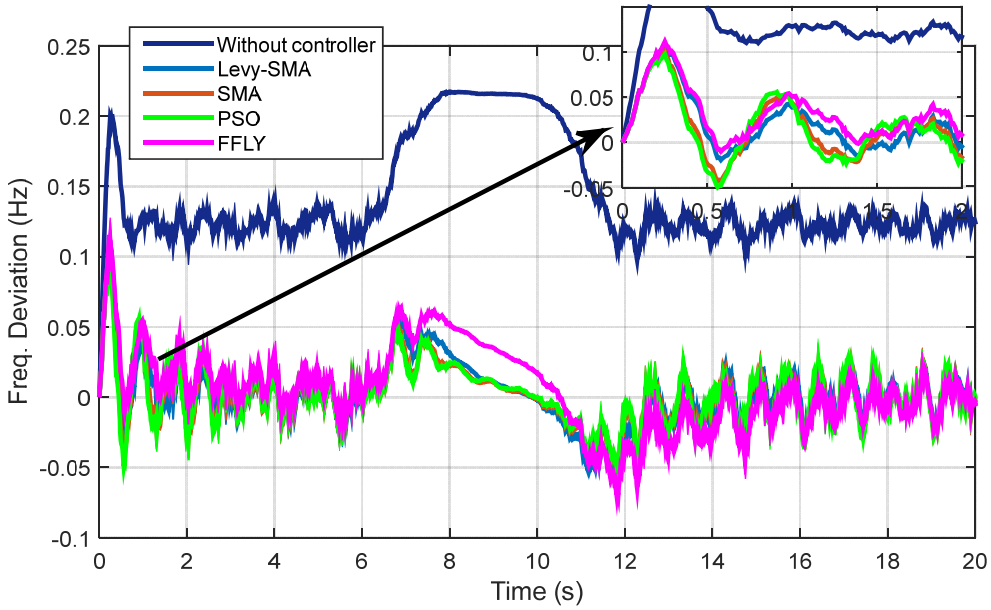

Figure 5.8: Comparison of system response with wind perturbations for 6secs

Table 5.4 Performance metric ITSE value for case-4

Algorithms	PI gains				Performance metric (ITSE)
	K_{p1}	K_{i1}	K_{p2}	K_{i2}	
Proposed Levy-SMA	3.6360	5.0000	5.0000	5.0000	0.0570
SMA	4.3291	4.3265	2.4781	4.1848	0.0653
PSO	2.4130	5.0000	5.0000	5.0000	0.0575
Firefly Algorithm	5.0000	5.0000	5.0000	5.0000	0.1225

Case-5: Parametric variation in the system

This case presents system response with parametric variation and studies the superiority of the proposed levy-SMA method by comparing with other algorithms. The parametric variation is incorporated as follows: R=+30%; D=-40%; H=+50%; T_t= -50%; T_g=+50%; Tb=-45%. The change is solar power is kept as 0.05p.u. and the load change is taken as 0.02p.u. whereas the wind velocity is maintained at 6.5m/s. The frequency deviation response is shown in Figure 5.9 and corresponding ITSE value comparison is presented in Table 5.5. The comparison shows that proposed levy-SMA is better when compared to all other algorithm presented in this chapter.

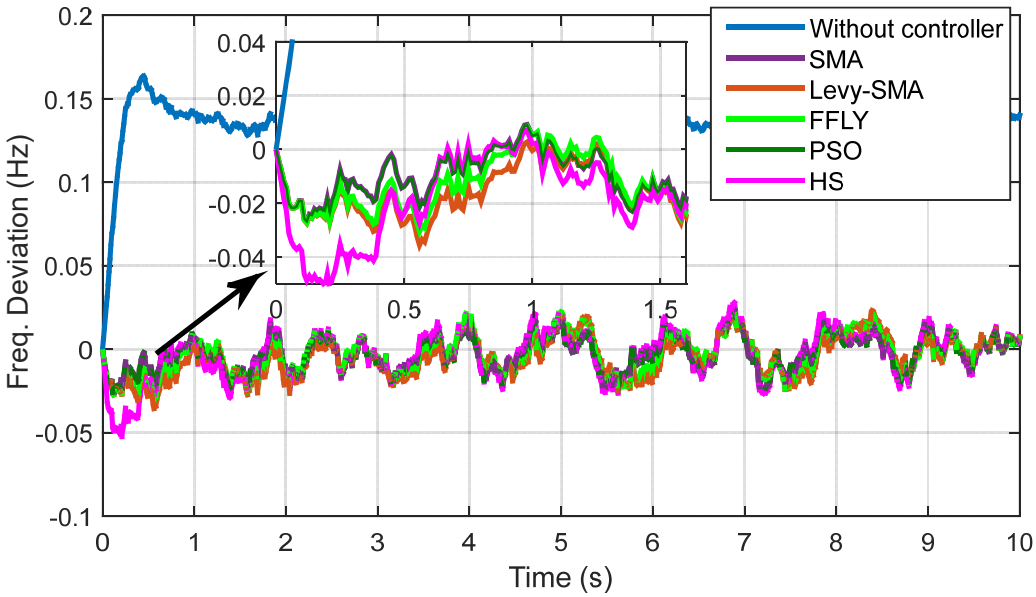

Figure 5.9: Comparison of system response for parametric variation

Table 5.5 Performance metric ITSE value for case-5

Algorithms	PI gains				Performance metric (ITSE)
	K_{p1}	K_{i1}	K_{p2}	K_{i2}	
Proposed Levy-SMA	5.000	0.1000	5.0000	4.4093	0.0050
SMA	2.2014	4.0216	4.7123	0.0619	0.0054
PSO	5.0000	4.7975	5.0000	0.1000	0.0051
Firefly Algorithm	5.0000	0.1	5.0000	5.0000	0.00617

5.5 Summary

In this chapter, a new eagle strategy by combining levy flights and spider monkey algorithm is proposed. The proposed strategy is utilized for optimizing the gains of PI controllers employed in the frequency control of the microgrid. The PI controllers are employed only for the dispatchable sources such as diesel engine and fuel cells. The proposed strategy implementation is a two-fold search process i.e., coarse search by levy flights and an intensive local search by spider monkey algorithm. The system response for different cases have been simulated and simulation results for various instances confirms the better performance of proposed algorithm compared with a few existing prominent algorithms. The performance index ITSE value is evaluated over simulation time to ascertain the superiority of the proposed strategy with few prominent algorithms

such PSO, Firefly Algorithm, and Harmony Search. This optimization algorithm is inspired from the foraging behavior of the spider monkey that includes the seven steps of implementation in the search procedure, which intensifies the search process resulting in promising solutions.

Chapter 6

Fuzzy Adaptive Model Predictive Control for Load Frequency Control of an Isolated Microgrid

Chapter 6

6 Fuzzy Adaptive Model Predictive Control for Load Frequency Regulation of an Isolated Microgrid

6.1 Introduction

This chapter presents a novel approach of fuzzy adaptive model prediction based load frequency control of an isolated microgrid. A generalized state space model of a typical isolated microgrid having controllable and uncontrollable generating power sources is derived and the same has been utilized to predict the future output and control inputs for the microgrid frequency control. The Model Predictive Control (MPC) is implemented with single input multi-output system model based on the controllable Distributed Energy Resources (DERs) in the microgrid. Apart from this, rule based fuzzy controller is employed to fuzzify the tuning parameter present in the cost function of MPC, which plays an important role in minimizing the frequency deviation in the system. The effectiveness of this proposed control has been evaluated with performance index ITSE (Integral time square error) value.

6.2 Outline of model predictive control (MPC)

An MPC is a model based advanced control strategy that employs an optimization procedure at each sampling time over prediction horizon to calculate the optimal control actions. As there is extensive literature on MPC, this section intends to presents only the outline of MPC [107].

The general discrete state-space model representation is given by:

$$x(k+1) = A_d x(k) + B_d u(k) + E_d w(k) \tag{6.1}$$

$$y(k) = C_d x(k) + D_d u(k) \tag{6.2}$$

Where, u - input variable vector; y - Process output vector; x - State variable vector; since moving horizon control requires current information of the plant for the prediction and control, it is implicitly assumed that $u(k)$ cannot affect output $y(k)$ but $u(k-1)$ at the k^{th} instant can. So, on taking difference on both sides of (6.1) and rearranging, we obtain

$$\begin{bmatrix} \Delta x(k+1) \\ y(k+1) \end{bmatrix} = A \begin{bmatrix} \Delta x(k) \\ y(k) \end{bmatrix} + B\Delta u(k) + E\Delta w(k) \tag{6.3}$$

$$y(k) = C \begin{bmatrix} \Delta x(k) \\ y(k) \end{bmatrix} \tag{6.4}$$

Where,

$$A = \begin{bmatrix} A_d & o_d^T \\ C_d A_d & 1 \end{bmatrix};\ B = \begin{bmatrix} B_d \\ C_d B_d \end{bmatrix};\ E = \begin{bmatrix} E_d \\ C_d E_d \end{bmatrix};\ C = \begin{bmatrix} o_d^T & 1 \end{bmatrix}$$

Where A, B and C are augmented state space model used in the design of predictive control. Since the disturbance in current step is not reflected in the future, the disturbance matrix is omitted in the predicting window. $o_d = [\overbrace{0 \quad 0}^{m} \quad \overbrace{0 \quad 0}]$ and m is the number of state variables.

The difference of future control trajectory at sampling instant k_i is given by

$$\Delta u(k_i), \Delta u(k_i+1), , \quad , , \Delta u(k_i + Nc - 1) \tag{6.5}$$

The rest of $\Delta u(k)$ for $k = Nc, Nc+1, ..., Np$ is assumed to be zero. Where Nc is the control horizon, it gives the number of future control inputs to be predicted. With given $x(k_i)$, future state variables and output are predicted for Np number of samples. The output is represented in compact form [107].

$$Y = Fx(k_i) + \Phi\Delta U \tag{6.6}$$

$$F = \begin{bmatrix} CA \\ CA^2 \\ CA^3 \\ . \\ . \\ CA^{Np} \end{bmatrix};\qquad \Phi = \begin{bmatrix} CB & 0 & 0 & . & . & 0 \\ CAB & CB & 0 & & & 0 \\ CA^2B & CA^2B & CB & & & 0 \\ . & . & & & & \\ . & . & & & & \\ CA^{Np-1}B & CA^{Np-2}B & CA^{Np-3}B & . & . & CA^{Np-Nc}B \end{bmatrix};$$

For a given reference signal $r(k_i)$ at sample k_i, the objective is to predict an output close to the reference signal. Moreover, this $r(k_i)$ remains constant in the optimization window. The control objective is given by:

$$\text{Min } J = (Y_s - Y)^T (Y_s - Y) + \Delta U^T \overline{R}_{in} \Delta U \tag{6.7}$$

Then the optimal control vector ΔU has been computed using $\frac{\partial J}{\partial \Delta U} = 0$;

$$\Delta U = (\Phi^T \Phi + \overline{R})^{-1} \Phi^T (Y_s - Fx(k_i)) \tag{6.8}$$

$$\overline{R}_{in} = R_w * I_{Nc*Nc};\ Y_s = [1 \quad 1 \quad . \quad 1]^T r(k_i) \tag{6.9}$$

6.3 MPC implementation for load frequency control of an isolated microgrid

The simplified load frequency model of a typical microgrid is considered in this thesis is shown in Figure 6.1. The microgrid consists of a diesel unit, fuel cell, wind, solar and battery storage of ratings given in [85]. The frequency control in the microgrid is achieved by predicting the future outputs and control signals i.e. frequency deviation and control actions to the controllable units respectively. The renewable sources are assumed to be operated at maximum power point. Hence, diesel unit and fuel cell are considered as controllable units in the microgrid. The prediction was accomplished by using model predictive control (MPC) design where a state space model of the system is used. From the model of the system shown in Figure 6.1, the dynamics of the system is defined with nine state equations with nine state variables for the microgrid considered. The nine state variables for the microgrid are explained with system dynamics in equations (6.10) - (6.18):

$$\dot{\Delta f} = \frac{1}{2H}(\Delta P_{s\_filt} + \Delta P_{md} + \Delta P_w - \Delta P_L + \Delta P_{f\_filt} - \Delta P_{bat} - D * \Delta f) \tag{6.10}$$

$$\Delta \dot{P}_{s\_inv} = \frac{1}{T_{inv}}\left(\Delta P_s - \Delta P_{s\_inv}\right) \tag{6.11}$$

$$\Delta \dot{P}_{s\_filt} = \frac{1}{T_{filt}}\left(\Delta P_{s\_inv} - \Delta P_{s\_filt}\right) \tag{6.12}$$

$$\Delta \dot{P}_{gd} = \frac{1}{T_g}\left(\Delta P_{cd} - \frac{\Delta f}{R} - \Delta P_{gd}\right) \tag{6.13}$$

$$\Delta \dot{P}_{md} = \frac{1}{T_t}\left(\Delta P_{gd} - \Delta P_{md}\right) \tag{6.14}$$

$$\Delta \dot{P}_{fc} = \frac{1}{T_{fc}}\left(\Delta P_{cf} - \frac{\Delta f}{R} - \Delta P_{fc}\right) \tag{6.15}$$

$$\dot{\Delta P}_{f\_inv} = \frac{1}{T_{inv}}\left(\Delta P_{fc} - \Delta P_{f\_inv}\right) \tag{6.16}$$

$$\dot{\Delta P}_{f\_filt} = \frac{1}{T_{filt}}\left(\Delta P_{f\_inv} - \Delta P_{f\_filt}\right) \tag{6.17}$$

$$\dot{\Delta P}_{bat} = \frac{1}{T_b}\left(\Delta f - \Delta P_{bat}\right) \tag{6.18}$$

In compact form, the state space model of above system dynamics and the output equation can be given as:

$$\begin{bmatrix} \dot{\Delta f} \\ \dot{\Delta P}_{s\_inv} \\ \dot{\Delta P}_{s\_filt} \\ \dot{\Delta P}_{gd} \\ \dot{\Delta P}_{md} \\ \dot{\Delta P}_{fc} \\ \dot{\Delta P}_{f\_inv} \\ \dot{\Delta P}_{f\_filt} \\ \dot{\Delta P}_{bat} \end{bmatrix} = \begin{bmatrix} -D/2H & 0 & 1/2H & 0 & 1/2H & 0 & 0 & 1/2H & -1/2H \\ 0 & -1/T_{inv} & 0 & 0 & 0 & 0 & 0 & 0 & 0 \\ 0 & 1/T_{filt} & -1/T_{filt} & 0 & 0 & 0 & 0 & 0 & 0 \\ -1/RT_g & 0 & 0 & -1/_{Tg} & 0 & 0 & 0 & 0 & 0 \\ 0 & 0 & 0 & 1/T_t & -1/T_t & 0 & 0 & 0 & 0 \\ -1/RT_{fc} & 0 & 0 & 0 & 0 & -1/T_{fc} & 0 & 0 & 0 \\ 0 & 0 & 0 & 0 & 0 & 1/T_{inv} & -1/T_{inv} & 0 & 0 \\ 0 & 0 & 0 & 0 & 0 & 0 & 1/T_{filt} & -1/T_{filt} & 0 \\ 1/T_b & 0 & 0 & 0 & 0 & 0 & 0 & 0 & -1/T_b \end{bmatrix} \begin{bmatrix} \Delta f \\ \Delta P_{s\_inv} \\ \Delta P_{s\_filt} \\ \Delta P_{gd} \\ \Delta P_{md} \\ \Delta P_{fc} \\ \Delta P_{f\_inv} \\ \Delta P_{f\_filt} \\ \Delta P_{bat} \end{bmatrix} + \begin{bmatrix} 0 & 0 \\ 0 & 0 \\ 0 & 0 \\ 1/T_g & 0 \\ 0 & 0 \\ 0 & 1/T_{fc} \\ 0 & 0 \\ 0 & 0 \\ 0 & 0 \end{bmatrix} \begin{bmatrix} \Delta P_{cd} \\ \Delta P_{cf} \end{bmatrix} + \begin{bmatrix} -1/2H & 1/2H & 0 \\ 0 & 0 & 1/T_{inv} \\ 0 & 0 & 0 \\ 0 & 0 & 0 \\ 0 & 0 & 0 \\ 0 & 0 & 0 \\ 0 & 0 & 0 \\ 0 & 0 & 0 \\ 0 & 0 & 0 \end{bmatrix} \begin{bmatrix} \Delta P_L \\ \Delta P_w \\ \Delta P_s \end{bmatrix}$$

…… (6.19)

$$\Delta f = \begin{bmatrix} 1 & 0 & 0 & 0 & 0 & 0 & 0 & 0 & 0 \end{bmatrix} \begin{bmatrix} \Delta f & \Delta P_{s\_inv} & \Delta P_{s\_filt} & \Delta P_{gd} & \Delta P_{md} & \Delta P_{fc} & \Delta P_{f\_inv} & \Delta P_{f\_filt} & \Delta P_{bat} \end{bmatrix}^T$$

..... (6.20)

The frequency regulation is achieved only through the controllable generating units in the system, therefore, the diesel unit and the fuel cell inputs are taken as controlled variables in the MPC formulation to minimize a control objective function to measure the predicted performance. Mathematically, it is formulated as follows:

$$\text{Min } J = (\Delta f^{ref} - \Delta f^{pred})^T (\Delta f^{ref} - \Delta f^{pred}) + \begin{bmatrix} \Delta P_{cd} \\ \Delta P_{cf} \end{bmatrix}^T \overline{R}_{in} \begin{bmatrix} \Delta P_{cd} \\ \Delta P_{cf} \end{bmatrix} \tag{6.21}$$

The first term in the objective function expression refers to the minimization of error between predicted output and the reference point whereas the second term considers the impact of predicted control input vectors in making J as small as possible. $\overline{R}_{in} = R_w * I_{Nc*Nc}$, is a diagonal matrix where $R_w$is tuning parameter for the desired closed loop performance. The prediction horizon for the output is taken as 10 time steps and the control horizon for the

control input is taken as 2 time steps with a sampling time step of 0.01s. These values are considered from the literature of typical load frequency problems using MPC.

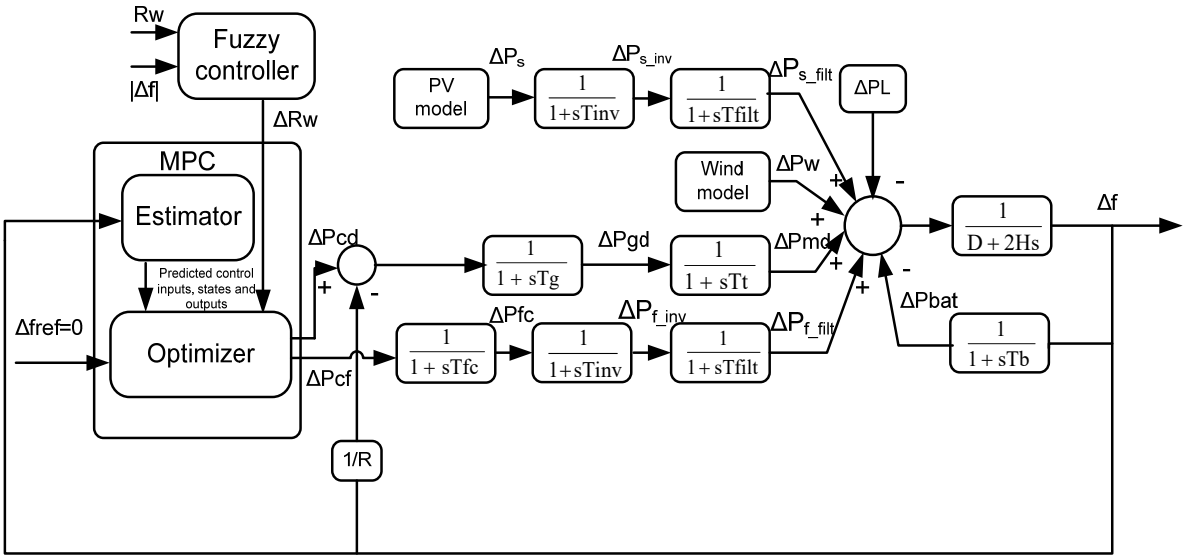

Figure 6.1: Load frequency control model of an isolated microgrid with fuzzy adaptive MPC

6.4 Fuzzy inference system for parameter (R_w) tuning

MPC is a simple and straightforward procedure with less computational efforts. However, it is parameter driven and it needs to be properly chosen for better performance of MPC. In MPC algorithm, we have some parameters - Prediction horizon (Np), Control horizon (Nc), Sampling time (Ts) and Input parameter (R_w). Adaptability of the MPC is achieved only through the extensive analysis of the qualitative and quantitative relationship of these parameters with the behavior of the control algorithm of MPC.

The impact of these parameters on MPC behavior is randomly studied by trial and error method for load frequency control. It is found that optimal values of these parameters for ideal behavior of MPC remains unchanged for different case studies except R_w. Thus, the idea of fuzzy adaptive MPC is proposed in the chapter where 'R_w' is a scalar and dynamically adjusted by the fuzzy controller over each prediction window of MPC keeping other procedures unchanged.

Three main components of fuzzy logic control are Fuzzification, Fuzzy inference engine (fuzzy rules) and defuzzification, which are described in the following subsections:

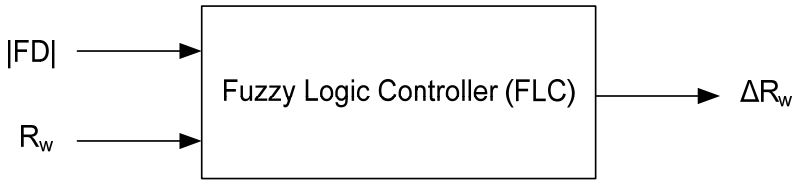

Figure 6.2: Inputs and output of fuzzy logic controller

6.4.1 Fuzzification

Fuzzification process is mapping the crisp value of inputs to linguistic variables using membership functions. Here inputs to fuzzification block are: Magnitude of Frequency Deviation (FD) and input parameter (R_w) and the output is the change in input parameter (ΔR_w) shown in Figure 6.2. The triangular memberships functions are considered for fuzzy mapping and the five linguistic variables are considered for each input variable. such as VS (very small), S (small), M (medium, B (big), VB (very big) whereas the output variable (ΔR_w) is represented in five linguistic values such as ZE (zero error), PS (positive small), PM (positive medium), PB (positive big), PL (positive large). The membership functions for inputs and outputs are shown in Figure 6.3. The universe of discourse for the magnitude of frequency deviation is taken as 0-0.25Hz whereas for R_w and ΔR_w it is taken as 1-75 and 1-25 respectively.

6.4.2 Fuzzy Inference System: Fuzzy Rules formulation

Fuzzy rules are formulated using Mamdani-type fuzzy rules which comprise "IF/THEN" conditional statements. In this work, a total of 25 (5×5=25) rules are formulated using "IF/THEN" statements with the membership functions of two input variables and one output variable, which are tabulated in Table 6.1.

In this chapter, the impact of parameter R_w in the cost function of MPC formulation is studied on load frequency control by trial and error method. The system response for different values of R_w is shown in Figure 6.4. Thus, based on the relationship of parameter R_w with the behaviour of the control algorithm of MPC, the logic for the rule base is established. Accuracy in solution is achieved by using more tuning rules at the cost of computational complexity. Since frequency deviation is expected to be tracked closely to the minimum value as far as possible, 25 rules are designed to determine the change in input parameter (ΔR_w). For example:

Rule 1: IF |FD| is S (small) AND R_w is S (small) THEN the output ΔR_w is PS (positive small). As the frequency deviation is small, it can still be reduced to very small values by increasing R_w to a small extent that corresponds to PS (positive small) in output of ΔR_w.

Rule 2: IF |FD| is B (big) AND R_w is S (small) THEN the output ΔR_w is PL (positive large). The frequency deviation is big and it demands a higher increment in R_w that corresponds to PS (positive small) in the output ΔR_w. All other rules are similarly fixed based on the logic established between the inputs and outputs.

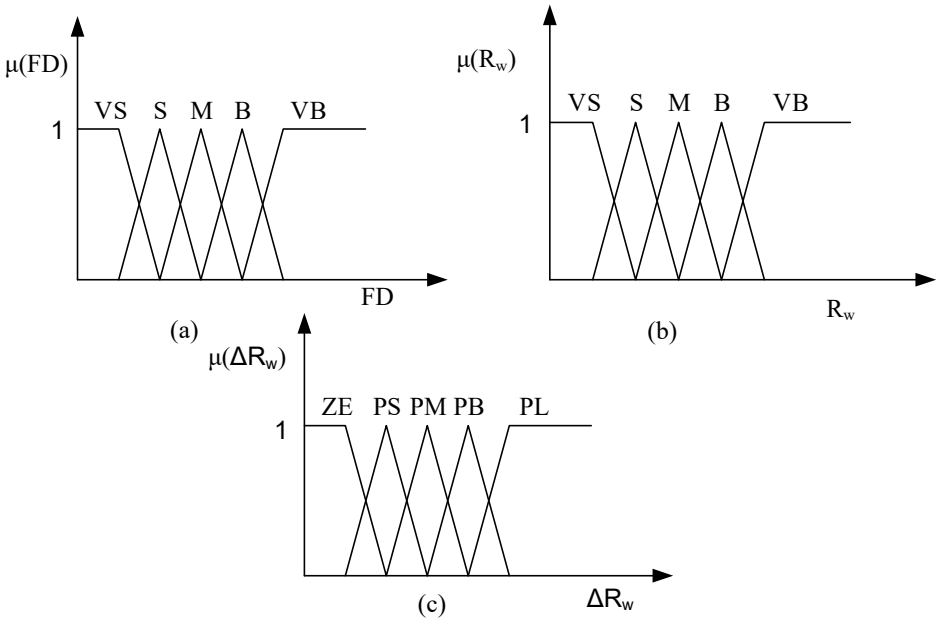

Figure 6.3: Membership Functions a) Magnitude of Frequency Deviation (|FD|)
b) Input parameter (R_w) c) Change in R_w (ΔR_w)

6.4.3 Defuzzification

There are two input variables, R_w and ΔR_w, with triangular membership functions, So, among the 25 designed rules, at any instant, a maximum of four rules may fire and a minimum of one rule will fire. The output i.e. frequency deviation |FD| obtained from the fuzzy controller is fuzzy in nature, so defuzzification is required to convert from fuzzy to crisp value. Centroid method is used here for defuzzification of inputs and output. The defuzzified value of output denoted using Center Of Gravity (COG) is defined as:

$$\Delta R_w^{*} = \frac{\sum_{i=1}^{n} \Delta R_w * \mu(\Delta R_w)}{\sum_{i=1}^{n} \mu(\Delta R_w)} \tag{6.22}$$

where, ΔR_w^{*} - Defuzzified value of output; $\mu(\Delta R_w)$ - Membership function of output

n- number of sample element.

Table 6.1 Fuzzy rules for variation of ΔR_w

Rules	Input variables		Output
	|FD|	R_w	ΔR_w
1	VS	VS	ZE
2	S	VS	PS
3	M	VS	PM
4	B	VS	PB
5	VB	VS	PL
6	VS	S	ZE
7	S	S	PS
8	M	S	PM
9	B	S	PB
10	VB	S	PL
11	VS	M	ZE
12	S	M	PS
13	M	M	PM
14	B	M	PB
15	VB	M	PL
16	VS	B	ZE
17	S	B	PS
18	M	B	PM
19	B	B	PB
20	VB	B	PL
21	VS	VB	ZE
22	S	VB	PS
23	M		PM
24	B	VB	PB
25	VB	VB	PL

6.5 Simulation results and discussion

This section presents the simulation and discussion of various cases of load frequency control in a typical isolated microgrid. The cases include the load and generation variation and parametric variation in the system. All the cases have been compared to the system response with constant Rw value of 15, which is chosen randomly from Figure 6.4.

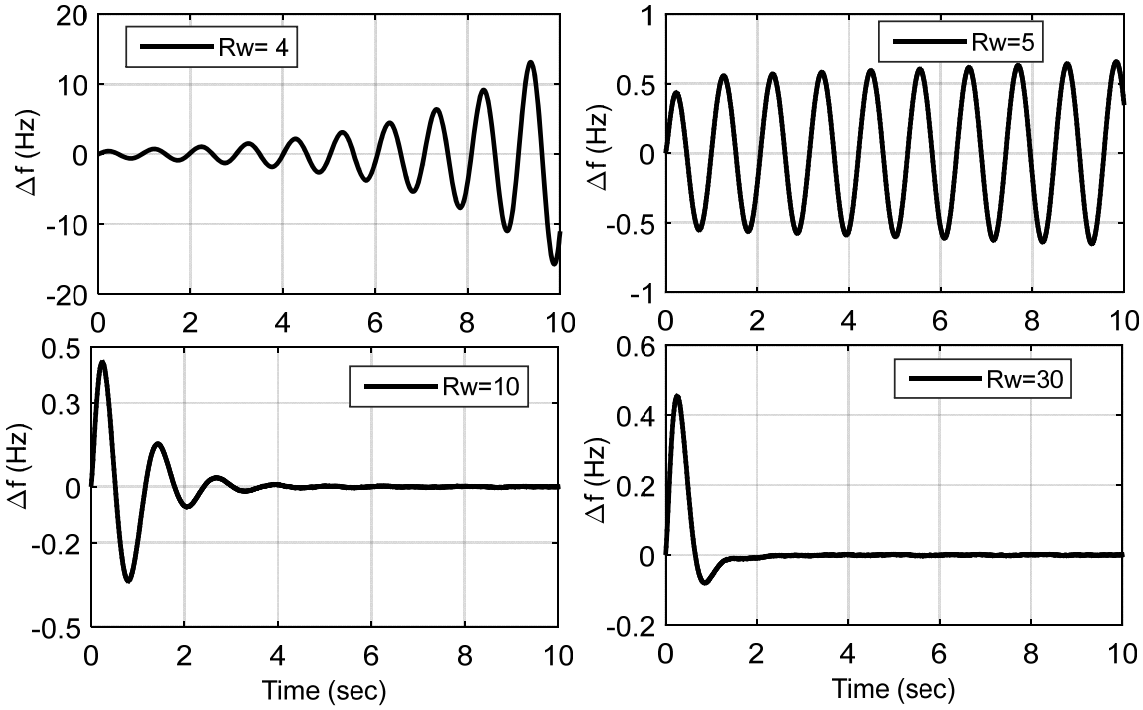

Figure 6.4: System response of the microgrid for different values of R_w

Case-1: Base case system response with all DERs

The load frequency control of a microgrid with all sources such as PV, Wind, fuel cell, diesel and battery storage is simulated in this case. This case presents the frequency deviation response of the system with step of 0.02 p.u load change and solar power change i.e. ΔPs taken as 0.2 p.u. The mean wind velocity for this case is taken as 7m/s. Appropriate value of R_w is selected by the fuzzy controller using rule base system. The comparison of frequency deviation response is shown in Figure 6.5(a). The proposed fuzzy MPC gives better and faster response when compared to PI controller. Figure 6.5(b) shows the response of cost function evaluated in the MPC procedure, which has to be minimized to achieve the desired frequency response in the system. Since it is an isolated microgrid, the frequency regulation is supposed to be taken care of by the dispatchable diesel unit and the fuel cell and thus become the controlled outputs from the MPC block. The response of control inputs i.e. change in diesel and fuel cell units is shown in Figure 6.5(c) and (d) respectively. The simulation period and sampling time are taken as 10s and 0.01s respectively. The prediction horizon and the control horizon are taken as 10 and 2 time steps respectively. The optimal R_w value from the proposed MPC is 38.5 for this case.

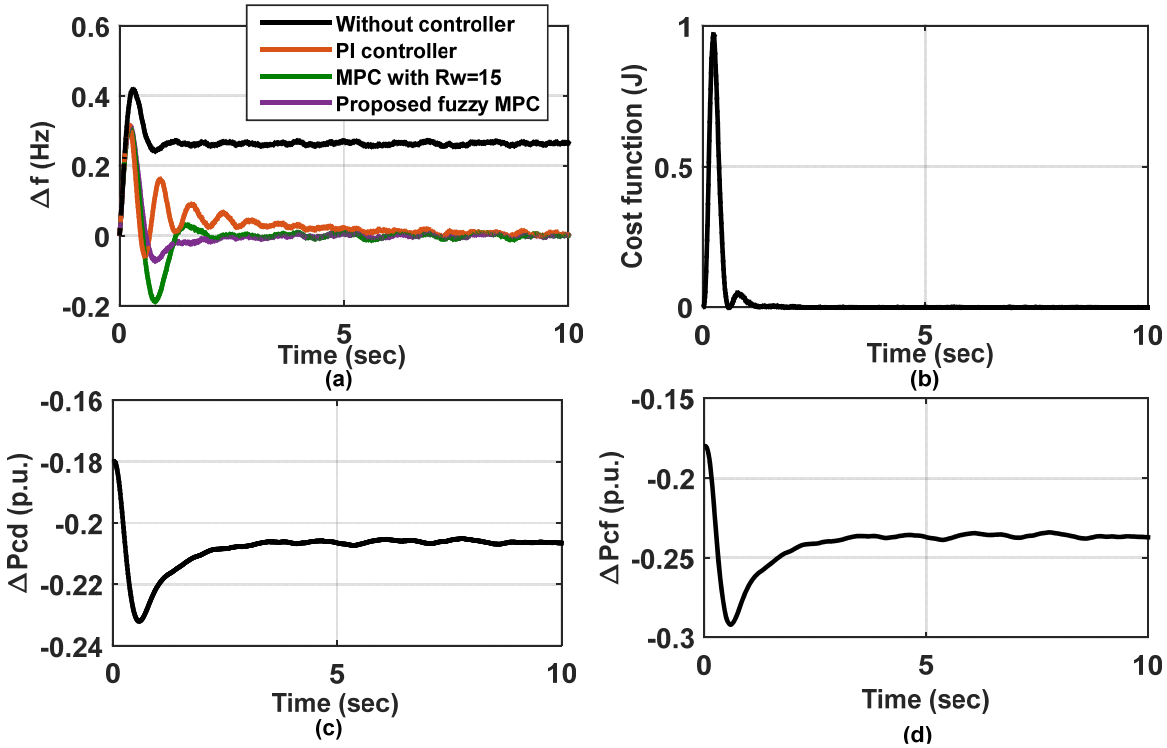

Figure 6.5: (a).Comparison of system response of the microgrid for case-1 (b). Response of Cost functions of MPC over simulation period for case-1 (c) & (d). Response of control inputs to diesel and fuel cell for case-1

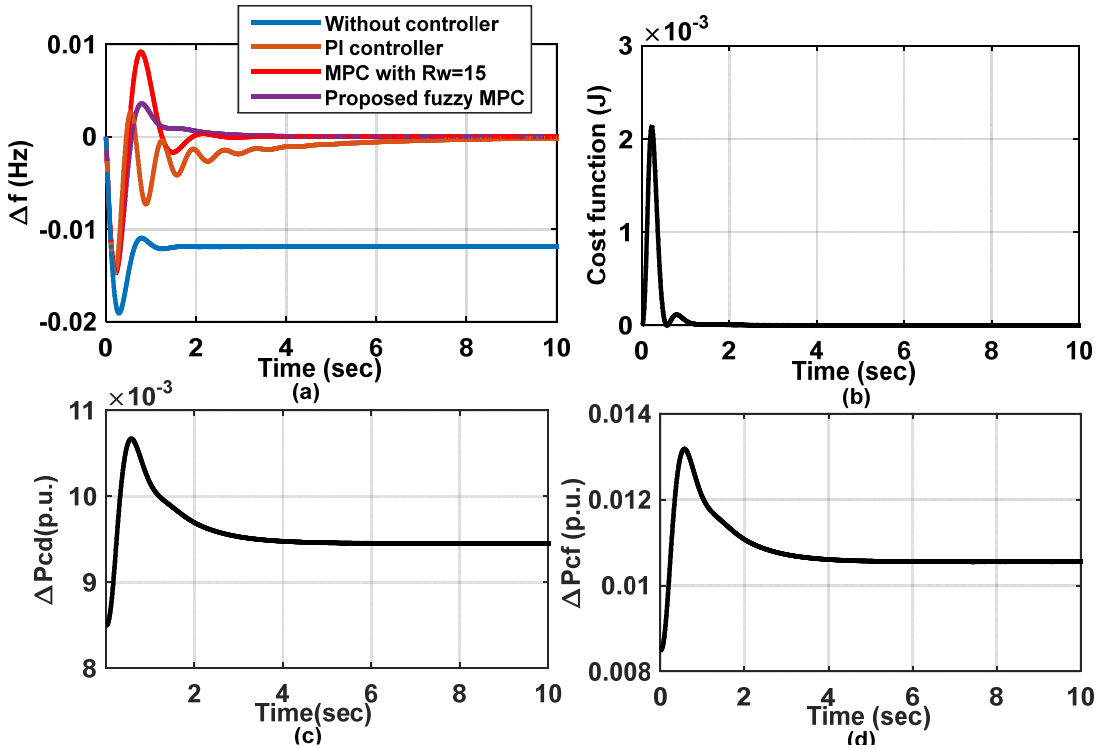

Figure 6.6: (a).Comparison of system response of the microgrid for case-2 (b). Response of Cost functions of MPC over simulation period for case-2 (c) & (d). Response of control inputs to diesel and fuel cell for case-2

Case-2: System response with dispatchable DERs

This case studies the frequency regulation in the system when there are only dispatchable units such as diesel unit, fuel cell and battery in the system. The load change is 0.02p.u. The comparison of system response is shown in Figure 6.6(a). Since there are only two dispatchable generation units in this case, the response shows the negative frequency deviation for the load change. The corresponding response of cost function and the change in control inputs are respectively shown in Figure 6.6(b) and Figure 6.6(c) and (d) respectively. The tuned R_w value for this case is 41. There is increase in the control inputs to reduce the frequency deviation in the system. The simulation period and sampling time is taken as 10s and 0.01s respectively.

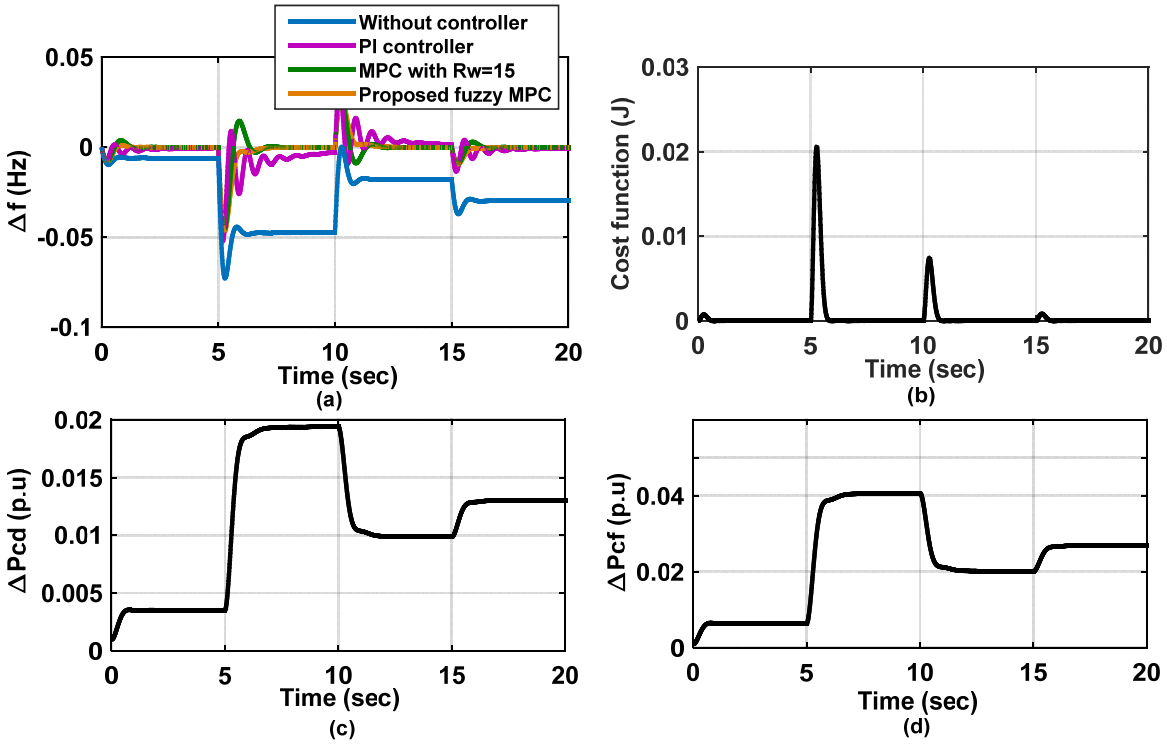

Figure 6.7: (a) Comparison of system response of the microgrid for case-3 (b). Response of Cost functions of MPC over simulation period for case-3 (c) & (d). Response of control inputs to diesel and fuel cell for case-3

Case-3: System response with series of step load variation

This case evaluates the system response of the microgrid with series step changes in the load. The load changes are implemented with increase and decrease in value of ΔP_L. The system response for this case is shown in Figure 6.7(a). Figure 6.7(b) and Figure 6.7(c) and (d) shows the response of cost function and control inputs respectively for the step load

variation in the system. The control inputs are accordingly varied by MPC to meet the load changes for minimum frequency deviation in the system. The optimal value of R_w is found to be 30 for this case.

Case-4: System response with wind perturbation of 2m/s

In this case, the wind gust component of magnitude 2m/s is introduced for 6s in the wind velocity and the mean velocity of the wind is taken as 6.5m/s. The change in solar power is maintained constant at 0.05p.u. and load change of 0.02p.u. The system response for this case is shown in Figure 6.8(a). The performance of the proposed method is better and faster than PI controller. Corresponding cost function and the control inputs are shown in Figure 6.8(b) and Figure 6.8(c) and (d) respectively. The control inputs to diesel and fuel cell are lowered by MPC when there is an increase in wind power generation due to increase in wind velocity in the system. The optimized value of R_w is found to be 16.5 for this case.

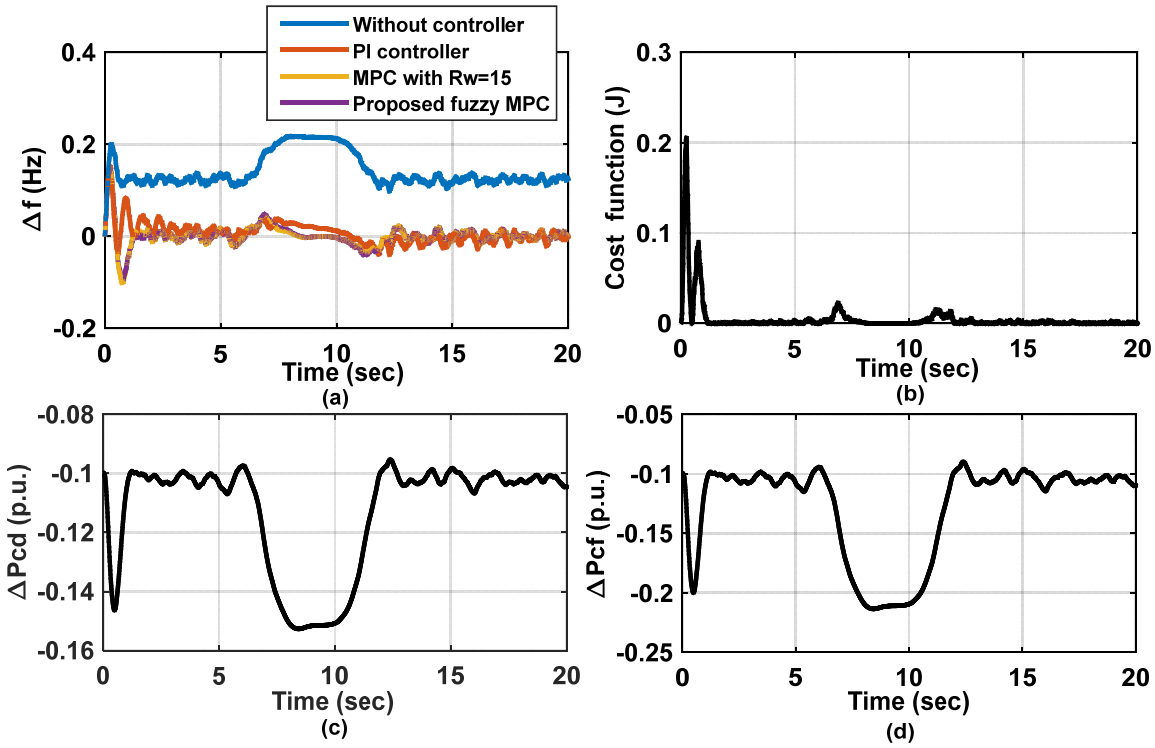

Figure 6.8: (a) Comparison of system response of the microgrid for case-4 (b). Response of Cost functions of MPC over simulation period for case-4 (c) & (d). Response of control inputs to diesel and fuel cell for case-4

Case-5: System response with step Changes in solar power (ΔP_s)

This case considers a series step increase in solar power. In this case, the wind power change (ΔP_w) is simply taken as 0.05p.u. throughout the simulation and the load change of

0.02p.u. The corresponding system response is shown in Figure 6.9(a). The cost function of MPC and the control inputs to the controllable units are shown in Figure 6.9(b) and Figure 6.9(c) and (d) respectively. As there is increasing step change in solar power, the control inputs to diesel and fuel cells are lowered accordingly by MPC so as to maintain zero frequency deviation. The obtained value of R_w for this case is 28.

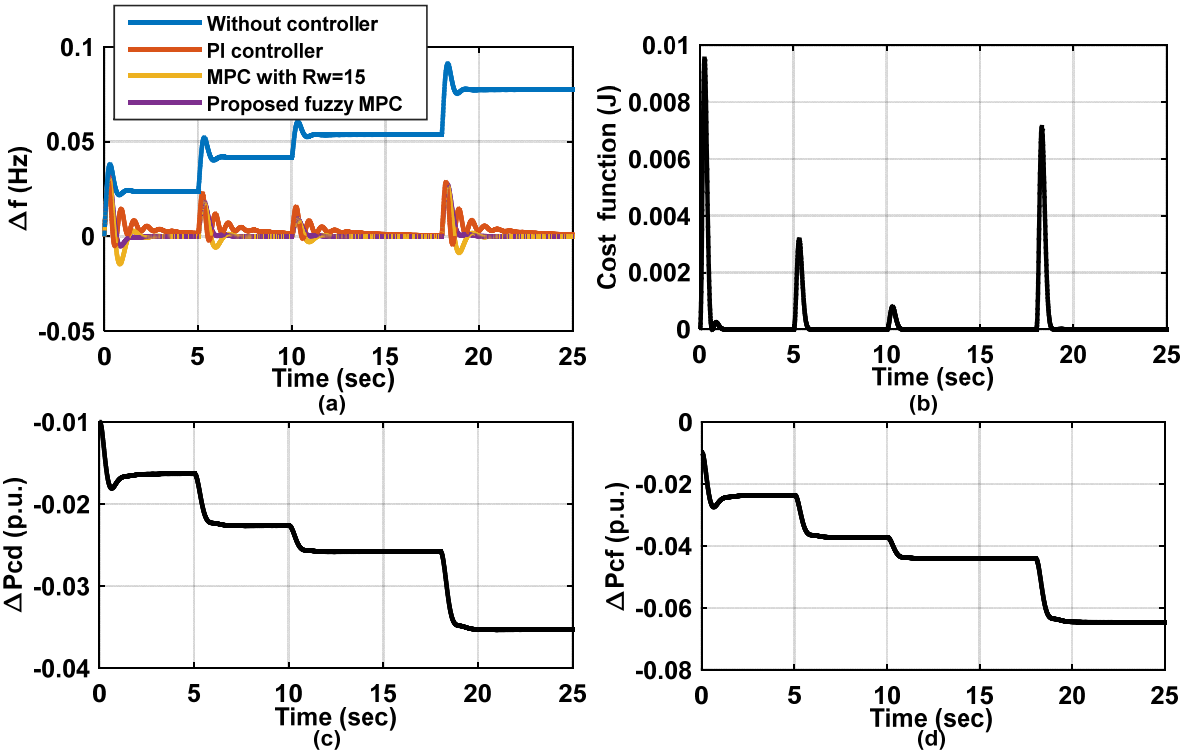

Figure 6.9: (a) Comparison of system response of the microgrid for case-5 (b).Response of Cost functions of MPC over simulation period for case-5 (c) & (d). Response of control inputs to diesel and fuel cell for case-5

Case-6: All disturbances such as ΔP_L, ΔP_w and ΔP_s in the Systems

This case presents the system response when all possible disturbances exist in the system. This case applies the disturbance considered in case-3, case-4 and case-5 simultaneously. The frequency deviation response of the microgrid for this case is shown in Figure 6.10(a). The cost function of MPC and the control inputs to diesel and fuel cell are shown in Figure 6.10(b) and Figure 6.10(c) and (d) respectively. The optimal value of R_w for this case is found to be 19.5. The comparison of proposed fuzzy MPC with PI controller is assessed by comparing the performance index ITSE value for all cases of simulation and has been tabulated in Table 6.2. It is evident that the optimal value of R_w obtained in each case of

simulation is unique and has to be optimally selected for different operating conditions of the system. Hence, the proposed method is found to be efficient for load frequency control.

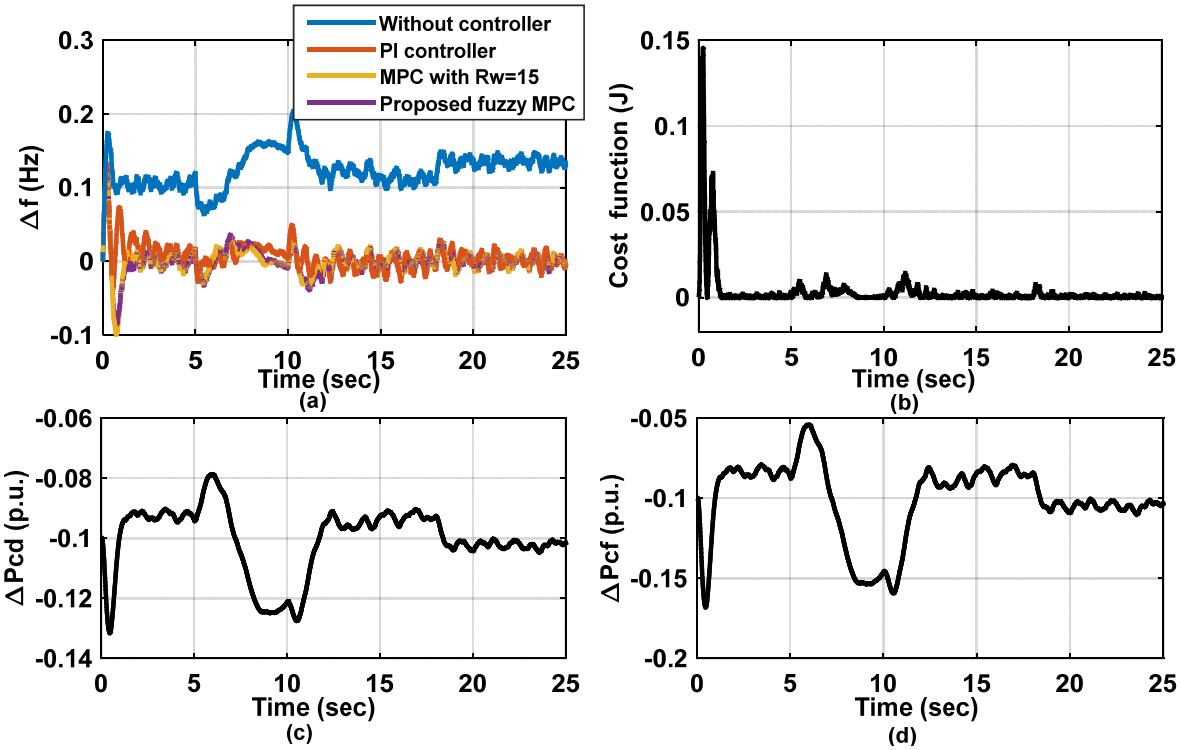

Figure 6.10: (a) Comparison of system response of the microgrid for case-6 (b). Response of Cost functions of MPC over simulation period for case-6 (c) & (d). Response of control inputs to diesel and fuel cell for case-6

Table 6.2 Comparison of performance index

Cases	Without controller	PI controller	MPC controller	**Proposed Fuzzy MPC**
Case -1 (ITSE)	0.3472	0.02871	0.01702	0.009268
Case – 2 (ITSE)	0.00709	5.578e-5	3.594e-5	1.835e-5
Case –3 (ITSE)	0.1874	0.009652	0.007288	0.00674
Case – 4 (ITSE)	4.1130	0.04772	0.04336	0.03714
Case – 5 (ITSE)	1.3010	0.00769	0.005746	0.00535
Case – 6(ITSE)	5.286	0.04508	0.03961	0.03193
Case – 7(ITSE)	0.9282	0.0101	0.00554	0.0036

Case-7: Parametric variation in the system

This case introduces the parametric variation and studies the system response by the proposed fuzzy MPC method. The parametric variation is incorporated as follows: R=+30%; D=-40%; H=+50%; T_t= -50%; T_g=+50%; Tb=-45%. The change in solar power is kept as 0.05p.u. and the load is 0.02p.u. whereas the wind velocity is maintained as 6.5m/s. The response comparison is shown in Figure 6.11(a) The respective cost function and the control

inputs are shown in Figure 6.11(b) and Figure 6.11 (c) and (d) respectively. The optimal R_w is found to 27.5 for this case.

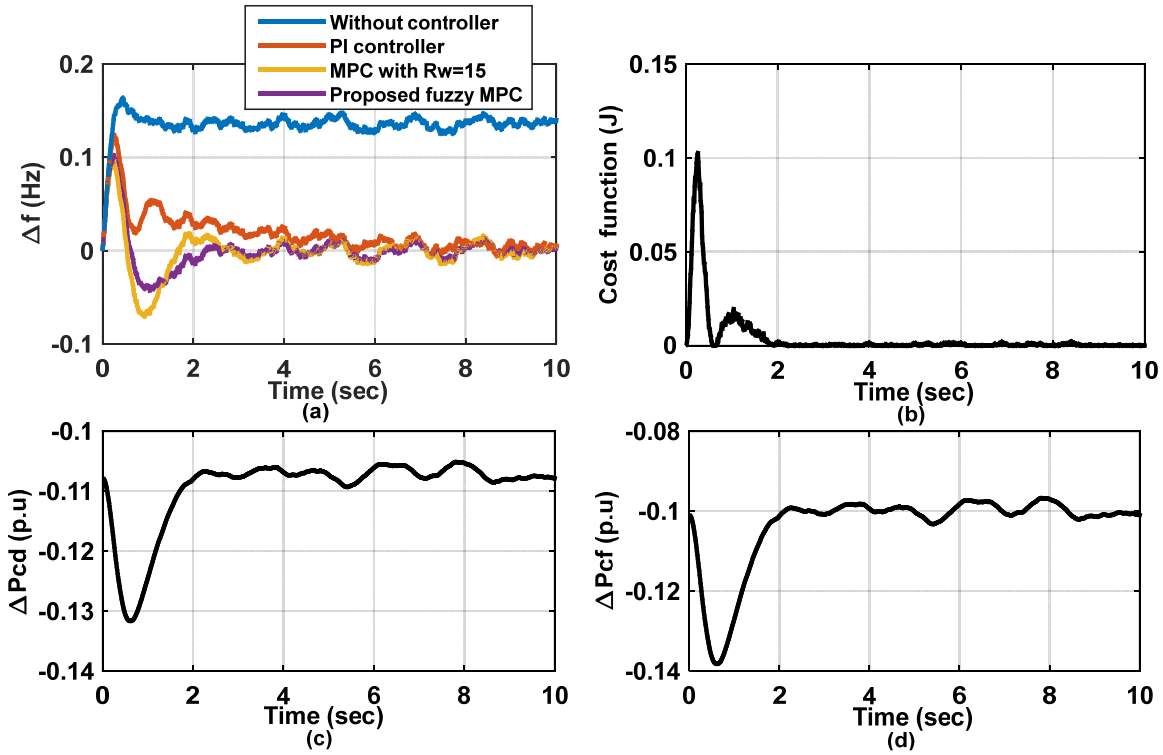

Figure 6.11: (a) Comparison of system response of the microgrid for case-7 (b). Response of Cost functions of MPC over simulation period for case-7 (c) & (d). Response of control inputs to diesel and fuel cell for case-7

6.6 Summary

This chapter has proposed a fuzzy adaptive MPC for effective and faster load frequency control for an isolated microgrid. The impact of tuning parameter R_w on the performance of the model predictive control is discussed in this chapter for the load frequency regulation. The adaptability of MPC is achieved by tuning parameter 'R_w' using fuzzy controller. The parameter R_w has been dynamically adjusted with fuzzy "IF/THEN" rule base to make it robust control irrespective of different scenarios of the problem. The proposed fuzzy adaptive MPC is implemented for load frequency control of a typical microgrid, while results and comparison show that the proposed method of control is effective in obtaining better and faster system response with damped oscillations for different case studies. Thus, the proposed fuzzy MPC can be used for effective frequency regulation in smart grid applications.

Chapter 7

Conclusions

Chapter 7

7 Conclusions

7.1 General

In this thesis, the planning of active distribution network operation is optimized using proposed meta-heuristic optimization algorithms in multi-objective frame. Apart from this, load frequency control of an isolated microgrid is also analyzed using PI controller and model predictive controller. This chapter briefs the important findings proposed in this thesis and future extension of the proposed research work.

7.2 Summary of important findings

This chapter presents the overall conclusions of the research work presented in this thesis and future scope of the research work. The following conclusions have been arrived at from research work carried out and reported in the earlier chapters in this thesis.

(i) The overall objective of the research work is to plan the optimal and economical operation of active distribution system and to analyze the load frequency control of isolated microgrid.

- First of all, basic planning of active distribution network i.e. optimally locating and sizing the distributed generation in a distribution network is attempted to minimize active power loss and voltage deviation in the system.
- For optimizing the location and sizing the DG units, a new form of Teaching Learning Based Optimization (TLBO) algorithm i.e. Peer enhanced Multi-objective TLBO (PeMOTLBO) is proposed.
- To prove effectiveness of the proposed algorithm, it was tested on IEEE 33-bus system, IEEE 69-bus system and Indian 85-bus distributed system and results were compared with well-known multi-objective NSGA-II technique and with the basic multi-objective TLBO algorithm.
- A statistical comparison and significance of the proposed PeMOTLBO algorithm was also evaluated with performance metrics and demonstrated with box plots.

(ii) While planning the DG location and size, cost of investment and operation are also to be considered for economic operation of active distribution network. This cost may vary with different DG technologies such as dispatchable units like diesel and gas engines and environment friendly non-dispatchable sources such as wind and solar DGs.

- Hence, in this thesis, the planning of optimal and economic operation of DGs in distribution networks was analyzed by considering different DG technologies.
- Multi-objective problem has been formulated to minimize simultaneously the active power loss, voltage deviation and the cost of DG integration in the system.
- For this planning, a new Grid based Multi-Objective Harmony search (GrMHS) was proposed. In the proposed GrMHS algorithm, the grid strategy has been incorporated as secondary selection criterion in the objective space to improve the efficiency of the optimization process.
- The proposed GrMHS algorithm has been tested on IEEE 33-bus system, IEEE 69-bus system and Indian 85-bus system. The results were validated with extensive comparison with prominent multi-objective NSGA-II and multi-objective harmony search algorithm.

(iii) The active management of load in the distribution grid is directly linked with the frequency of operation in this system. Thus load frequency control of isolated microgrid is also attempted in this thesis.

- The load frequency control of the isolated microgrid is attempted with Proportional Integral (PI) controller.
- The PI controller gains are tuned using the proposed levy based spider monkey algorithm (Levy-SMA).
- The performance of the proposed algorithm has been evaluated with the integral time square error (ITSE) and has been compared with other algorithms such as Particle Swarm Optimization (PSO), Harmony Search (HS), Firefly Algorithm (FA).

- The obtained system response has been compared with other algorithms and results are found better with less ITSE value for the proposed Levy-Spider Monkey Algorithm.

(iv) The load frequency control is the one which needs a simple and faster control. One such simple straightforward control is the model predictive control (MPC).

- In this thesis, a fuzzy adaptive Model Predictive Control has been proposed for better load frequency control. A fuzzy controller is embedded into MPC block to tune its input parameter which improves the system performance.
- The performance of load frequency control in microgrid is evaluated with ITSE value.
- The system response obtained using the proposed method has been compared with PI controller response and the MPC control with constant input parameter value and the results found better in fuzzy MPC.

7.3 Scope for Future Work

In this thesis, distributed generation planning and their optimal resource mix has been identified for economical operation of active distribution networks and load frequency control of a typical isolated microgrid is also attempted. The future work can be extended on the following aspects:

- Voltage and frequency stability studies can be implemented with large penetrations of renewable energy sources into active distribution network operation.
- Coordinated control of electrically distanced Distributed Energy Resources and loads for better frequency regulation in the active distribution network operation for both grid connected and islanded mode of operation can be explored.
- In the planning of active distribution network operation, meta-heuristic algorithms were dominantly applied, so investigations can be carried out on the new hybrid methods for better convergence and for exploring the diversified search space.

References

[1] Li, Qilin, and Mingtian Zhou, "The future-oriented grid-smart grid," *Journal of Computers*, vol. 6, no.1, pp 98-105, 2011.

[2] Smith, Merrill, "Overview of the US Department of energy's research & development activities on microgrid technologies," *Proceedings of the Symposium Presentations on Micro-Grid*, 2009.

[3] Farhangi, Hassan, "The path of the smart grid," *IEEE power and energy magazine*, vol.8, no.1, 2010.

[4] Agrawal, Poonum, "Overview of DOE microgrid activities," *Symposium on Microgrid, Montreal*, vol. 23, 2006.

[5] Zamora, Ramon, and Anurag K. Srivastava, "Controls for microgrids with storage: Review, challenges, and research needs," *Renewable and Sustainable Energy Reviews,* vol.14, no.7, pp. 2009-2018, 2010.

[6] Coster, Edward J., Johanna MA Myrzik, Bas Kruimer, and Wil L. Kling. "Integration issues of distributed generation in distribution grids," *Proceedings of the IEEE*, vol.99, no. 1, pp.28-39, 2011.

[7] Keane, Andrew, Luis F. Ochoa, Carmen LT Borges, Graham W. Ault, Arturo D. Alarcon-Rodriguez, Robert AF Currie, Fabrizio Pilo, Chris Dent, and Gareth P. Harrison, "State-of-the-art techniques and challenges ahead for distributed generation planning and optimization," *IEEE Transactions on Power Systems,* vol.28, no.2, pp. 1493-1502, 2013.

[8] Georgilakis, Pavlos S., and Nikos D. Hatziargyriou, "Optimal distributed generation placement in power distribution networks: models, methods, and future research," *IEEE Transactions on Power Systems*, vol.28, no. 3, pp.3420-3428, 2013.

[9] Theo, Wai Lip, Jeng Shiun Lim, Wai Shin Ho, Haslenda Hashim, and Chew Tin Lee, "Review of distributed generation (DG) system planning and optimization techniques: Comparison of numerical and mathematical modelling methods," *Renewable and Sustainable Energy Reviews*, vol.67, pp.531-573, 2017.

[10] N. Acharya, P. Mahat, and N. Mithulananthan, "An analytical approach for DG allocation in primary distribution network," *Int. J. Elect. Power Energy Syst.*, vol. 28, no. 10, pp. 669–678, 2006.

[11] S.-H. Lee and J.-W. Park, "Selection of optimal location and size of multiple distributed generations by using Kalman filter algorithm," *IEEE Trans. Power Syst.*, vol. 24, no. 3, pp. 1393–1400, 2009.

[12] T. Gözel and M. H. Hocaoglu, "An analytical method for the sizing and siting of distributed generators in radial systems," *Elect. Power Syst. Res.*, vol. 79, no. 6, pp. 912-918, 2009.

[13] D. Q. Hung, N. Mithulananthan, and R. C. Bansal, "Analytical expressions for DG allocation in primary distribution networks," *IEEE Transactions on energy conversion,* vol. 25, no. 3, pp. 814–820, 2010.

[14] D.Q. Hung and N. Mithulananthan, "Multiple distributed generators placement in primary distribution networks for loss reduction," *IEEE Transactions Industrial Electronics.*, vol. 60, no. 4, pp. 1700–1708, 2013.

[15] Tah, Avisha, and Debapriya Das, "Novel analytical method for the placement and sizing of distributed generation unit on distribution networks with and without considering P and PQV buses," *International Journal of Electrical Power & Energy Systems*, vol.78, pp.401-413, 2016.

[16] P. Vovos and J. Bialek, "Direct incorporation of fault level constraints in optimal power flow as a tool for network capacity analysis," *IEEE Transaction on Power Systems*, vol. 20, no. 4, pp. 2125–2134, 2005.

[17] A. Keane and M. O'Malley, "Optimal allocation of embedded generation on distribution networks," *IEEE Transactions on Power System*, vol. 20, no.3, pp. 1640–1646, 2005.

[18] M. F. AlHajri, M. R. AlRashidi, and M. E. El-Hawary, "Improved sequential quadratic programming approach for optimal distribution generation deployments via stability and sensitivity analyses," *Electric Power Components and System*, vol. 38, no. 14, pp. 1595–1614, 2010.

[19] Y. M. Atwa and E. F. El-Saadany, "Probabilistic approach for optimal allocation of wind-based distributed generation in distribution systems," *IET Renewable Power Generation.*, vol. 5, no. 1, pp. 79–88, 2011.

[20] Y. M. Atwa, E. F. El-Saadany, M. M. A. Salama, and R. Seethapathy, "Optimal renewable resources mix for distribution system energy loss minimization," *IEEE Transactions on Power System*, vol. 25, no. 1, pp. 360–370, 2010.

[21] S. Porkar, P. Poure, A. Abbaspour-Tehrani-Fard, and S. Saadate, "Optimal allocation of distributed generation using a two-stage multi-objective mixed-integer-nonlinear programming," *European Transaction on Electric Power*, vol. 21, no. 1, pp. 1072–1087, 2011.

[22] A. Kumar and W. Gao, "Optimal distributed generation location using mixed integer non-linear programming in hybrid electricity markets," *IET Generation Transmission and Distribution*, vol. 4, no. 2, pp. 281–298, 2010.

[23] Al Abri, R. S., Ehab F. El-Saadany, and Yasser M. Atwa, "Optimal placement and sizing method to improve the voltage stability margin in a distribution system using distributed generation," *IEEE Transactions on power systems*, vol.28, no. 1, pp.326-334, 2013.

[24] Esmaili, Masoud, Esmail Chaktan Firozjaee, and Heidar Ali Shayanfar, "Optimal placement of distributed generations considering voltage stability and power losses

with observing voltage-related constraints," Applied *energy*, vol.113, pp.1252-1260, 2014.

[25] R. A. Jabr and B. C. Pal, "Ordinal optimisation approach for locating and sizing of distributed generation," *IET Generation Transmission Distribution.*, vol. 3, no. 8, pp. 713–723, 2009.

[26] Gampa, Srinivasa Rao, and D. Das, "Optimum placement and sizing of DGs considering average hourly variations of load," *International Journal of Electrical Power & Energy Systems*, vol.66, pp.25-40, 2015.

[27] Ogunjuyigbe, A. S. O., T. R. Ayodele, and O. A. Akinola, "Optimal allocation and sizing of PV/Wind/Split-diesel/Battery hybrid energy system for minimizing life cycle cost, carbon emission and dump energy of remote residential building," *Applied Energy*, vol.171, pp.153-171, 2016.

[28] Singh, Bindeshwar, V. Mukherjee, and Prabhakar Tiwari, "Genetic algorithm for impact assessment of optimally placed distributed generations with different load models from minimum total MVA intake viewpoint of main substation," *Renewable and Sustainable Energy Reviews*, vol.57, pp.1611-1636, 2016.

[29] Muttaqi, Kashem M., An DT Le, Jamshid Aghaei, Esmaeil Mahboubi-Moghaddam, Michael Negnevitsky, and Gerard Ledwich, "Optimizing distributed generation parameters through economic feasibility assessment," *Applied Energy*, vol.165, pp. 893-903, 2016.

[30] Kowsalya, M, "Optimal size and siting of multiple distributed generators in distribution system using bacterial foraging optimization," Swarm *and Evolutionary computation*, vol.15, pp.58-65, 2014.

[31] Mitra, Joydeep, Mallikarjuna R. Vallem, and Chanan Singh, "Optimal deployment of distributed generation using a reliability criterion," *IEEE Transactions on Industry Applications*, vol. 52, no. 3, pp.1989-1997, 2016.

[32] Prabha DR, Jayabarathi T, "Optimal placement and sizing of multiple distributed generating units in distribution networks by invasive weed optimization algorithm," Ain Shams Engineering Journal, vol. 7, pp.683–694, 2016.

[33] Sultana, Sneha, and Provas Kumar Roy, "Krill herd algorithm for optimal location of distributed generator in radial distribution system," *Applied Soft Computing*, vol.40, pp.391-404, 2016.

[34] A.Soroudi and M.afrasiab, "Binary PSO-based dynamic multiobjective model for distributed generation planning under uncertainty", *IET Generation Transmission Distribution*, vol.6, no.2, pp.67-78, 2012.

[35] Moradi MH, Zeinalzadeh A, Mohammadi Y, Abedini M, "An efficient hybrid method for solving the optimal sitting and sizing problem of DG and shunt capacitor banks simultaneously based on imperialist competitive algorithm and genetic algorithm," *Electric Power Energy System*, vol. 54, pp.101–111, 2014.

[36] Nayeripour M, Mahboubi-Moghaddam E, Aghaei J, Azizi-Vahed A, "Multiobjective placement and sizing of DGs in distribution networks ensuring transient stability using hybrid evolutionary algorithm," *Renewable Sustainable Energy Reviews*, vol. 25, pp.759–767, 2013.

[37] R.V. Rao, V.J. Savsani and J. Balic, "Teaching-learning based algorithm for unconstrained and constrained real-parameter optimization problems*," Engineering Optimization-Taylor and Francis*, vol. 44, no. 12, pp.1447-1462, 2012.

[38] T. Niknam, R. Azizipanah-Abarghooee, M. R. Narimani, "A new multi objective optimization approach based on TLBO for location of automatic voltage regulators in distribution systems," *Engineering Applications of Artificial Intelligence*, vol.25, no.8, pp.1577-1588, 2012.

[39] M. R. Nayak, C. K. Nayak, P. K. Rout, "Application of Multi-Objective Teaching Learning based Optimization Algorithm to Optimal Power Flow Problem," *Procedia Technology*, vol. 6, pp. 255-264, 2012.

[40] K. Deb, A. Samir, P. Amrit, and T. Meyarivan, "A fast elitist non- dominated sorting genetic algorithm for multi-objective optimization: NSGA-II," *IEEE Transaction on Evolutionary Computation,* vol. 6, no. 2, pp.103–112, 2002.

[41] Lopes, JA Pecas, N. Hatziargyriou, J. Mutale, P. Djapic, and N. Jenkins, "Integrating distributed generation into electric power systems: A review of drivers, challenges and opportunities," *Electric power systems research*, vol. 77, no. 9, pp.1189-1203, 2007.

[42] Coster, Edward J., Johanna MA Myrzik, Bas Kruimer, and Wil L. Kling, "Integration issues of distributed generation in distribution grids," *Proceedings of the IEEE*, vol. 99, no. 1, pp.28-39, 2011.

[43] Wang, David T-C., Luis F. Ochoa, and Gareth P. Harrison, "DG impact on investment deferral: Network planning and security of supply," *IEEE Transactions on Power Systems*, vol. 25, no. 2, pp.1134-1141, 2010.

[44] Kayalvizhi S., and D M Vinod Kumar, "Dispatchable DG planning in distribution networks considering costs," *International Conference on Recent Developments in Control, Automation and Power Engineering (RDCAPE),* pp. 320-325, 2015.

[45] Kumar, Ashwani, and Wenzhong Gao, "Optimal distributed generation location using mixed integer non-linear programming in hybrid electricity markets," *IET Generation, Transmission & Distribution*, vol. 4, no. 2, pp. 281-298, 2010.

[46] El-Khattam, W., Hegazy, Y. G., & Salama, M. M. A., "An integrated distributed generation optimization model for distribution system planning," *IEEE Transactions on Power Systems*, vol. 20, no. 2, pp.1158-1165, 2005.

[47] Ochoa, L. F., & Harrison, G. P., "Minimizing energy losses: Optimal accommodation and smart operation of renewable distributed generation," *IEEE Transactions on Power Systems,* vol. 26, no. 1, pp.198-205, 2011.

[48] Atwa, Y. M., El-Saadany, E. F., Salama, M. M. A., and Seethapathy, R., "Optimal renewable resources mix for distribution system energy loss minimization," *IEEE Transactions on Power Systems*, vol. 25, no. 1, pp.360-370, 2010.

[49] Harrison, G. P., Piccolo, A., Siano, P., & Wallace, A. R., "Exploring the tradeoffs between incentives for distributed generation developers and DNOs," *IEEE Transactions on Power Systems*, vol. 22, no. 2, pp. 821-828, 2007.

[50] Haghifam, M. R., Falaghi, H., and Malik, O. P., "Risk-based distributed generation placement," *IET Generation Transmission and Distribution*, vol. 2, no. 2, pp.252-260, 2008.

[51] Di Silvestre, M. L., Graditi, G., and Sanseverino, E. R., "A generalized framework for optimal sizing of distributed energy resources in micro-grids using an indicator-based swarm approach," *IEEE Transactions on Industrial Informatics*, vol.10, no. 1, pp. 152-162, 2014.

[52] Guo, L., Liu, W., Jiao, B., Hong, B., and Wang, C., "Multi-objective stochastic optimal planning method for stand-alone microgrid system," *IET Generation, Transmission and Distribution*, vol. 8, no. 7, pp. 1263-1273, 2014.

[53] Mohammadi, S., Soleymani, S., and Mozafari, B., "Scenario-based stochastic operation management of microgrid including wind, photovoltaic, micro-turbine, fuel cell and energy storage devices," *International Journal of Electrical Power & Energy Systems,* vol. 54, pp. 525-535, 2014.

[54] Zhang, L., and Li, Y, "Optimal energy management of wind-battery hybrid power system with two-scale dynamic programming," IEEE *Transactions on Sustainable Energy*, vol.4, no. 3, pp. 765-773, 2013.

[55] Moradi, M. H., and Eskandari, M., "A hybrid method for simultaneous optimization of DG capacity and operational strategy in microgrids considering uncertainty in electricity price forecasting," *Renewable Energy*, vol. 68, pp. 697-714, 2014.

[56] Chen, C., Duan, S., Cai, T., Liu, B., and Hu, G., "Smart energy management system for optimal microgrid economic operation," IET *renewable power generation*, vol. 5, no. 3, pp. 258-267, 2011.

[57] J.A. Pecas Lopes, C.L. Moreira and A.G. Madureira, "Defining control strategies for microgrids," *IEEE Transaction on Power Systems*, vol. 21, no. 2, pp. 916-924, 2006.

[58] Miao, Zhixin, Alexander Domijan, and Lingling Fan, "On Integration of Distributed Energy Resources to Microgrids—An Overview," *International Journal of Power and Energy Systems*, vol. 32, no. 4, pp.149, 2012.

[59] Ritwik Majumdar, Saikat Chakrabarti, and Gerald ledwich, "Advance battery storage control for an autonomous microgrid," *Electric Power Components and Systems*; vol. 41, pp.157-181, 2013.

[60] Jin-Hong Jeon, Jong-Yul kim, and Seul-ki kim, "Unified compensation control of a hybrid energy storage system for enhancing power quality and operation efficiency in

a diesel and wind-turbine based stand-alone microgrid," *3rd IEEE international symposium on PEDG*, pp. 264-270, 2012.

[61] Mokheimer, Esmail MA, Abdullah Al-Sharafi, Mohamed A. Habib, and Iyad Alzaharnah, "A new study for hybrid PV/wind off-grid power generation systems with the comparison of results from homer," *International journal of green energy*, vol. 12, no. 5, pp. 526-542, 2015.

[62] Yang, H., Zhou, W., Lu, L. and Fang, Z., "Optimal sizing method for stand-alone hybrid solar–wind system with LPSP technology by using genetic algorithm," *Solar energy*, vol. 82, no. 4, pp.354-367, 2008.

[63] Rajan Singaravel M.M, and Arul Daniel S., "Studies on battery storage requirement of PV fed wind-driven induction generators," *Energy Conversion and Management*; vol. 67, pp. 34-43, 2013.

[64] Xinda ke, Ning Lu, and Chunlian Jin, "Control and size energy storage systems for managing imbalance of variable resources," *IEEE Transactions on Sustainable Energy*, vol. 6, pp.70-78, 2015.

[65] Zhao, B., Zhang, X., Li, P., Wang, K., Xue, M. and Wang, C., "Optimal sizing, operating strategy and operational experience of a stand-alone microgrid on Dongfushan Island," *Applied Energy*, vol. 113, pp.1656-1666, 2014.

[66] Ting-chia Qu and chih-Ming Hong, "Dynamic operation and control of microgrid hybrid power system," *Energy*, vol. 66, pp. 314-323, 2014

[67] Hussain, Mohammed T., and Abu HMA Rahim, "Performance of a microgrid including photovoltaic and wind generation systems," *International Journal of Power and Energy System*, vol. 33, pp. 22-29, 2013.

[68] Ritwik Majumder, "Some aspects of stability in Microgrid," *IEEE Transactions on Power systems*, vol. 28, no. 3, pp. 3243-3252, 2013.

[69] Marwali M.N,Dai M, Keyhani A., "Stability analysis of load sharing control for distributed generation systems," *IEEE Transactions on Energy Conversion*, vol. 22, no. 3, pp. 737–745, 2007.

[70] Kamel R, Chaouachi A, and Nagasaka K., "Detailed analysis of micro-grid stability during islanding mode under different load conditions," *Engineering (Scientific Research)*, vol. 3, no. 5, pp. 508–516, 2011.

[71] Alaboudy A.H, Zeineldin H H, and Kirtley J L, "Microgrid stability characterization subsequent to fault-triggered islanding incidents," *IEEE Transactions on Power Delivery*, vol. 27, no. 2, pp. 658–669, 2012.

[72] Ustun, Taha Selim, Cagil Ozansoy, and Aladin Zayegh, "Recent developments in microgrids and example cases around the world—A review," *Renewable and Sustainable Energy Reviews*, vol.15, no.8, pp. 4030-4041, 2011.

[73] Olivares, D.E., Mehrizi-Sani, A., Etemadi, A.H., Cañizares, C.A., Iravani, R., Kazerani, M., Hajimiragha, A.H., Gomis-Bellmunt, O., Saeedifard, M., Palma-

Behnke, R. and Jimenez-Estevez, G.A., "Trends in microgrid control," *IEEE Transactions on smart grid*, vol. 5, no. 4, pp.1905-1919, 2014.

[74] Majumder, Ritwik, Arindam Ghosh, and Gerard Ledwich, "Load Frequency Control in a Microgrid: Challenges and Improvements," *Smart Power Grids 2011*, pp. 49-82. Springer Berlin Heidelberg, 2012.

[75] Pandey, Shashi Kant, Soumya R. Mohanty, and Nand Kishor, "A literature survey on load–frequency control for conventional and distribution generation power systems," *Renewable and Sustainable Energy Reviews*, vol.25, pp.318-334, 2013.

[76] J. M. Guerrero, J. C. Vasquez, J. Matas, L. G. de Vicuña, and M. Castilla, "Hierarchical control of droop-controlled AC and DC microgrids—A general approach toward standardization," *IEEE Transaction on Industrial Electronics*, vol. 58, no. 1, pp. 158–172, 2011

[77] Latha R, Palanivel R and Kanagaraj J, "Frequency control of microgrid based on compressed air energy storage system", *Distributed Generation and Alternative Energy Journal,* vol.27, no.4, pp. 8-19, 2012.

[78] Serban I and Marinescu C, "Control strategy of three-phase battery storage system for frequency support in microgrids and with uninterruptible supply of local loads," *IEEE Transactions on Power Electronics*, vol. 29, no.9, pp.5010-5020, 2014.

[79] Dunghuan Zhu, Gabriela Hug-Glanzmann, "Coordination of storage and generation in power system frequency control using H∞ approach," *IET Generation Transmission Distribution*, vol.7, no.11, pp.1263-1271, 2013.

[80] Dipayan guha, Provas Kumar and Subrata Banerjee, "Load frequency control of interconnected power system using grey wolf optimization," *Swarm and Evolutionary Computation*, vol.27, pp. 97-115, 2016.

[81] Sahu R.K, Panda S and Padhan S, "A novel hybrid gravitational search and pattern search algorithm for load frequency control of nonlinear power system," *Applied Soft Computing*, vol. 29, pp.310-327, 2015.

[82] Ali E.S and Abd-Elazim S.M, "BFOA based design of PID-controller for two area load frequency control with nonlinearities," *Int. Journal of Electric Power and Energy System*, vol.51, pp.224-231, 2013.

[83] Barisal A.K, "Comparative performance analysis of teaching learning based optimization for automatic load frequency control of multi-sources power systems", *Int. Journal of Electric Power and Energy System,* vol. 66, pp.67-77, 2015.

[84] Sahu R.K, Panda S and Padhan S, "A novel hybrid gravitational search and pattern search algorithm for load frequency control of nonlinear power system", *Applied Soft Computing*. vol.29, pp.310-327, 2015.

[85] H. Bevrani, F. Habibi, P. Babahajyani, M. Watanabe, and Y. Mitani, "Intelligent frequency control in an AC microgrid: Online PSO-based fuzzy tuning approach," *IEEE Transactions on Smart Grid*, vol. 3, no. 4, pp. 1935–1944, 2012.

[86] M. J. Hossain, H. R. Pota, M. A. Mahmud, and M. Aldeen, "Robust control for power sharing in microgrids with low-inertia wind and PV generators," *IEEE Transactions. Sustainable Energy*, vol. 6, no. 3, pp. 1067–1077, 2014.

[87] Y.Han, P.M.Young, A. Jain, and D. Zimmerle, "Robust control for microgrid frequency deviation reduction with attached storage system," *IEEE Transactions Smart Grid*, vol. 6, no. 2, pp. 557–565, 2015.

[88] Bevrani, Hassan, Mohammad Ramin Feizi, and Sirwan Ataee, "Robust Frequency Control in an Islanded Microgrid: H∞ and μ-Synthesis Approaches," *IEEE Transactions on Smart Grid*, vol.7, no. 2, pp.706-717, 2016.

[89] Lam, Quang Linh, Antoneta Iuliana Bratcu, and Delphine Riu, "Robustness Analysis of Primary Frequency H∞ Control in Stand-alone Microgrids with Storage Units," *IFAC-Papers On Line*, vol. 49, no. 27, pp.123-128, 2016.

[90] Gallestey, Eduardo, Alec Stothert, Marc Antoine, and Steve Morton, "Model predictive control and the optimization of power plant load while considering lifetime consumption," *IEEE Transactions on Power Systems*, vol.17, no.1, pp. 186-191, 2002.

[91] Ma, Miaomiao, Hong Chen, Xiangjie Liu, and Frank Allgöwer, "Distributed model predictive load frequency control of multi-area interconnected power system," *International Journal of Electrical Power & Energy Systems,* vol.62, pp.289-298, 2014.

[92] Mohamed TH, Morel J, Bevrani H, Hiyama T, "Model predictive based load frequency control_design concerning wind turbines," *Int. Journal of Electrical Power & Energy Systems*, vol.43, no.1, pp.859-867, 2012.

[93] Galus, Matthias D., Stephan Koch, and Göran Andersson, "Provision of load frequency control by PHEVs, controllable loads, and a cogeneration unit," *IEEE Transactions on Industrial Electronics*, vol.58, no.10, pp.4568-4582, 2011.

[94] Pahasa, Jonglak, and Issarachai Ngamroo, "Coordinated control of wind turbine blade pitch angle and PHEVs using MPCs for load frequency control of microgrid," *IEEE Systems Journa* , vol.10, no. 1, pp.97-105, 2016.

[95] Jiang H, Lin J, Song Y, You S, and Zong Y., "Explicit model predictive control applications in power systems: an AGC study for an isolated industrial system," *IET Generation, Transmission & Distribution*, vol.10, no.4, pp.964-971, 2016.

[96] Yang, X. S., "Harmony search as a metaheuristic algorithm. In Music-inspired harmony search algorithm, Springer Berlin Heidelberg. pp. 1-14, 2009.

[97] Yang, S., Li, M., Liu, X., & Zheng, J., "A grid-based evolutionary algorithm for many-objective optimization," IEEE *Transactions on Evolutionary computation*, vol. 17, no. 5, pp. 721-736, 2013.

[98] Nekooei, K., Farsangi, M. M., Nezamabadi-Pour, H., & Lee, K. Y., "An improved multi-objective harmony search for optimal placement of DGs in distribution systems," *IEEE Transactions on smart grid*, vol. 4, no.1, pp.557-567, 2013.

[99] http://www.nrel.gov/midc/nwtc_m2/ accessed 20 February 2015.

[100] Teng, J-H., "Modelling distributed generations in three-phase distribution load flow," *IET Generation, Transmission & Distribution, vol.* 2, no. 3, pp.330-340, 2008.

[101] Yang X.S. and Deb S, "Eagle strategy using Levy walk and firefly algorithms for stochastic optimization, in: Nature Inspired Cooperative Strategies for Optimization," Springer, vol. 284, pp. 101-111, 2010.

[102] Xin she Yang, "Nature inspired meta heuristic algorithms," Luniver Press, United Kingdom, second edition, 2010.

[103] Bansal, J.C., Sharma, H., Jadon, S.S. and Clerc, M., "Spider monkey optimization algorithm for numerical optimization," *Memetic computing*, vol. 6, no. 1, pp.31-47, 2014.

[104] Bompard, E., Enrico Carpaneto, Gianfranco Chicco, and Roberto Napoli, "Convergence of the backward/forward sweep method for the load-flow analysis of radial distribution systems," *International journal of electrical power & energy systems*, vol.22, no. 7, pp. 521-530, 2000.

[105] Das, D., D. P. Kothari, and A. Kalam, "Simple and efficient method for load flow solution of radial distribution networks," I*nternational Journal of Electrical Power & Energy Systems,*vol.17, no. 5 ,pp. 335-346, 1995.

[106] Pinheiro, J. M. S., C. R. R. Dornellas, M. Th Schilling, A. C. G. Melo, and J. C. O. Mello, "Probing the new IEEE reliability test system (RTS-96): HL-II assessment," *IEEE Transactions on Power Systems*, vol.13, no. 1, pp. 171-176, 1998.

[107] Wang, Liuping. Model predictive control system design and implementation using MATLAB®. Springer Science & Business Media, 2009.

Appendix

IEEE 33-bus Distribution System Data

Number of Buses: 33

Number of lines: 32

Base voltage: 12.66kV

Total active power load: 3.715 MW

Total reactive power load: 2.3 MVAR

System active power loss: 0.202 MW

System reactive power loss: 0.134 MVAR

Minimum voltage bus in the system: 0.9132 at 18th Bus

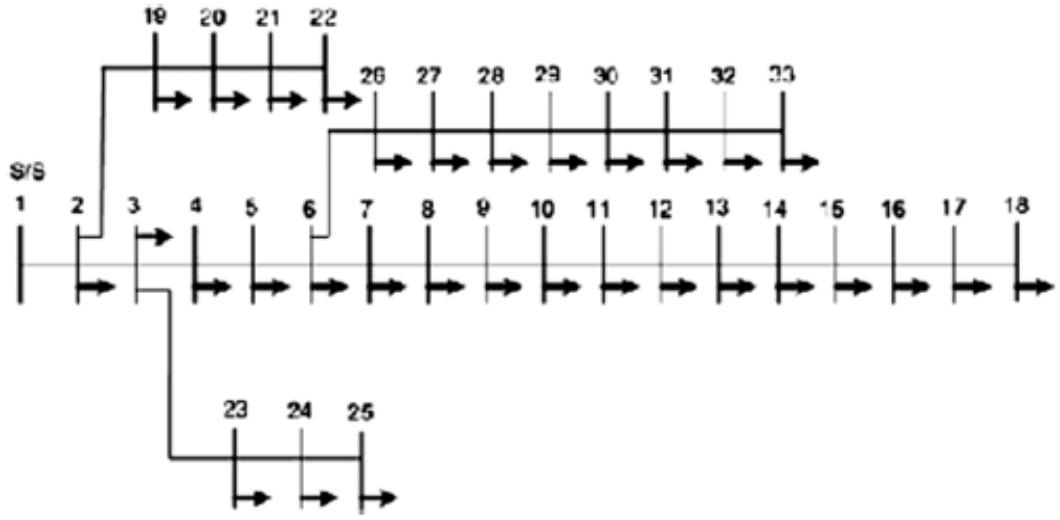

Figure A. 1: IEEE 33-bus distribution system

Table A. 1 Input data of IEEE 33-bus distribution system

Line number	From Bus	To Bus	R (Ohms)	X (Ohms)	Pload (kW)	Qload (kVAR)
1	1	2	0.0922	0.0477	100	60
2	2	3	0.493	0.2511	90	40
3	3	4	0.366	0.1864	120	80
4	4	5	0.3811	0.1941	60	30
5	5	6	0.819	0.707	60	20
6	6	7	0.1872	0.6188	200	100

7	7	8	0.7114	0.2351	200	100
8	8	9	1.03	0.74	60	20
9	9	10	1.04	0.74	60	20
10	10	11	0.1966	0.065	45	30
11	11	12	0.3744	0.1238	60	35
12	12	13	1.468	1.155	60	35
13	13	14	0.5416	0.7129	120	80
14	14	15	0.591	0.526	60	10
15	15	16	0.7463	0.545	60	20
16	16	17	1.289	1.721	60	20
17	17	18	0.732	0.574	90	40
18	2	19	0.164	0.1565	90	40
19	19	20	1.5042	1.3554	90	40
20	20	21	0.4095	0.4784	90	40
21	21	22	0.7089	0.9373	90	40
22	3	23	0.4512	0.3083	90	50
23	23	24	0.898	0.7091	420	200
24	24	25	0.896	0.7011	420	200
25	6	26	0.203	0.1034	60	25
26	26	27	0.2842	0.1447	60	25
27	27	28	1.059	0.9337	60	20
28	28	29	0.8042	0.7006	120	70
29	29	30	0.5075	0.2585	200	600
30	30	31	0.9744	0.963	150	70
31	31	32	0.3105	0.3619	210	100
32	32	33	0.341	0.5302	60	40

IEEE 69-bus Distribution System Data

Number of Buses: 69

Number of lines: 68

Base voltage: 12.66 kV

Total active power load: 3.80 MW

Total reactive power load: 2.69 MVAR

System active power loss: 0.226 MW

System reactive power loss: 0.098 MVAR

Minimum voltage bus in the system: 0.908 p.u. at 65^{th} Bus

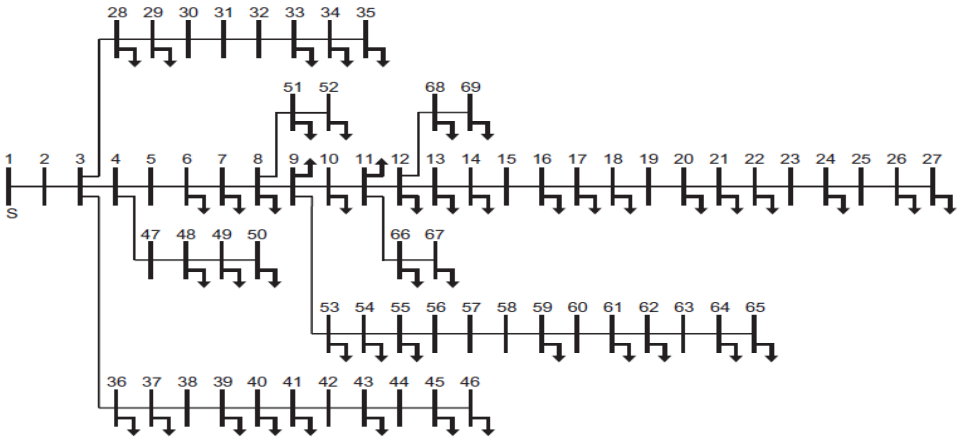

Figure A. 2: IEEE 69-bus distribution system

Table A. 2 Input data of IEEE 69-bus distribution system

Line number	From Bus	To Bus	R (Ohms)	X (Ohms)	Pload (kW)	Qload (kVAR)
1	1	2	0.0005	0.0012	0	0
2	2	3	0.0005	0.0012	0	0
3	3	4	0.0015	0.0036	0	0
4	4	5	0.0251	0.0294	0	0
5	5	6	0.366	0.1864	2.6	2.20
6	6	7	0.3811	0.1941	40.4	30.00
7	7	8	0.0922	0.047	75	54.00
8	8	9	0.0493	0.0251	30	22.00
9	9	10	0.819	0.2707	28	19.00
10	10	11	0.1872	0.0619	145	104.0
11	11	12	0.7114	0.2351	145	104.0
12	12	13	1.03	0.34	8	5.50
13	13	14	1.044	0.345	8	5.50
14	14	15	1.058	0.3496	0	0
15	15	16	0.1966	0.065	45.5	30.0
16	16	17	0.3744	0.1238	60	35.0
17	17	18	0.0047	0.0016	60	35.0
18	18	19	0.3276	0.1083	0	0
19	19	20	0.2106	0.069	1	0.6
20	20	21	0.3416	0.1129	114	81.0
21	21	22	0.014	0.0046	5.3	3.5
22	22	23	0.1591	0.0526	0	0
23	23	24	0.3463	0.1145	28	20.0
24	24	25	0.7488	0.2475	0	0

25	25	26	0.3089	0.1021	14	10.0
26	26	27	0.1732	0.0572	14	10.0
27	3	28	0.0044	0.0108	26	18.6
28	28	29	0.064	0.1565	26	18.6
29	29	30	0.3978	0.1315	0	0
30	30	31	0.0702	0.0232	0	0
31	31	32	0.351	0.116	0	0
32	32	33	0.839	0.2816	14	10.0
33	33	34	1.708	0.5646	19.5	14.0
34	34	35	1.474	0.4873	6	4.0
35	3	36	0.0044	0.0108	26	18.55
36	36	37	0.064	0.1565	26	18.55
37	37	38	0.1053	0.123	0	0
38	38	39	0.0304	0.0355	24	17.00
39	39	40	0.0018	0.0021	24	17.00
40	40	41	0.7283	0.8509	1.2	1.00
41	41	42	0.31	0.3623	0	0
42	42	43	0.041	0.0478	6	4.30
43	43	44	0.0092	0.0116	0	0
44	44	45	0.1089	0.1373	39.22	26.3
45	45	46	0.0009	0.0012	39.22	26.30
46	4	47	0.0034	0.0084	0	0
47	47	48	0.0851	0.2083	79	56.40
48	48	49	0.2898	0.7091	384.7	274.5
49	49	50	0.0822	0.2011	384.7	274.5
50	8	51	0.0928	0.0473	40.5	28.30
51	51	52	0.3319	0.1114	3.6	2.70
52	9	53	0.174	0.0886	4.35	3.50
53	53	54	0.203	0.1034	26.4	19.00
54	54	55	0.2842	0.1447	24	17.20
55	55	56	0.2813	0.1433	0	0
56	56	57	1.59	0.5337	0	0
57	57	58	0.7837	0.263	0	0
58	58	59	0.3042	0.1006	100	72.00
59	59	60	0.3861	0.1172	0	0
60	60	61	0.5075	0.2585	1244	888.0
61	61	62	0.0974	0.0496	32	23.00
62	62	63	0.145	0.0738	0	0
63	63	64	0.7105	0.3619	227	162.0
64	64	65	1.041	0.5302	59	42.00
65	11	66	0.2012	0.0611	18	13.00

66	66	67	0.0047	0.0014	18	13.00
67	12	68	0.7394	0.2444	28	20.00
68	68	69	0.0047	0.0016	28	20.00

Indian 85 - bus Distribution System Data

Number of Buses: 85

Number of lines: 84

Base voltage: 11 kV

Total active power load: 2.5708 MW

Total reactive power load: 2.6218 MVAR.

System active power loss: 0.3163 MW

System reactive power loss: 0.134 MVAR

Minimum voltage bus in the system: 0.8713 at 56th Bus

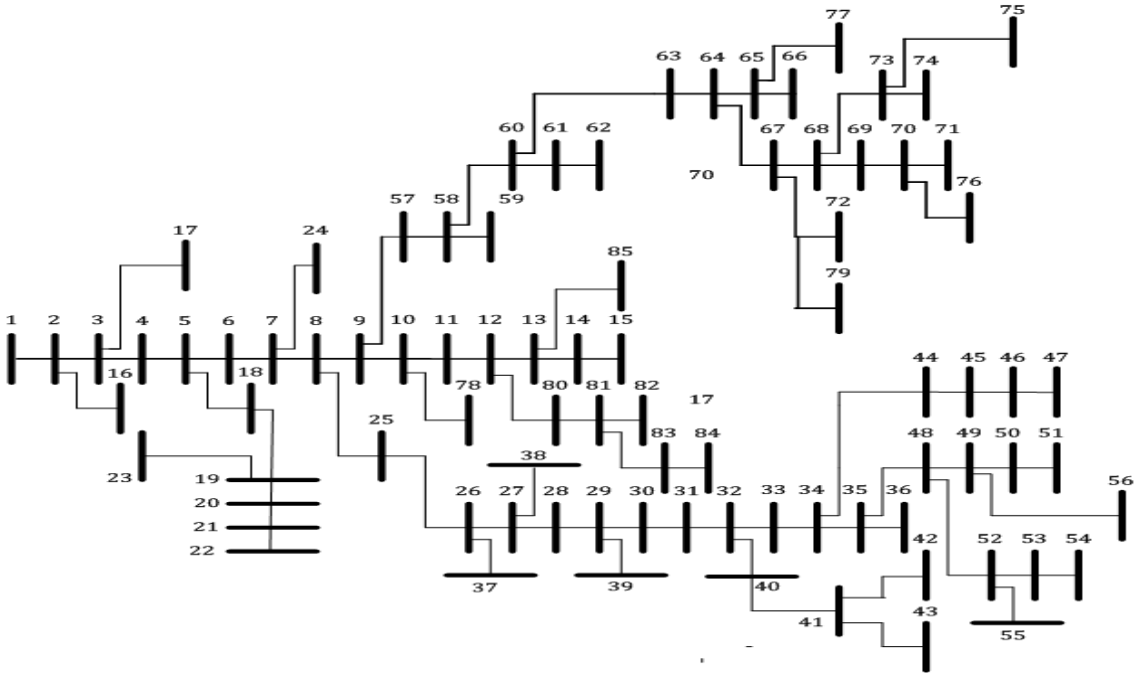

Figure A. 3: Indian 85-bus distribution system

Table A. 3 Input data for Indian 85-bus distribution system

Line Number	From bus	To bus	R (ohms)	X (ohms)	Pload (kw)	Qload (kVAR)
1	1	2	0.108	0.075	0	0
2	2	3	0.163	0.112	0	0
3	3	4	0.217	0.149	0	0
4	4	5	0.108	0.074	56	57.1312
5	5	6	0.435	0.298	0	0
6	6	7	0.272	0.186	35.28	35.99266
7	7	8	1.197	0.82	0	0
8	8	9	0.108	0.074	35.28	35.99266
9	9	10	0.598	0.41	0	0
10	10	11	0.544	0.373	0	0
11	11	12	0.544	0.373	56	57.1312
12	12	13	0.598	0.41	0	0
13	13	14	0.272	0.186	0	0
14	14	15	0.326	0.223	35.28	35.99266
15	2	16	0.728	0.302	35.28	35.99266
16	3	17	0.455	0.189	35.28	35.99266
17	5	18	0.82	0.34	112	114.2624
18	18	19	0.637	0.264	56	57.1312
19	19	20	0.455	0.189	56	57.1312
20	20	21	0.819	0.34	35.28	35.99266
21	21	22	1.548	0.642	35.28	35.99266
22	19	23	0.182	0.075	35.28	35.99266
23	7	24	0.91	0.378	56	57.1312
24	8	25	0.455	0.189	35.28	35.99266
25	25	26	0.364	0.151	35.28	35.99266
26	26	27	0.546	0.226	56	57.1312
27	27	28	0.273	0.113	0	0
28	28	29	0.546	0.226	56	57.1312
29	29	30	0.546	0.226	0	0
30	30	31	0.273	0.113	35.28	35.99266
31	31	32	0.182	0.075	35.28	35.99266
32	32	33	0.182	0.075	0	0
33	33	34	0.819	0.34	14	14.2828
34	34	35	0.637	0.264	0	0
35	35	36	0.182	0.075	0	0
36	26	37	0.364	0.151	35.28	35.99266
37	27	38	1.002	0.416	56	57.1312
38	29	39	0.546	0.226	56	57.1312
39	32	40	0.455	0.189	56	57.1312

40	40	41	1.002	0.416	35.28	35.99266
41	41	42	0.273	0.113	0	0
42	41	43	0.455	0.189	35.28	35.99266
43	34	44	1.002	0.416	35.28	35.99266
44	44	45	0.911	0.378	35.28	35.99266
45	45	46	0.911	0.378	35.28	35.99266
46	46	47	0.546	0.226	35.28	35.99266
47	35	48	0.637	0.264	14	14.2828
48	48	49	0.182	0.075	0	0
49	49	50	0.364	0.151	0	0
50	50	51	0.455	0.189	36.28	37.01286
51	48	52	1.366	0.567	56	57.1312
52	52	53	0.455	0.189	0	0
53	53	54	0.546	0.226	35.28	35.99266
54	52	55	0.546	0.226	56	57.1312
55	49	56	0.546	0.226	56	57.1312
56	9	57	0.273	0.113	14	14.2828
57	57	58	0.819	0.34	56	57.1312
58	58	59	0.182	0.075	0	0
59	58	60	0.546	0.226	56	57.1312
60	60	61	0.728	0.302	0	0
61	61	62	1.002	0.415	112	114.2624
62	60	63	0.182	0.075	56	57.1312
63	63	64	0.728	0.302	14	14.2828
64	64	65	0.182	0.075	0	0
65	65	66	0.182	0.075	0	0
66	64	67	0.455	0.189	56	57.1312
67	67	68	0.91	0.378	0	0
68	68	69	1.092	0.453	0	0
69	69	70	0.455	0.189	56	57.1312
70	70	71	0.546	0.226	0	0
71	67	72	0.182	0.075	35.28	35.99266
72	68	73	1.184	0.491	56	57.1312
73	73	74	0.273	0.113	0	0
74	73	75	1.002	0.416	56	57.1312
75	70	76	0.546	0.226	35.28	35.99266
76	65	77	0.091	0.037	56	57.1312
77	10	78	0.637	0.264	14	14.2828
78	67	79	0.546	0.226	56	57.1312
79	12	80	0.728	0.302	35.28	35.99266
80	80	81	0.364	0.151	56	57.1312

81	81	82	0.091	0.037	0	0
82	81	83	1.092	0.453	56	57.1312
83	83	84	1.002	0.416	35.28	35.99266
84	13	85	0.819	0.34	14	14.2828
					35.28	35.99266

Publications

Refereed Journal Publication:

1. S. Kayalvizhi and D.M. Vinod Kumar, "***Distributed Generation Planning using Peer enhanced Multi-Objective Teaching-Learning based Optimization in Distribution Networks***", Institution of Engineers (India), Springer, vol. 98, no.2, pp.203-211, 2017.
2. S. Kayalvizhi and D.M. Vinod Kumar, "***Planning of Autonomous Microgrid with Energy Storage using Grid-based Multi-Objective Harmony Search Algorithm***", International Journal of Power and Energy Systems, vol. 37, no.1, 2017.
3. S. Kayalvizhi and D.M. Vinod Kumar, "***Frequency Control of Microgrid with wind perturbations using Levy walks with Spider Monkey Optimization Algorithm***", International Journal of Renewable Energy Research-IJRER vol.7, no.1, pp.146-156, 2017.
4. S. Kayalvizhi and D.M. Vinod Kumar, "***Load Frequency Control of an Isolated Microgrid using Fuzzy Adaptive Model Predictive Control***", IEEE Access, vol. 5, pp. 16241-16251.
5. S. Kayalvizhi and D.M. Vinod Kumar, "***Distributed generation- Planning, control and management: state-of-the-art***", *International Journal of Advanced Technology & Engineering Research (IJATER),* vol.4, special issue (2), *pp.53-59, 2014.*

Conference Publications:

1. S. Kayalvizhi and D.M. Vinod Kumar, "***Dispatchable DG Planning in Distribution Network considering cost"*** IEEE International conference on Recent Development in Control, Automation and Power Engineering (RDCAPE'15), Mar'2015 at Amity University, UP.
2. S. Kayalvizhi and D.M. Vinod Kumar, "***Optimal Operation of Autonomous microgrid for minimization of energy loss, cost and voltage deviation***", IEEE Workshop on Computational Intelligence: Theories, application and future directions, Dec 2015 at IIT Kanpur.

Journal Communicated:

1. S. Kayalvizhi and D.M. Vinod Kumar, "Optimal Planning of active distribution networks with hybrid Distributed Energy Resources using Grid-based Multi-Objective Harmony Search Algorithm", Applied Soft Computing, Elsevier.

Curriculum - Vitae

Name	:	Ms. S. Kayalvizhi
Date of Birth	:	9th August 1989
Gender	:	Female
Contact number	:	+919790050752, +918142497171
Email id	:	kayaleee89@gmail.com

Academic Qualification

Program	Institution	%/CGPA	Year of completion
M.E. (Power Systems Engineering)	College of Engineering Guindy, Anna University, Chennai	8.64	2012
B.E (EEE)	Krishnasamy College of Engineering and Technology, Cuddalore.	77	2010